UNIVERSITY OF CALIFORNIA

SANTA CRUZ

# INVESTIGATING THE ALLOSTERIC ACTIVATION AND SUBSTRATE PREFERENCES OF HUMAN LIPOXYGENASE ENZYMES

A dissertation submitted in partial satisfaction
of the requirements for the degree of

DOCTOR OF PHILOSOPHY

in

CHEMISTRY

by

**Christopher Joseph Smyrniotis**

June 2014

The Dissertation of Christopher Joseph Smyrniotis is approved:

_____
Professor Seth M. Rubin, Chair

_____
Professor Theodore R. Holman

_____
Professor Michael D. Stone

_____
Tyrus Miller
Vice Provost and Dean of Graduate Studies

## Table of Contents

## List of Figures

**Chapter 1**



**Chapter 2**



**Chapter 4**

## List of Tables

**Chapter 2**



**Chapter 3**



**Chapter 4**

## List of Schemes

**Chapter 2**



**Chapter 3**

**Abstract**

**Investigating the allosteric activation and substrate preferences of human lipoxygenase enzymes**

Christopher J. Smyrniotis

The research in this dissertation describes the allosteric activation and inhibition of 5-LOX human lipoxygenase as well as the substrate preferences for all 3 main LOX isozymes, 5-LOX, 12-LOX, and 15-LOX-1, to generate higher-order lipid mediators. 5-LOX is both a hydroperoxidase of arachidonic acid (AA) and an epoxidase of 5(S)-hydroperoxy-6E,8Z,11Z,14Z-eicosatetraenoic acid (5(S)-HpETE) to form leukotrienes from a single polyunsaturated fatty acid (PUFA). This dissertation investigates the kinetic mechanism of these two processes and the role of ATP in their activation. Specifically, it was determined that epoxidation of 5(S)-HpETE has a significantly lower rate of substrate capture ($V_{max}/K_m$) than AA hydroperoxidation, however, hyperbolic kinetic parameters for ATP activation suggest a larger activation with 5(S)-HpETE. Solvent isotope effect (SIE) results for both hydroperoxidation and epoxidation indicate that a specific step in its molecular mechanism is changed, possibly due a change in the dependency of the rate-limiting step on hydrogen-bond rearrangement toward substrate rearrangement. The products of 5-LOX, leukotrienes and resolvins, both promote and inhibit inflammation, respectively, and therefore changes in ATP concentration in the cell could have wide implications in their relative concentrations and ultimately the regulation of cellular inflammation.

5-LOX inhibition was also profiled with the discovery of a novel dual inhibitor targeting fungal sterol 14α-demethylase (CYP51 or Erg11) and 5-LOX. A phenylenediamine core was translated into the structure of ketoconazole, a highly effective anti-fungal medication for seborrheic dermatitis, to generate a novel compound, ketaminazole. Docking of ketaminazole confirmed kinetic results showing that the drug binds in the active site presenting the phenylenediamine core for effective reduction of the 5-LOX catalytic iron. This novel dual anti-fungal/anti-inflammatory inhibitor could potentially have therapeutic uses against fungal infections that have an anti-inflammatory component.

Epoxidation and hydroperoxidation mechanisms were also investigated in the other main LOX isozymes, 12-LOX and 15-LOX-1. Only 15-LOX-1 was found to effectively hydroperoxidate some of the oxylipins tested, with the hydroxide/hydroperoxide causing a change in the positioning of the substrate in the active site and changing the enzyme's regiospecificity. In contrast, all three LOX isozymes can epoxidate hydroperoxides and this ability is dependent on their respective hydrogen atom abstraction specificity. ATP activation of 5-LOX is also further profiled and found to be more substrate-selective than previously noted. These epoxidation mechanisms may be implicated in higher-order lipids being formed such as lipoxins, eoxins, and hepoxilins, all unique in their ability to mediate inflammation.

**Acknowledgements**

I would first like to thank my advisor, Theodore R. Holman, for his training and support for doing fun research in his lab, and for being eager to explore a different research direction with lipoxygenase. Thank you to Seth M. Rubin for his support as my committee chair, and for his phone call nearly 5 years ago, asking me if I wanted to switch into the newly formed MSCB program (I'm glad I did). Thanks to Michael D. Stone for all of the great advice and moral support he's given me, as it has helped me make the most out of grad school. In addition, I'd like to thank Pradip K. Mascharak for letting me rotate into his lab and for the many edifying conversations there. And thanks to William G. Scott for his scholarly advice when I was first starting out on my research projects. I also owe thanks to Carrie L. Partch for a lot of advice given with some different cell preparations I was trying out. It's been great having professors like you all around.

For my fellow grad student colleagues, I'd like to especially thank Eric Hoobler for being an awesome mentor and friend, and Kenny Ikei for first welcoming me into the lab (I miss you buddy). Thanks to my ever-helpful team of undergrads: Shannon Barbour, Jason Xia, and Anhquan Nguyen. Shannon in particular has helped so much in making this research possible, and I wish her lots of luck with her own research career. Thanks to the rest of my lab mates over the past 5 years: Victor, Josh, Netra, Brian, Steve, Cody, Gio, Michelle and Thomas. And thanks to all the others I've had the pleasure of researching and teaching with: Andy, Ryan, Eric

Evans, Denise, Jason Burke, Gabe, Ana, Jaime, Genevieve, Eefei, Mark Hixon, Jack Lee, Chris Bailey, Damon, Valerie, Jason Cooper, Qiangli, Charles, and Kyle Brown.

Lastly, I'd like to thank my family for their unending love and support. My parents, Maria and Chuck Smyrniotis, have always been there for me, and their support and encouragement has helped me become who I am today. I'm proud to be your son. My sisters, Erica and Victoria, are the best sisters a brother could have. My godmother Tata and Lynn, thank you for putting the oil on me all those years ago and for the support and encouragement ever since. And thank you to my fiancée Toshiko for sticking with me and helping me succeed in finally making it to graduation. It always helped knowing that, even after a tiring day in lab, I still got to come home to you and our kitties, Sushi and Ravi. Lastly, thanks to all of my extended family, whom I don't see as often as I'd like: Uncle Jim and family, the Clancys, Aunt Rose, Uncle Carl, and all of my theas, theos, and cousins.

The text of this document includes permitted reprints of the following previously published material:

**1)** Hoobler, E. K., Rai, G., Warrilow, A. G. S., Perry, S. C., Smyrniotis, C. J., Jadhav, A., Simeonov, A., Parker, J. E., Kelly, D. E., Maloney, D. J., Kelly, S. L., and Holman, T. R. (2013) Discovery of a novel dual fungal CYP51/human 5-lipoxygenase inhibitor: implications for anti-fungal therapy. *PLoS One 8*, e65928.

The coauthor listed in this publication, Theodore R. Holman, directed and supervised the research that forms the basis for this dissertation.

# Chapter 1

# Introduction

## 1.1 Lipoxygenase

Lipoxygenases (linoleate:oxygen oxidoreductase, EC 1.13.11.12) form a unique family of lipid-peroxidizing metalloenzymes that utilize a non-heme iron center for catalysis.[1-6] Ubiquitous in nature, these enzymes function to dioxygenate polyunsaturated fatty acids (PUFAs), which are the precursors to biologically active eicosanoids such as leukotrienes and lipoxins. These lipoxygenase products play varied roles within the biological context of their organism, such as regulating inflammation pathways in mammals,[7,8] promoting wound healing and defense processes in plants,[9] and regulating mycotoxin production and the life cycle in fungi.[10] Noting such roles, inhibitor and antagonist studies have been performed and have helped described in great detail all of the nuances of the enzyme's kinetics,[11,12] as have studies probing the varied properties of lipoxygenase isoforms.[13-15] Furthermore, the impact of lipoxygenase products on pathogenesis and cancer has been well characterized.[16-19] Like other non-heme iron-containing dioxygenases, lipoxygenase undergoes redox chemistry at its active site, and much has been answered about the role of iron in this mechanism.[20]

## 1.2 Non-heme Iron Center and its Reduction-Oxidation Properties

The importance of the iron center in lipoxygenase was first overlooked when the first soybean lipoxygenase was crystallized, due to the authors not finding any metal or prosthetic groups in the absorption spectrum of the enzyme.[21] Nearly 30

years later, it was determined that lipoxygenase is indeed an iron-containing enzyme through experiments that characterized a stoichiometry of 1 Fe to every 1 mol enzyme, established that iron is tightly bound to enzyme and unable to be removed even in the presence of strong complexing chelators, and highlighted the importance of iron in catalysis due to the necessity of bound ferric Fe(III) for native function.[20,22,23]

Non-heme iron-containing dioxygenases, like lipoxygenase, are ubiquitous and compose a grouping of enzymes with a variety of functions, such as cleavage of aromatic rings, oxidation of sulfur-containing compounds, and the dioxygenation of PUFAs. Non-heme iron is the most common type of cofactor in dioxygenases, although there are examples of enzymes that prefer either the ferric state or ferrous state for catalytic activity.[24]

While noting the importance of iron to catalytic activity, it had not been established which residues for chelating iron were necessary and which were necessary for the mechanism. Data obtained from primary sequences gleaned from the cDNAs of soybean, human, and rat 5-lipoxygenase had highlighted the existence of a conserved cluster of 5 His residues in all primary sequences that may potentially be the iron-binding site (Figure 1.1).[25] Nguyen *et al.* (1991) were able to show through site-directed mutagenesis that His at positions 363, 391, and 400 of human 5-lipoxygenase were able to be replaced by Ser residues without loss of activity, which indicated that these residues are not essential for lipoxygenase activity.[26] However, the authors cautioned that this didn't qualify the 3 sites as unnecessary to iron

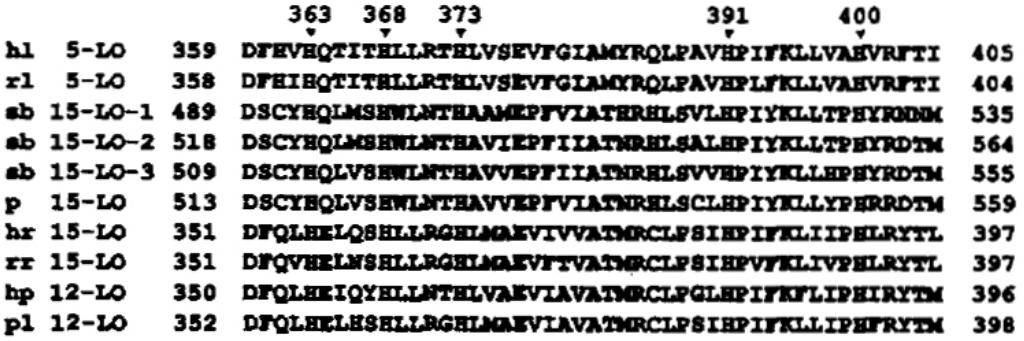


**Figure 1.1.** Comparison of primary sequences and the conserved His-$(X)_4$-His-$(X)_4$-His-$(X)_{17}$-His-$(X)_8$-His motif of 5-lipoxygenases in human leukocyte (hl) and rat leukocyte (rl); 15-lipoxygenase types 1-3 in soybean (sb), pea seed (p), human reticulocyte (hr), and rabbit reticulocyte (rr); and 12-lipoxygenase in human platelet (hp) and porcine leukocytes (pl)[26]

binding, but suggested that these 3 sites were necessary for maintaining native state structure, as these mutants tended to form aggregates and become inactivated much easier than native protein. To prove this point, a Lys residue was instead swapped into the His-363 position and enzyme activity was assayed, and the group found that the mutant had lost all activity. Their results also suggested that His-368 and His-373 were most important for maintaining enzyme activity. Zhang *et al.* (1993) independently confirmed these data by their own site-directed mutagenesis experiments, and found that His-367 mutants were inactive although retained partial iron content, while His-372 and His-550 mutants were inactive and contained zero iron content.[27] Further still, Steczko and Axelrod (1992) also reported that mutating out 3 histidines of soybean lipoxygenase-1 in comparable positions to above for human 5-lipoxygenase lead to the apo-form of the enzyme.[28] Taken together, these sources suggest the role of these 3 conserved histidine residues for iron-binding, with other conserved residues needed for adopting native structure.

Suzuki *et al.* (1994) performed site-directed mutagenesis on porcine leukocyte 12-lipoxygenase to determine the iron-binding capabilities of this histidine cluster, and found that His-361, -366, and -541 were essential for iron binding, as site mutations at these residues caused a loss of activity while also depleting the iron content of the enzyme.[29]

**1.3 Spectroscopic Methods**

X-ray absorption spectra indicated that ferrous Fe(II) in native state soybean lipoxygenase L-1 is held in an octahedral coordinate sphere containing 4 ± 1 nitrogen

atoms (imidazole) and 2 ± 1 oxygen atoms, although upon enzyme activation, a nitrogen atom from imidazole is replaced with an oxygen atom.[30] Dunham *et al.* (1990) utilized Mössbauer spectroscopy to determine that iron is spherically coordinated within the lipoxygenase.[31] Zhang *et al*. (1991) utilized magnetic circular dichroism to uncover an octahedral 6-coordinate system with a slight rhombic distortion, and determined that diatomic oxygen was not itself a ligand during the mechanism.[32]

The X-ray crystal structure of soybean lipoxygenase type 1 was solved in 1993 by multiple anomalous isomorphous replacement (Figure 1.2), and to higher resolution in 1996 (Figure 1.3), which determined the location of the active site iron atom and also identified 1 water group and 5 protein groups which act as its ligands: the C-terminal carboxylate group of Ile-839, the imidazole groups of His-499, His-504, and His-690, and the side chain of Asn-694, confirming the importance of these conserved histidines in binding iron.[33,34]

**1.4 Lipoxygenase Structure and Mechanism**

The model for soybean lipoxygenase shown in Figure 1.3 confirms not only the active site structure surrounding iron, but also provides a wealth of other structural information that helps define the lipoxygenase mechanism of dioxygenase of PUFAs. The enzyme can be divided into two spatially isolated domains: the N-terminal domain (residues 1-146 in soybean lipoxygenase-1), which resembles a β-barrel sandwich; and the C-terminal domain (residues 147-839), which comprises mostly α-helical secondary structure. It is thought that the N-terminal domain may be

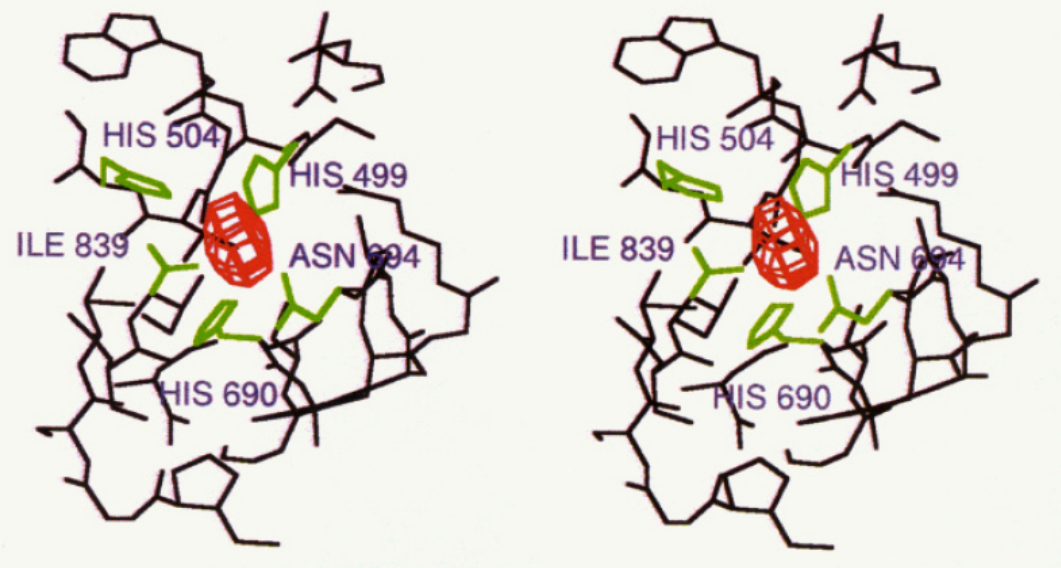


**Figure 1.2.** Stereoscopic view of the active Fe center of soybean lipoxygenase-1.[33] These residues correspond to the 5-lipoxygenase model in the following way: His-499 (sl) corresponds to His-367 (5-LO); His-504 (sl) corresponds to His-372 (5-LO); His-690 (sl) corresponds to His-550 (5-LO).

**Figure 1.3.** Soybean lipoxygenase-1 crystal structure refined to 1.4 Å.[34]

involved in substrate- or membrane-binding, whereas iron is found in the C-terminal domain that is required for catalytic activity.[10,35,36] The active site lies within a multihelix bundle, and there exists 2 major cavities (Cavity I & II) within the C-terminal domain that substrates can travel through.

Recently, Dainese *et al.* (2010) isolated a 60-kDa C-terminal region they referred to as a miniLOX, which lacks an α-helix that normally occludes access to iron, and found that it possesses higher catalytic efficiency compared to the native form of the enzyme due partially to a more substrate-accessible active site.[37] Furthermore, miniLOX has a more flexible coordination of Asn, which is already a weak-field ligand for Iron in the native state, allowing it to undergo reaction quicker and achieving a higher $k_{cat}$ value. In these experiments the authors were also able to generate an apo-miniLOX, the first time iron has been extracted successfully to yield such an apo-form. Removal of iron yields an inactive, more relaxed form of miniLOX, suggesting iron is also necessary for maintaining functional structure. More specifically, the membrane-binding activity of apo-miniLOX is lost compared to miniLOX (which has a relatively higher membrane-binding ability than native state lipoxygenase due to a larger exposure of hydrophobic regions in the former), suggesting iron also has a role in promoting proper structure for membrane-binding.

**1.5 Mechanism of Dioxygenation of Polyunsaturated Fatty Acids (PUFAs)**

Lipoxygenases are designated as 5-, 12-, or 15-lipoxygenases according to their selectivity for the indicated carbon of their substrate, arachidonic acid in animals or linoleic acid in plants.[38] Considerable detail of their mechanism has been

elucidated by a wealth of kinetic studies (Figure 1.4). The first and rate-determining step in the catalytic cycle is the activation of the substrate by ferric-state iron, which is accomplished by first abstracting hydrogen through homolytic cleavage and thus producing a substrate radical and a ferrous species.[39] By forming a peroxy radical, the substrate is made viable to react with triplet-state (unpaired high-energy electrons) $O_2$. Steady-state kinetic data from Glickman *et al.* disproved the possibility of a ternary complex of enzyme-substrate-dioxygen forming, and tied with evidence of a carbon-centered linoleic free radical,[40] direct observation of the peroxyl radical by EPR,[41] a very high reduction potential of the ferric iron (~0.6V),[42] and lack of any spectroscopic evidence of a bound oxygen species to lipoxygenase in the absence of substrate, this conclusively points to a radical mechanism for hydrogen abstraction prior to dioxygen binding (Figure 1.5).

After hydrogen abstraction, dioxygen reacts with the substrate. To demonstrate this, it was shown that in the absence of $O_2$, hydrogen abstraction will occur causing the enzyme to be reduced to its ferrous state while lipid radicals will be generated and form homodimers. Analysis of this mechanism shows that it can be described by a purely quantum-mechanical pathway, with hydrogen tunneling occurring in the first step to overcome the energy barrier of radical formation and dissociation, as prompted by the iron cofactor operating as an electron sink.[43] Also detailed in Figure 1.4 is the activation pathway of resting ferrous state enzyme, through interaction with the hydroperoxide product.

Since this abstraction of the hydrogen atom is rate-limiting, it is a key step to

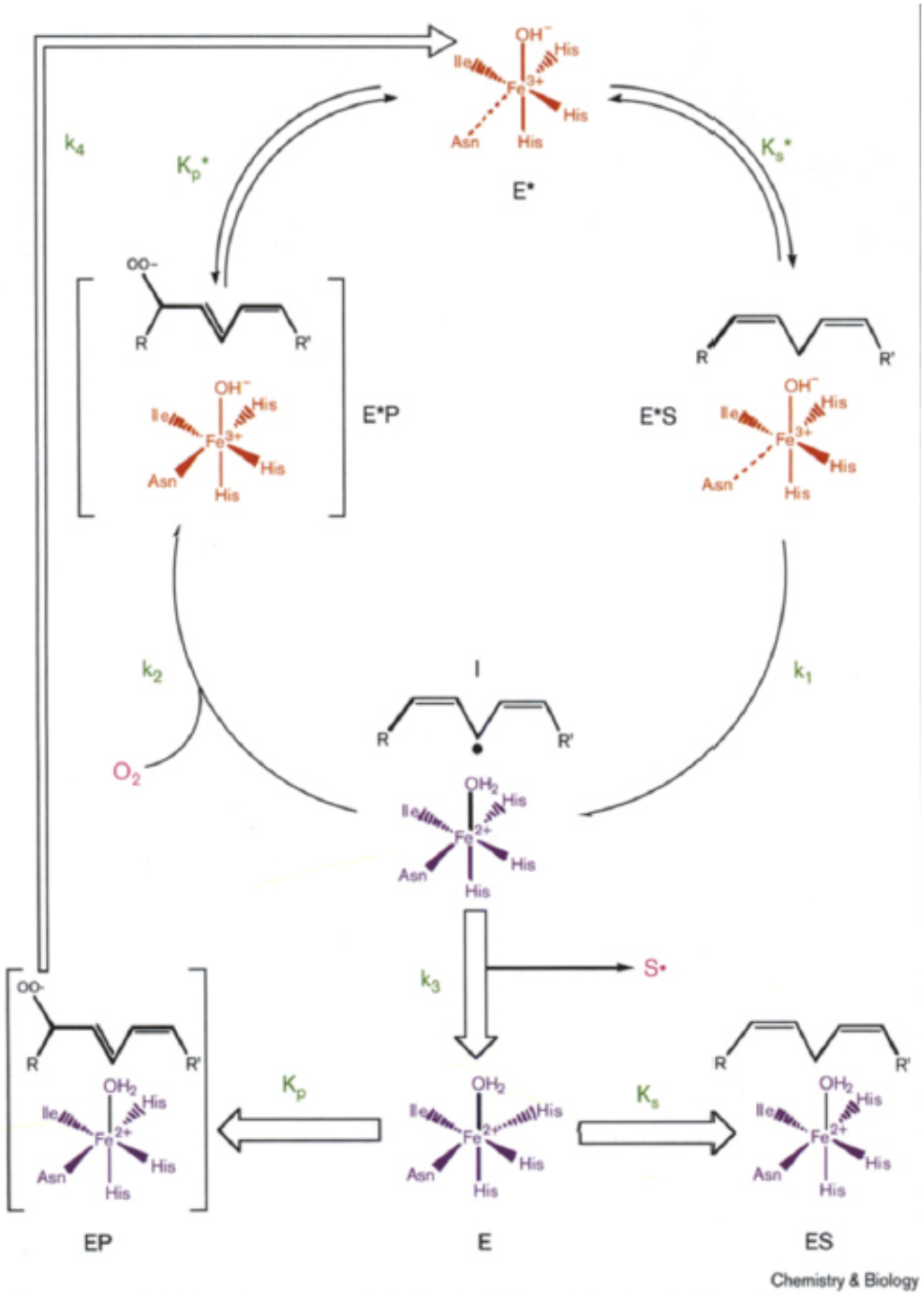


**Figure 1.4.** Reaction scheme of dioxygenation of substrate by lipoxygenase.[38] The second step in this mechanism is a relaxation process where an electron is transferred from the metastable radical intermediate back to hydroxide ligand and finally to the iron cofactor, oxidizing it back to the ferric Fe(III) state.

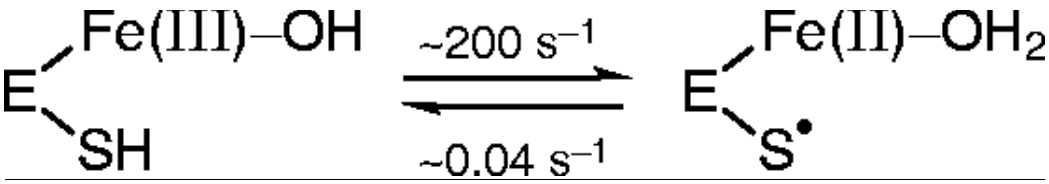


**Figure 1.5.** Hydrogen abstraction step of the lipoxygenase dioxygenation mechanism.[38]

the lipoxygenase mechanism.[38] Studies with EPR have determined that the iron cofactor in its ferric state has a pseudo-5C geometry with a weak Fe-Asn bond, whereas the ferrous state has a pure 6C geometry with fully bound Asn. This geometry is essential for ensuring that the coordinated water has a high $pK_a$ that is also required for proton transfer. The ferrous 6C coordination site has a high amount of electron density as compared to the ferric pseudo-5C coordination geometry, and thus the ferrous state decreases the inductive polarization of the OH bond by pushing electron density out to the water ligand.

### 1.6 Regiospecificity and Stereospecificity of Products

While sharing the same catalytic mechanism, lipoxygenases are selective as to the stereochemistry of the products they each produce. In soybean lipoxygenase, the linoleic acid substrate can be converted to either the 9-hydroperoxy (9-HPODE) product by introducing molecular oxygen at carbon atom 9, or the 13-hydroperoxy (13-HPODE) product by alternatively introducing molecular oxygen at carbon atom 13.[10] As the nomenclature suggests, 9-lipoxygenase will selectively turn over 9-HPODE, and 13-lipoxygenase turns over 13-HPODE. Regioisomers of these fatty acid products are selected by their respective enzyme through stereoselective hydrogen removal at C-11 and $O_2$ insertion at either C-9 or C-13 (Figure 1.6). There is no entirely accepted model for this high regiospecificity, although there are 2 competing hypotheses: the space-related model and the orientation-dependent model, which implicate a number of critical amino acids at the active site for influencing regiospecificity.

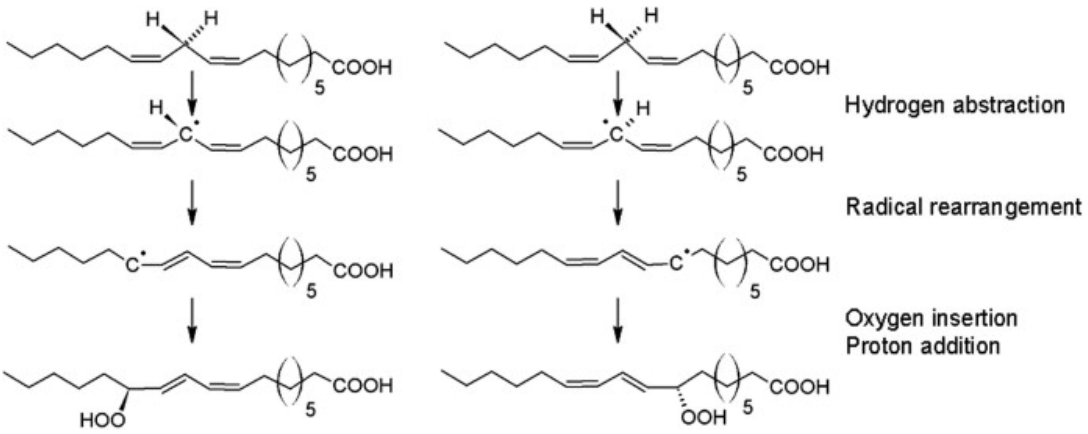


**Figure 1.6.** Dioxygenation mechanism and generation of stereoisomer products. Left: 13-LO generating 13-HPODE. Right: 9-LO generating 9-HPODE.[10]

The orientation-dependent model was described by Gardner *et al*. for soybean lipoxygenase-1 as a model for the plausible active site structure of lipoxygenase.[44] It was reasoned that due to the pH dependence of the selective formation of 2 distinct HPODE products (13S-HPODE and 9S-HPODE), the carboxylic acid and carboxylate anion of substrate interact differently with the active site structure of the enzyme, determining the orientation of the substrate as either "head-to-tail" or "tail-to-head" before hydrogen abstraction occurs. In all 13-lipoxygenases, a space-filling histidine or phenylalanine can be found, whereas for 9-lipoxygenases a smaller valine residue is identified at this same amino acid position. Hornung *et al.* (1999) were able to convert a 13-lipoxygenase to a 9-lipoxygenase simply by site-directed mutagenesis of this particular amino acid, and structural modeling of this enzyme/substrate interaction suggests that such a point mutation allows substrate access to a conserved arginine residue, which promotes stabilization of a head-to-tail orientation (Figure 1.7, bottom panel).[45]

In contrast, the space-related model suggests that the tail-to-head orientation of substrate in the active site pocket is conserved throughout all lipoxygenases, and the size of the pocket itself is the determinant of the regiospecificity of products turned over by enzyme (Fig. 7, top panel). This model does not account for the conserved nature of the arginine residue as described above, and thus the orientation-dependent model is the more preferred hypothesis at this time.

Each lipoxygenase prefers to create one particular regiospecific and stereospecific hydroperoxy product. For the arachidonic acid substrate, there are 12

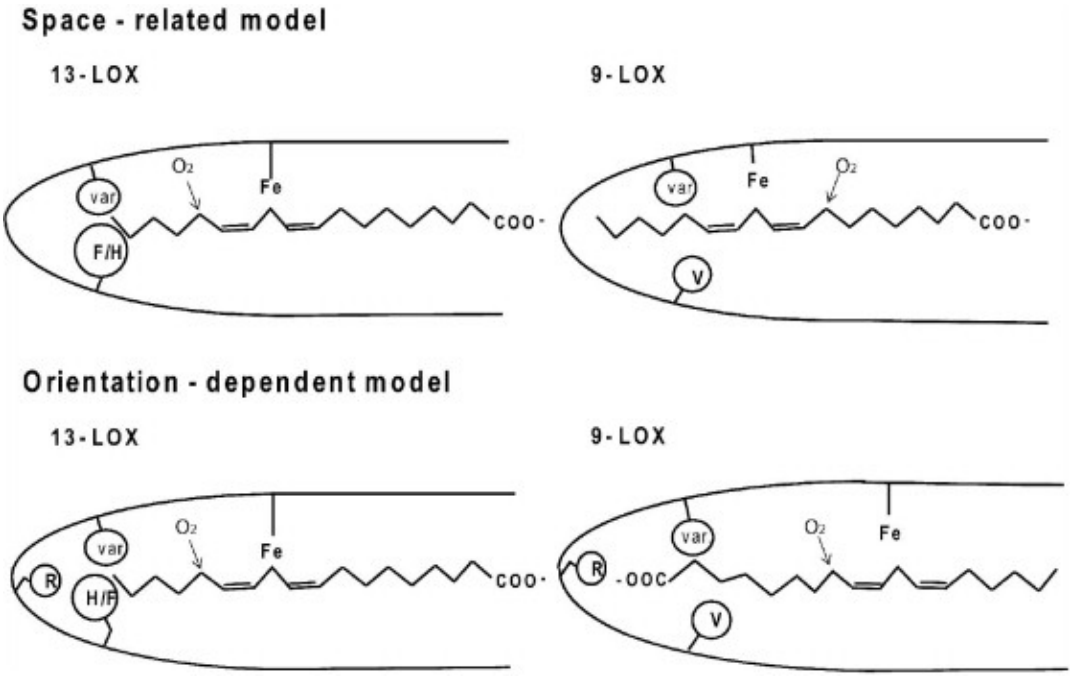


**Figure 1.7.** Two models that explain the regiospecificity of lipoxygenase.[10]

theoretical mono-hydroperoxide derivative products that can be formed, and 9 different stereospecific lipoxygenases have been characterized, each with a preference for one single product (5S-, 5R-, 8S-, 8R-, 9S-, 11R-, 12R-, 12S-, and 15S-specificities), with the exception of 12-lipoxygenase and its homologue 15-lipoxygenase-1 which form a mixture of 12S- and 15S- products.[46] It is a fact of all lipoxygenases that oxygenation and hydrogen abstraction observe an antarafacial relationship, meaning they occur on opposite faces of the substrate. Coffa *et al*. (2005) identified a conserved Ala in S-lipoxygenases and a corresponding conserved Gly in R-lipxoygenases, and site-specific mutation to switch this residue impacted the stereoselectivity of the HPODE product formed, for example by modulating an 8S-lipoxygenase, which turns over only 8S-HPODE products, into turning over both 8S- and 12-R products.[46] This Gly/Ala residue is referred to as the "Coffa site" after the authors, and is thought to function by sterically allowing for oxygenation at the opening of the active site pocket when a glycine is present (R stereoselectivity), whereas an alanine sterically prevents oxygenation at that site, and presumably $O_2$ must be reacted with the activated substrate at a point further in the active site pocket (Figure 1.8). In conclusion, substrate orientation, hydrogen abstraction, and the "Coffa site" Gly/Ala residue all impact the reaction specificity of a particular lipoxygenase.

**1.7 Inhibitors**

The environment of the lipoxygenase iron-binding site can be explored with synthetically derived inhibitor compounds. In 1996, Abeysinghe *et al*. synthesized

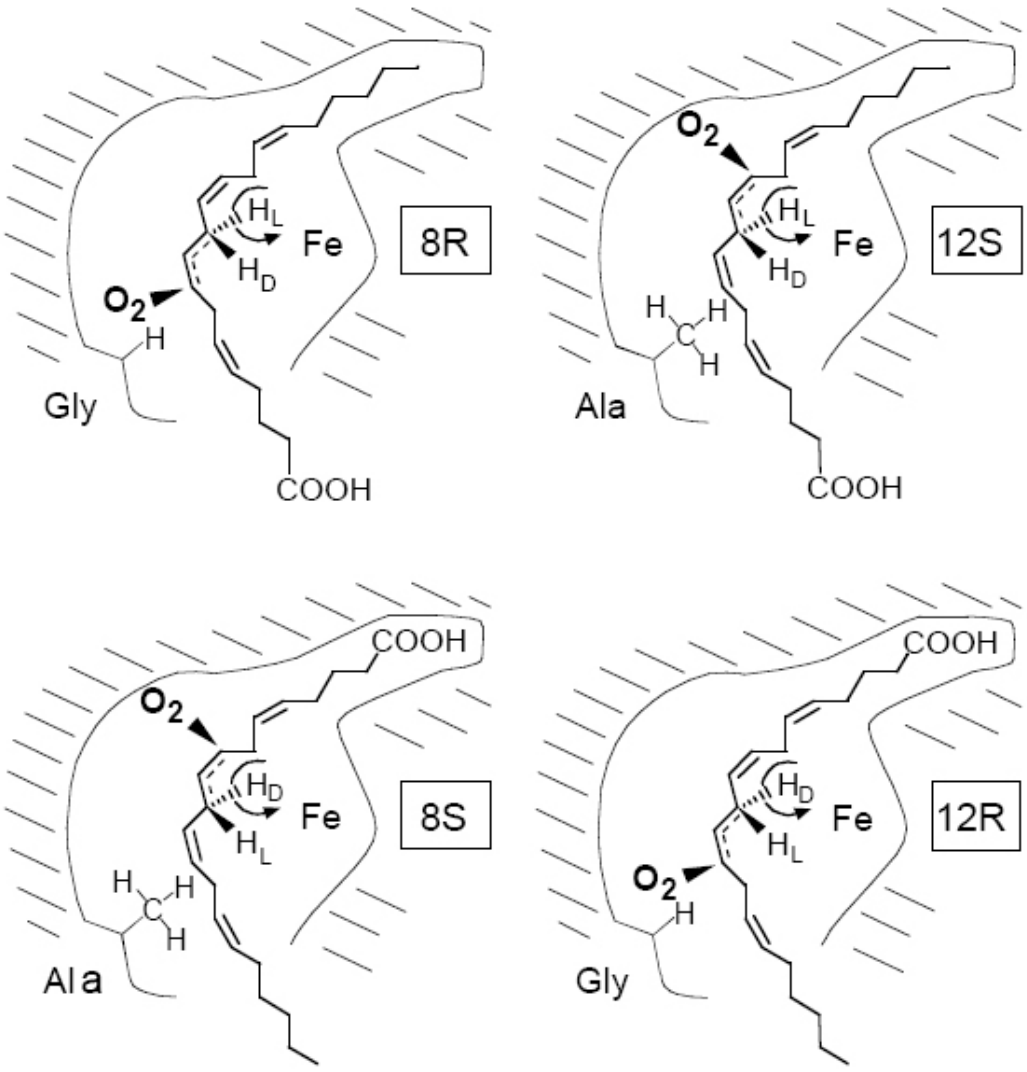


**Figure 1.8.** Arachidonic acid situation in different orientations within the active site of lipoxygenase.[46] The "Coffa site" Gly/Ala is shown, along with the regio- and stereo-specificity of the product each active site promotes. The exposed arginine residue forming a salt bridge with the carboxylate head group in the bottom 2 panels is not shown.

hydroxypyridinone and hydroxypyranone iron chelators and investigated their inhibitory activity on 5-lipoxygenase and soybean lipoxygenase.[47] The authors discovered that the iron chelating properties of the inhibitors indeed are able to bind and even remove iron to inactive the enzyme, but also that the inhibitory potential is influenced by its lipid solubility. Apart from iron chelating inhibitors, lipoxygenases can also be inhibited by redox switching compounds. Isoflavones are antioxidants that inhibit both soybean lipoxygenase and 5-lipoxygenase, and they noncompetitively inhibit enzyme by reducing active state iron to the ferrous state, and further prevent enzyme activation.[48]

**1.8 Allosteric Regulation**

Investigating the inhibitory effects of oleic acid on soybean lipoxygenase-1 and human 15-lipoxygenase, Mogul *et al*. (2000) found that inhibition was more complex than originally assumed.[49] Steady-state kinetics with a novel inhibitor they synthesized, (Z)-9-octadecenyl sulfate (oleyl sulfate), determined that there is an allosteric binding site in both soybean lipoxygenase-1 and human 15-lipxoygenase-1 that when bound to inhibitor, lowers the specificity constant ($k_{cat}/K_m$) by 80%. In 2008, Wecksler *et al*. utilized a novel competitive substrate capture assay to better probe the importance of this allosteric site and regulatory effect on the enzyme.[50] Their results confirmed the presence of an allosteric site and how it is responsible for induced changes to substrate specificity. This allosteric site likely has biological implications, as it was found that HpODE products were able to bind the allosteric site in human 15-lipoxygenase, which modulated their substrate specificity toward

linoleic acid or arachidonic acid substrates in the form of a product-feedback loop. Similar findings were also found in soybean lipoxygenase-1[15] and in human 15-lipoxygenase-2[13] (Figure 1.9).

**1.9 Products and Biological Impacts of Arachidonic Acid Metabolism**

A large number of products are formed by metabolism of arachidonic acid, a 20:4 ω6 essential fatty acid with 2 (1Z,4Z)-pentadiene moieties. As shown in Figure 1.10, arachidonic acid is a precursor to many important derivatized target eicosanoids.[51] Prostaglandin H synthases, sometimes referred to as cyclooxygenases (COX-1 and COX-2), are responsible for the conversion of arachidonic acid into prostaglandins and thromboxanes, which have varied biological roles from vasoconstriction to pain response.[52] In comparison, 5-, 12-, and 15-lipoxygenases also use arachidonic acid as a substrate, for different end results depending on their cellular context, and thus their activity and product profile has to be strictly regulated to prevent unwanted side-effects, like oxidative stress-related death.[53,54] For example, due to the implications of 5-lipoxygenase in a number of inflammatory and allergic disorders, there is much work undertaken with regards to designing inhibitors for these enzymes.[55,56]

Lipoxygenase products can be subdivided into 3 general categories: (1) peptidoleukotrienes ($LTC_4$, $LTD_4$, and $LTE_4$), (2) non-peptidyl leukotrienes ($LTA_4$ and $LTB_4$), and (3) hydroperoxy eicosatetraenoic acids (HPETE), hydroxyl eicosatetraenoic acids (HETE), and lipoxins (LX).[51] The former two make up a general class of leukotrienes, which function to activate, migrate and adhere

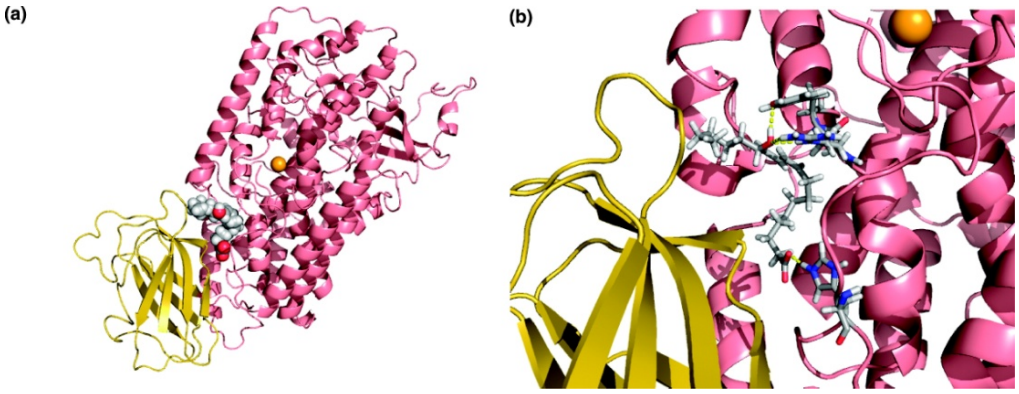


**Figure 1.9.** Human 15-lipoxygenase-2 docked with 13-HODE in the proposed allosteric site.[13]

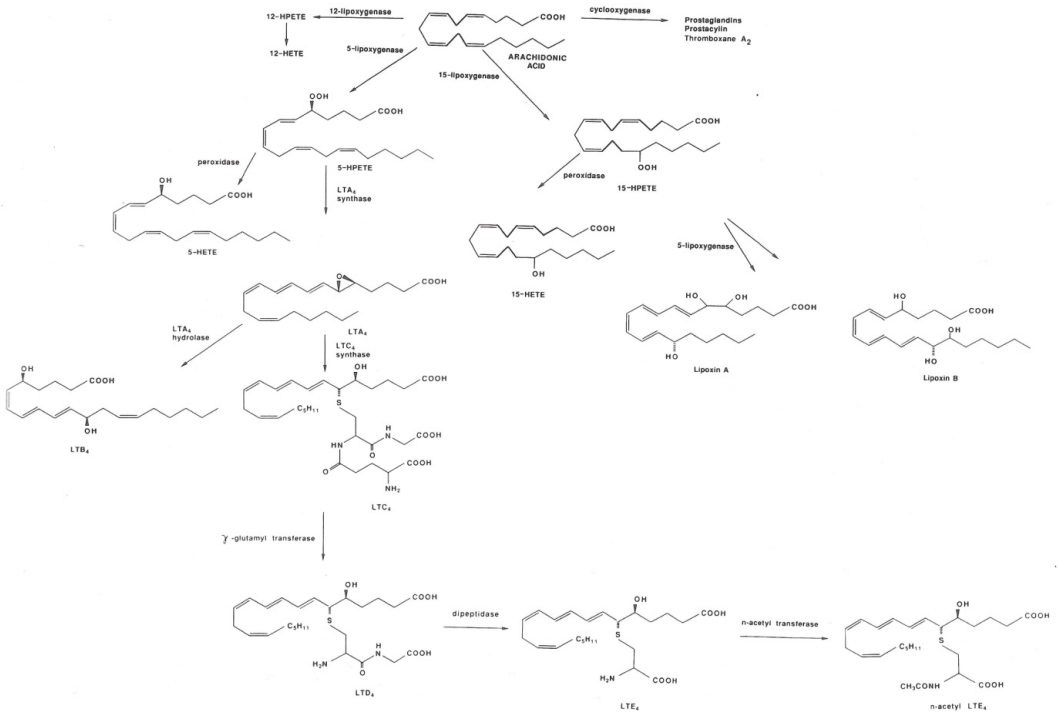


**Figure 1.10.** Arachidonic acid is the primary precursor for a number of biologically relevant eicosanoid signalling molecules.[51]

leukocytes to their target destination (Figure 1.11), while the latter is thought to be involved in dilating cardiovasculature and inhibiting natural killer cell cytotoxicity.

**1.10 Peptidoleukotrienes**

The $LTC_4$ synthase ($LTC_4H$) conjugates a glutathione to $LTA_4$ to create this class of leukotrienes.[52] It is well established that a major function of peptidoleukotrienes is for smooth muscle contraction and inflammation of airway tissues; $LTC_4$ and $LTD_4$ are actually ~1000x more potent than histamine in signaling an inflammation response. [51,57] Intravenous administration of peptidoleukotrienes causing bronchoconstriction is delayed by cyclooxygenase inhibition[58] or thromboxane synthase inhibition,[59] and other studies with guinea pigs have shown that leukotriene-elicited contractions are attenuated by inhibitors that target cyclooxygenase,[60] suggesting convergent biosynthetic pathways. $LTC_4$ and $LTD_4$ also have concentration-dependent vasoconstrictive effects and function likely through direct activation of specific peptidoleukotrienes receptors,[51] although other studies showed that these contractile effects are not seen in thoracic aorta or pulmonary artery of the rat or rabbit.[61]

**1.11 Leukotrienes**

$LTA_4$ is hydrolyzed to $LTB_4$ by leukotriene $A_4$ hydrolase ($LTA_4H$) in a variety of immune cells such as polymorphonuclear leukocytes, mast cells, T-lymphocytes, alveolar macrophages, and keratinocytes,[51] and this form of leukotriene can cause relatively weak contractions in the trachea and lungs.[62] In line with effects seen with its peptidyl counterpart, overlap with cyclooxygenase is suggested by

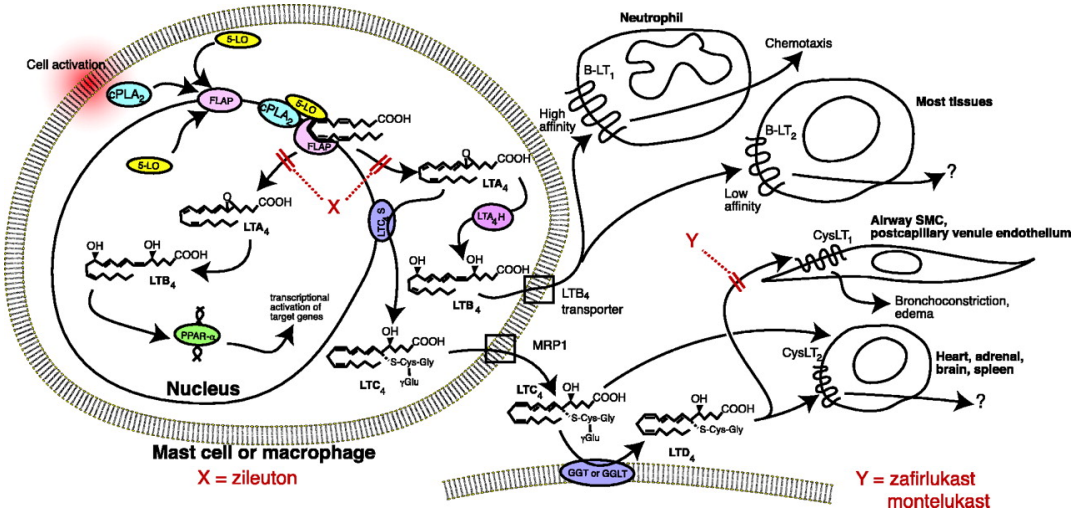


**Figure 1.11.** Leukotriene synthesis and actions. 5-Lipoxygenase catalyzes the first step in this biosynthetic pathway from the arachidonic acid substrate.[51]

studies that have shown that cyclooxygenase products mediate these leukotriene-prompted contractions.[63] $LTB_4$ is a potent neutrophil chemoattractant and stimulator of leukocyte adhesion to endothelial cells.[52]

### 1.12 Lipoxins and HPETE/HETE products

Lipoxins are so named because they are lipoxygenase interaction products, formed by the function of both 5- and 15-lipoxygenase. LXA and LXB are the primary lipoxins, with a number of immunoregulatory and smooth muscle contractile properties, and are created from their 15-HETE and 15-HPETE precursors by activated leukocytes.[64] Lipoxins are anti-inflammatory and function by signaling macrophages to enhance phagocytosis and thus remove the remains of apoptotic and necrotic neutrophils, which are typically the body's first line of defense and the cause of a locally contained inflammation.[65] 12- and 15-HPETE products have been shown to have concentration-dependent effects on vasoconstriction through the alteration in transmembrane calcium fluxes.[66,67]

### 1.13 Scope of Dissertation

Much of the chemistry behind the biological roles of lipoxygenase has been elucidated by the many research groups referenced herein. As an all-encompassing topic of interest, lipoxygenase has been studied through structural analysis, kinetic profiling, mechanistic characterization, and cell-based *in vivo* assays to name just a few methods, and there are still many directions future studies can take for this ubiquitous enzyme that has a critical role in the biology of many different organisms. A full characterization of the allosteric site and the impact of product-feedback loops

on inter- and intra-cell signaling, along with a more detailed characterization of the stereo- and regio-specificity of lipoxygenase, are currently some of the more actively researched topics related to lipoxygenase, and in the near future this research may generate new understandings of the inner workings of lipoxygenase.

This dissertation focuses on two main additions to the lipoxygenase literature: probing allosteric regulation induced by common biomolecules in the cell, and elucidating pathways of higher-order lipid formation that occur when multiple lipoxygenases are involved in catalysis of bioactive products. Chapter 2 provides kinetic evidence for ATP as an allosteric activator of 5-LOX for both HPETE and $LTA_4$ formation, suggesting a potential biologically relevant link between increased ATP concentration in certain disease states and 5-LOX activation leading to increased generation of pro-inflammatory products. Chapter 3 utilizes HETE and HPETE substrates to demonstrate kinetic parameters of epoxidation for 5-LOX, 12-LOX, and 15-LOX-1, and discusses what these parameters suggest about the unique substrate specificity of each enzyme. The final chapter of this dissertation, Chapter 4, discusses the discovery by our laboratory of a novel reductive inhibitor that is highly selective for 5-LOX in addition to being a potent anti-fungal drug, suggesting potential therapeutic uses against fungal infections that include inflammation as a symptom.

## 1.14 References

(1) Hamberg, M., and Samuelsson, B. (1974) Prostaglandin endoperoxides. Novel transformations of arachidonic acid in human platelets. *Proc. Natl. Acad. Sci. U.S.A. 71*, 3400–3404.

(2) Borgeat, P., Hamberg, M., and Samuelsson, B. (1976) Transformation of arachidonic acid and homo-gamma-linolenic acid by rabbit polymorphonuclear leukocytes. Monohydroxy acids from novel lipoxygenases. *J. Biol. Chem. 251*, 7816–7820.

(3) Gardner, H. W. (1991) Recent investigations into the lipoxygenase pathway of plants. *Biochim. Biophys. Acta 1084*, 221–239.

(4) Yamamoto, S. (1992) Mammalian lipoxygenases: molecular structures and functions. *Biochim. Biophys. Acta 1128*, 117–131.

(5) Brash, A. R. (1999) Lipoxygenases: occurrence, functions, catalysis, and acquisition of substrate. *J. Biol. Chem. 274*, 23679–23682.

(6) Rådmark, O. (2002) Arachidonate 5-lipoxygenase. *Prostaglandins & Other Lipid Mediators 68-69*, 211–234.

(7) Serhan, C. N. (2007) Resolution phase of inflammation: novel endogenous anti-inflammatory and proresolving lipid mediators and pathways. *Annu Rev Immunol*.

(8) Kühn, H., and O'Donnell, V. B. (2006) Inflammation and immune regulation by 12/15-lipoxygenases. *Prog. Lipid Res. 45*, 334–356.

(9) Liavonchanka, A., and Feussner, I. (2006) Lipoxygenases: occurrence, functions and catalysis. *J. Plant Physiol. 163*, 348–357.

(10) Andreou, A., and Feussner, I. (2009) Lipoxygenases - Structure and reaction mechanism. *Phytochemistry 70*, 1504–1510.

(11) Mogul, R., and Holman, T. R. (2001) Inhibition Studies of Soybean and Human 15-Lipoxygenases with Long-Chain Alkenyl Sulfate Substrates †. *Biochemistry 40*, 4391–4397.

(12) Kenyon, V., Rai, G., Jadhav, A., Schultz, L., Armstrong, M., Jameson, J. B., Perry, S., Joshi, N., Bougie, J. M., Leister, W., Taylor-Fishwick, D. A., Nadler, J. L., Holinstat, M., Simeonov, A., Maloney, D. J., and Holman, T. R. (2011) Discovery of potent and selective inhibitors of human platelet-type 12- lipoxygenase. *J. Med. Chem. 54*, 5485–5497.

(13) Wecksler, A. T., Kenyon, V., Garcia, N. K., Deschamps, J. D., van der Donk, W. A., and Holman, T. R. (2009) Kinetic and structural investigations of the allosteric site in human epithelial 15-lipoxygenase-2. *Biochemistry 48*, 8721–8730.

(14) Wecksler, A. T., Jacquot, C., van der Donk, W. A., and Holman, T. R. (2009) Mechanistic Investigations of Human Reticulocyte 15- and Platelet 12-Lipoxygenases with Arachidonic Acid. *Biochemistry 48*, 6259–6267.

(15) Wecksler, A. T., Garcia, N. K., and Holman, T. R. (2009) Substrate specificity effects of lipoxygenase products and inhibitors on soybean lipoxygenase-1. *Bioorg. Med. Chem. 17*, 6534–6539.

(16) Samuelsson, B. (1983) Leukotrienes: mediators of immediate hypersensitivity reactions and inflammation. *Science 220*, 568–575.

(17) Shimizu, T., Radmark, O., and Samuelsson, B. (1984) Enzyme with dual lipoxygenase activities catalyzes leukotriene A4 synthesis from arachidonic acid. *Proc. Natl. Acad. Sci. U.S.A. 81*, 689–693.

(18) Borgeat, P., and Samuelsson, B. (1979) Metabolism of arachidonic acid in polymorphonuclear leukocytes. Structural analysis of novel hydroxylated compounds. *J. Biol. Chem. 254*, 7865–7869.

(19) Ueda, N., Yamamoto, S., Oates, J. A., and Brash, A. R. (1986) Stereoselective hydrogen abstraction in leukotriene A4 synthesis by purified 5-lipoxygenase of porcine leukocytes. *Prostaglandins 32*, 43–48.

(20) Pistorius, E. K., and Axelrod, B. (1974) Iron, an essential component of lipoxygenase. *J. Biol. Chem. 249*, 3183–3186.

(21) Theorell, H., Holman, R. T., and Akeson, A. (1947) Crystalline lipoxidase. *Acta Chem Scand 1*, 571–576.

(22) Chan, H. W. (1973) Soya-bean lipoxygenase: an iron-containing dioxygenase. *Biochim. Biophys. Acta 327*, 32–35.

(23) Roza, M., and Francke, A. (1973) Product specificity of soyabean lipoxygenases. *Biochim. Biophys. Acta 316*, 76–82.

(24) Hayaishi, O., Nozaki, M., and Abbott, M. T. (1975) 3 Oxygenases: Dioxygenases, in *sciencedirect.com*, pp 119–189. Elsevier.

(25) Shibata, D., Steczko, J., Dixon, J. E., Andrews, P. C., Hermodson, M., and

Axelrod, B. (1988) Primary structure of soybean lipoxygenase L-2. *J. Biol. Chem. 263*, 6816–6821.

(26) Nguyen, T., Falgueyret, J. P., Abramovitz, M., and RIENDEAU, D. (1991) Evaluation of the role of conserved His and Met residues among lipoxygenases by site-directed mutagenesis of recombinant human 5-lipoxygenase. *J. Biol. Chem. 266*, 22057–22062.

(27) Zhang, Y. Y., Lind, B., Radmark, O., and Samuelsson, B. (1993) Iron content of human 5-lipoxygenase, effects of mutations regarding conserved histidine residues. *J. Biol. Chem. 268*, 2535–2541.

(28) Steczko, J., and Axelrod, B. (1992) Identification of the iron-binding histidine residues in soybean lipoxygenase L-1. *Biochem. Biophys. Res. Commun. 186*, 686–689.

(29) Suzuki, H., Kishimoto, K., Yoshimoto, T., Yamamoto, S., Kanai, F., Ebina, Y., Miyatake, A., and Tanabe, T. (1994) Site-directed mutagenesis studies on the iron-binding domain and the determinant for the substrate oxygenation site of porcine leukocyte arachidonate 12-lipoxygenase. *Biochim. Biophys. Acta 1210*, 308–316.

(30) Feiters, M. C., Boelens, H., Veldink, G. A., Vliegenthart, J. F. G., Nolting, H. F., Hermes, C., Navaratnam, S., and Allen, J. C. (1990) X-Ray absorption spectroscopic studies on iron in soybean lipoxygenase: A model for mammalian lipoxygenases. *Recl. Trav. Chim. Pays-Bas 109*, 133–146.

(31) Dunham, W. R., Carroll, R. T., Thompson, J. F., Sands, R. H., and Funk, M. O. (1990) The initial characterization of the iron environment in lipoxygenase by Mössbauer spectroscopy. *Eur J Biochem 190*, 611–617.

(32) Zhang, Y., Gebhard, M. S., and Solomon, E. I. (1991) Spectroscopic studies of the non-heme ferric active site in soybean lipoxygenase: magnetic circular dichroism as a probe of electronic and geometric structure. Ligand-field origin of zero-field splitting. *J. Am. Chem. Soc. 113*, 5162–5175.

(33) Minor, W., Steczko, J., Bolin, J. T., Otwinowski, Z., and Axelrod, B. (1993) Crystallographic determination of the active site iron and its ligands in soybean lipoxygenase L-1. *Biochemistry 32*, 6320–6323.

(34) Minor, W., Steczko, J., Stec, B., Otwinowski, Z., Bolin, J. T., Walter, R., and Axelrod, B. (1996) Crystal structure of soybean lipoxygenase L-1 at 1.4 A resolution. *Biochemistry 35*, 10687–10701.

(35) Walther, M., Anton, M., Wiedmann, M., Fletterick, R., and Kühn, H. (2002) The

N-terminal domain of the reticulocyte-type 15-lipoxygenase is not essential for enzymatic activity but contains determinants for membrane binding. *J. Biol. Chem. 277*, 27360–27366.

(36) Walther, M., Hofheinz, K., Vogel, R., Roffeis, J., and Kühn, H. (2011) The N-terminal Î²-barrel domain of mammalian lipoxygenases including mouse 5-lipoxygenase is not essential for catalytic activity and membrane binding but exhibits regulatory functions. *Archives of Biochemistry and Biophysics* 1–9.

(37) Dainese, E., Angelucci, C. B., Sabatucci, A., De Filippis, V., Mei, G., and Maccarrone, M. (2010) A novel role for iron in modulating the activity and membrane-binding ability of a trimmed soybean lipoxygenase-1. *The FASEB Journal 24*, 1725–1736.

(38) Solomon, E. I., Zhou, J., Neese, F., and Pavel, E. G. (1997) New insights from spectroscopy into the structure/function relationships of lipoxygenases. *Chem. Biol. 4*, 795–808.

(39) Glickman, M. H., and Klinman, J. P. (1996) Lipoxygenase reaction mechanism: demonstration that hydrogen abstraction from substrate precedes dioxygen binding during catalytic turnover. *Biochemistry 35*, 12882–12892.

(40) De Groot, J., Garssen, G. J., and Vliegenthart, J. (1973) The detection of linoleic acid radicals in the anaerobic reaction of lipoxygenase. *Biochimica et Biophysica ….*

(41) Chamulitrat, W., and Mason, R. P. (1989) Lipid peroxyl radical intermediates in the peroxidation of polyunsaturated fatty acids by lipoxygenase. Direct electron spin resonance investigations. *J. Biol. Chem. 264*, 20968–20973.

(42) Nelson, M. J. (1988) Catecholate complexes of ferric soybean lipoxygenase 1. *Biochemistry 27*, 4273–4278.

(43) Moiseyev, N., Rucker, J., and Glickman, M. H. (1997) Reduction of ferric iron could drive hydrogen tunneling in lipoxygenase catalysis: implications for enzymatic and chemical mechanisms. *J. Am. Chem. Soc. 119*, 3853–3860.

(44) Gardner, H. W. (1989) Soybean lipoxygenase-1 enzymically forms both (9S)- and (13S)-hydroperoxides from linoleic acid by a pH-dependent mechanism. *Biochim. Biophys. Acta 1001*, 274–281.

(45) Hornung, E., Walther, M., Kuhn, H., and Feussner, I. (1999) Conversion of cucumber linoleate 13-lipoxygenase to a 9-lipoxygenating species by site-directed mutagenesis. *Proc. Natl. Acad. Sci. U.S.A. 96*, 4192–4197.

(46) Coffa, G., Schneider, C., and Brash, A. R. (2005) A comprehensive model of positional and stereo control in lipoxygenases. *Biochem. Biophys. Res. Commun. 338*, 87–92.

(47) Abeysinghe, R. D., Roberts, P. J., Cooper, C. E., MacLean, K. H., Hider, R. C., and Porter, J. B. (1996) The environment of the lipoxygenase iron binding site explored with novel hydroxypyridinone iron chelators. *J. Biol. Chem. 271*, 7965–7972.

(48) Mahesha, H. G., Singh, S. A., and Rao, A. G. A. (2007) Inhibition of lipoxygenase by soy isoflavones: evidence of isoflavones as redox inhibitors. *Archives of Biochemistry and Biophysics 461*, 176–185.

(49) Mogul, R., Johansen, E., and Holman, T. R. (2000) Oleyl sulfate reveals allosteric inhibition of soybean lipoxygenase-1 and human 15-lipoxygenase. *Biochemistry 39*, 4801–4807.

(50) Wecksler, A. T., Kenyon, V., Deschamps, J. D., and Holman, T. R. (2008) Substrate Specificity Changes for Human Reticulocyte and Epithelial 15-Lipoxygenases Reveal Allosteric Product Regulation †. *Biochemistry 47*, 7364–7375.

(51) Wasserman, M. A., Smith, E. F., III, Underwood, D. C., and Barnette, M. A. (1991) Pharmacology and Pathophysiology of 5-Lipoxygenase Products, in *sciencedirect.com*, pp 1–50. Elsevier.

(52) Funk, C. D. (2001) Prostaglandins and leukotrienes: advances in eicosanoid biology. *Science 294*, 1871–1875.

(53) Pallast, S., Arai, K., Wang, X., Lo, E. H., and van Leyen, K. (2009) 12/15-Lipoxygenase targets neuronal mitochondria under oxidative stress. *J. Neurochem. 111*, 882–889.

(54) Park, H.-A., Khanna, S., Rink, C., Gnyawali, S., Roy, S., and Sen, C. K. (2009) Glutathione disulfide induces neural cell death via a 12-lipoxygenase pathway. *Cell Death Differ. 16*, 1167–1179.

(55) Werz, O. (2007) Inhibition of 5-lipoxygenase product synthesis by natural compounds of plant origin. *Planta Med. 73*, 1331–1357.

(56) Werz, O., and Steinhilber, D. (2006) Therapeutic options for 5-lipoxygenase inhibitors. *Pharmacol. Ther. 112*, 701–718.

(57) Piper, P. J., Letts, L. G., Samhoun, M. N., Tippins, J. R., and Palmer, M. A. (1982) Actions of leukotrienes on vascular, airway, and gastrointestinal smooth

muscle. *Adv. Prostaglandin Thromboxane Leukot. Res. 9*, 169–181.

(58) Weichman, B. M., Muccitelli, R. M., Osborn, R. R., Holden, D. A., Gleason, J. G., and Wasserman, M. A. (1982) In vitro and in vivo mechanisms of leukotriene-mediated bronchoconstriction in the guinea pig. *J. Pharmacol. Exp. Ther. 222*, 202–208.

(59) Muccitelli, R. M., Osborn, R. R., and Weichman, B. M. (1983) Effect of inhibition of thromboxane production on the leukotriene D4-mediated bronchoconstriction in the guinea pig. *Prostaglandins 26*, 197–206.

(60) Piper, P. J., and Samhoun, M. N. (1987) Leukotrienes. *British medical bulletin*.

(61) Berkowitz, B. A., Zabko-Potapovich, B., Valocik, R., and Gleason, J. G. (1984) Effects of the leukotrienes on the vasculature and blood pressure of different species. *J. Pharmacol. Exp. Ther. 229*, 105–112.

(62) Lawson, C., Bunting, S., Holzgrefe, H., and Fitzpatrick, F. (1986) Leukotriene B4 and 20-hydroxyleukotriene B4 contract guinea-pig trachea strips in vitro. *J. Pharmacol. Exp. Ther. 237*, 888–892.

(63) Piper, P. J., and Samhoun, M. N. (1982) Stimulation of arachidonic acid metabolism and generation of thromboxane A2 by leukotrienes B4, C4 and D4 in guinea-pig lung in vitro. *Br. J. Pharmacol. 77*, 267–275.

(64) Samuelsson, B., Dahlén, S. E., Lindgren, J. A., Rouzer, C. A., and Serhan, C. N. (1987) Leukotrienes and lipoxins: structures, biosynthesis, and biological effects. *Science 237*, 1171–1176.

(65) Serhan, C. N. (2008) Systems approach with inflammatory exudates uncovers novel anti-inflammatory and pro-resolving mediators. *Prostaglandins Leukot. Essent. Fatty Acids 79*, 157–163.

(66) Trachte, G. J., Lefer, A. M., Aharony, D., and Smith, J. B. (1979) Potent constriction of cat coronary arteries by hydroperoxides of arachidonic acid and its blockade by anti-inflammatory agents. *Prostaglandins 18*, 909–914.

(67) Aharony, D., Smith, J. B., Smith, E. F., III, and Lefer, A. M. (1981) Effects of arachidonic acid hydroperoxides on vascular and non-vascular smooth muscle. *Prostaglandins and Medicine 7*, 527–535.

# Chapter 2

# ATP allosterically activates the human 5-lipoxygenase molecular mechanism of both arachidonic acid and 5(S)-HpETE

## 2.1 Introduction

Human 5-lipoxygenase (5-LOX) is a non-heme iron-containing enzyme responsible for catalyzing the stereospecific and regiospecific peroxidation of natural polyunsaturated fatty acid (PUFA) substrates, specifically converting arachidonic acid (AA) into 5(S)-hydroperoxy-6-trans-8,11,14-cis-eicosatetraenoic acid (5(S)-HpETE).[1,2] 5-LOX shares this hydroperoxidation activity with other lipoxygenases, such as 12-LOX and 15-LOX, although these generate different products with different biological roles in the cell, e.g. 12(S)-HpETE and 15(S)-HpETE, respectively. A unique feature of 5-LOX is the additional catalytic step of converting 5(S)-HpETE into the epoxide-containing leukotriene $A_4$ ($LTA_4$) (Figure 2.1). This biomolecule is the first in a line of highly pro-inflammatory mediators that act as potent chemoattractants and are implicated in a variety of diseases from asthma to cancer.[3-6] Distinguishing the biological role of 5-LOX further, $LTA_4$ can also be shuttled into neighboring cells expressing 12/15-LOX via mechanisms of transcellular biosynthesis.[7,8] Ultimately, $LTA_4$ is converted to a series of anti-inflammatory biomolecules termed lipoxins and resolvins, both of which are important in attenuating chemotaxis and initiating clearance of exudate and cell debris.[9,10]

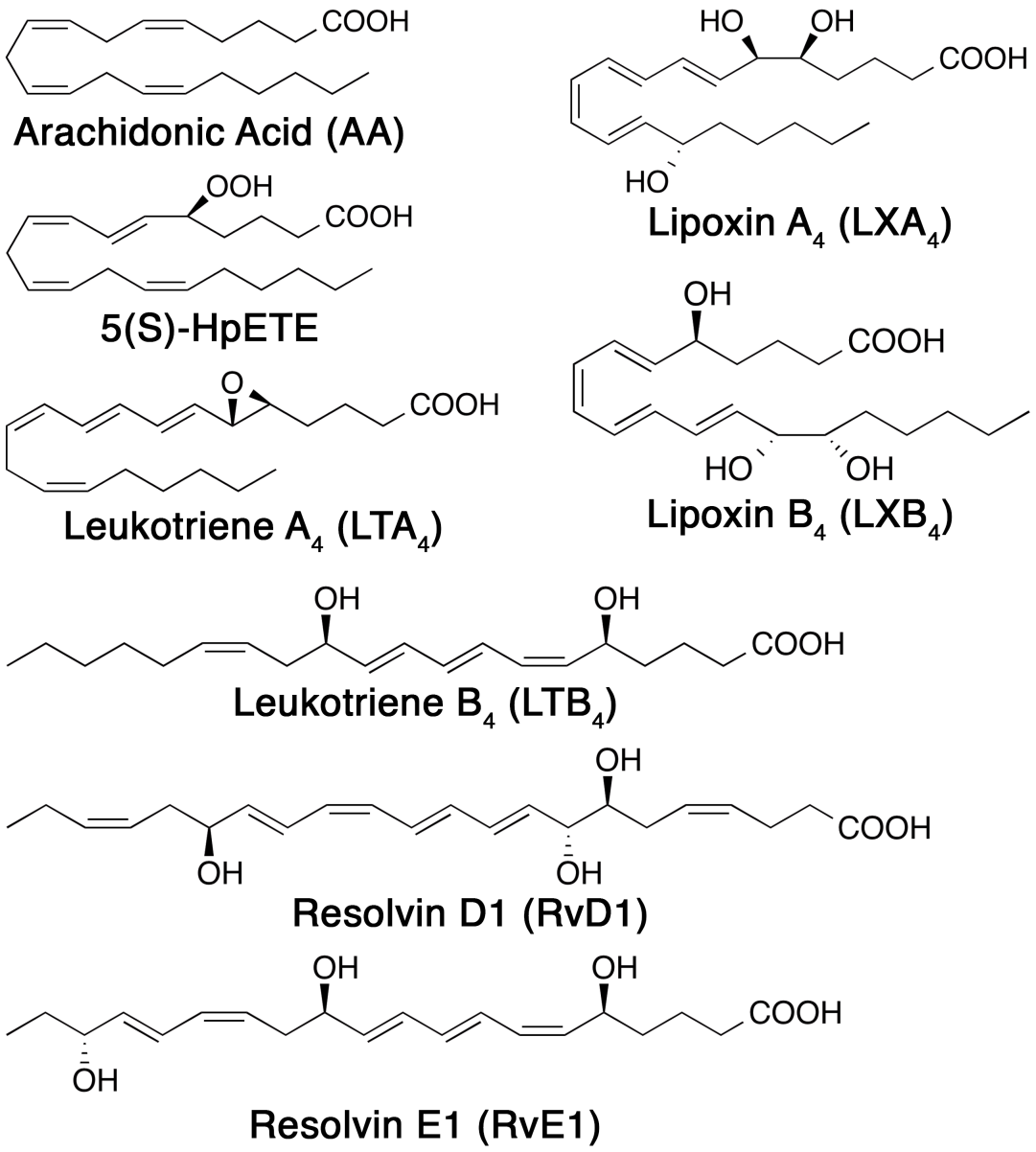


**Figure 2.1.** Important metabolites of inflammation regulation

5-LOX catalytic activity is regulated through several mechanisms by the cell. 5-LOX is recruited to the nuclear membrane upon cellular $Ca^{2+}$ influx. Calcium binds to allosteric sites in the 5-LOX N-terminal polycystin-1/lipoxygenase/alpha-toxin (PLAT) domain, promoting attachment to the membrane via conserved tryptophan residues that embed into the lipid bilayer.[11-13] There is also evidence that magnesium can substitute for calcium in this regard.[14] Membrane association leads to an increased hydroperoxide and leukotriene production.[15,16] 5-LOX must interact with 5-LOX-activating protein (FLAP) to secure PUFA substrates from the nuclear membrane and further promote leukotriene formation *in vivo*.[17,18] Evidence of an additional protein-protein interaction with coactosin-like protein (CLP), an actin binding protein, suggests CLP helps stabilize the membrane-docked 5-LOX and enhances leukotriene formation by 3-fold.[19,20] The fate of $LTA_4$ depends on where 5-LOX is localized in the cell when it is activated to bind the nuclear membrane, a phenomenon referred to as compartmentalization.[21-23] $LTA_4$ can be converted to $LTB_4$ by $LTA_4$ hydrolase, a soluble protein that can localize in the nucleus, or to $LTC_4$ by $LTC_4$ synthase, a membrane-bound protein embedded in the outer leaflet of the nuclear membrane. Compartmentalization implicates the importance of the 5-LOX nuclear localization sequences,[24] which may be further regulated by phosphorylation.[25] Lastly, the ability of 5-LOX to dimerize may provide yet another avenue of enzymatic regulation.[26]

In addition to the calcium-binding allosteric sites, there is an ATP-binding site(s) that contributes to 5-LOX activation.[27-29] Previous studies report a range of 5-

LOX activating potential, from a 5-fold increase in 5-LOX activity[27] to a 25-fold increase in $k_{cat}/K_m$ with $Ca^{2+}$ added,[30] both found in guinea pig peritoneal polymorphonuclear leukocytes (PMNLs). Furthermore, the substrate specificity of 5-LOX is affected by ATP, with the $k_{cat}/K_m$ ratio of AA to eicosapentaenoic acid (EPA) increasing 2-fold.[30] Unfortunately, the ATP-induced activation mechanism has eluded thorough understanding and is often explained with generalized statements, such as extending enzyme stability.[31] The recent crystal structure of Stable-5-LOX, a mutant with a longer half-life than wildtype, gave further impetus for characterizing ATP's effect on 5-LOX since the structural determinants for ATP-induced activation were not obvious from the structure.[32] To expand on what is currently known about ATP-induced activation and the complex set of regulatory controls imposed on 5-LOX activity, our laboratory conducted a detailed investigation of 5-LOX ATP activation.

In this report, we determine that ATP allosteric activation of 5-LOX promotes both 5(S)-HpETE and $LTA_4$ formation by a similar magnitude. ATP induces hyperbolic activation, allowing for the calculation of $K_i$, the strength of ATP binding, α, the change induced in $K_m$, and β, the change induced in $V_{max}$. Further kinetic investigations into the solvent and viscosity effects on product formation reveal changes in microscopic rate constants that promote activation, definitively proving that ATP is an allosteric activator of both hydroperoxidation and epoxidation mechanisms with 5-LOX. Finally, we review the literature on the role of ATP in inflammation and speculate that the ATP-induced allosteric activation of 5-LOX *in vitro* is a potentially relevant modulator of inflammation *in vivo*.

## 2.2 Materials and Methods

### 2.2.1 Ammonium sulfate precipitation of 5-LOX

Recombinant human 5-LOX in a pET21 plasmid was expressed in *E.coli* BL21 (DE3) cells as published previously.[33] Briefly, host cells were grown in LB (100 μg/ml ampicillin) to 0.6 OD at 37 $^{o}$C, at which time they were induced with 0.25 mM IPTG and cooled to 18 $^{o}$C for overnight growth. Cells were then centrifuged at 4700 g for 15 minutes, pelleted into smaller aliquots at 6200 g for 7 minutes, and snap frozen in liquid nitrogen. Frozen cell pellets were resuspended in a nitrogen-sparged, 4 $^{o}$C chilled buffer of 50 mM Hepes, 0.1 mM EDTA, pH 7.5, normalized to 50 mM ionic strength with NaCl (referred to as Buffer A in all subsequent methods). A French pressure cell press was used to lyse cells at 2000 psi, and the resulting lysate centrifuged at 46000 g for 25 min. Ammonium sulfate was added to the supernatant (50% w/v), inverted to mix, centrifuged at 46000 g for 20 minutes, divided into 200 mg aliquots and snap frozen in liquid nitrogen for long-term storage. When needed for enzymatic assays, an aliquot was resuspended in nitrogen-sparged, 4 $^{o}$C chilled Buffer A to a standard concentration and utilized within 3 hours to avoid enzyme degradation due to the inherent instability of 5-LOX.

### 2.2.2 Purification of LOX hydroperoxide and hydroxide enzymatic products

HPLC running solutions were made prior to experiment. Solution A was 99.9% ACN and 0.1% acetic acid; solution B was 99.9% $H_2O$ and 0.1% acetic acid. AA was used to generate 5(S)-HpETE. Two liters of 100 μM PUFA substrate in

Buffer A were reacted with 5-LOX and run to completion as monitored by a sample reaction on a UV/VIS spectrometer, promptly extracted three times with 900 mL total volume of dichloromethane, evaporated to dryness, and reconstituted in MeOH for HPLC purification. Products were injected onto a Higgins Haisil Semi-Preparative (5 μm, 250 × 10 mm) C-18 column with an elution protocol consisting of 3 mL/min isocratic mobile phase of 55% solution A and 45% solution B. Both products were tested using analytical HPLC and LC-MS/MS, demonstrating greater than 90% purity, with the other <10% being hydrolysis products of the hydroperoxide (5-hydroxides and 5-ketones), which were found to be inert when reacted with 5-LOX.

**2.2.3 Steady-state kinetic measurements**

Steady-state kinetic rates were determined by following the formation of the conjugated product at 234 nm ($\varepsilon$ = 27000 $M^{-1}$ $cm^{-1}$ for AA turnover; $\varepsilon$ = 50000 $M^{-1}$ $cm^{-1}$ for 5(S)-HpETE turnover) with a Perkin-Elmer Lambda 40 UV/vis spectrophotometer at room temperature (21 $^{o}$C). All assays were carried out in Buffer A. AA concentrated stock solutions were stored in 95% ethanol, and diluted into buffer so that the total ethanol concentration was less than 1%. Fatty acid concentrations were verified by full turnover with soybean-1 lipoxygenase and quantitating product concentration. Enzymatic reactions were initiated by the addition of approximately 100 to 300 nM ammonium sulfate precipitated wildtype enzyme. The catalytic activity relative to protein weight was measured by observing turnover of a 10 μM solution of AA by the production of 5(S)-HpETE at 234 nm, and was calculated to be ≈ 0.2 abs/sec/mg, or an absolute enzymatic activity of ≈ 60

μmol/min/mg (not standardized to metal content). Activities of all wildtype ammonium sulfate preparations used were within 20% of this value. Assays were 2 mL in volume with substrate concentrations ranging from 1 to 30 μM and were constantly stirred with a rotating magnetic bar. Higher substrate concentrations were avoided to prevent the formation of micelles, which would alter the free substrate concentration.[34] Initial rates (up to the first 20% of the reaction) for each substrate were fitted to the Michaelis-Menten equation using KaleidaGraph (Synergy) and kinetic parameters calculated. Calculation of $V_{max}/K_m$ parameters was done by plotting them as second-order rate constants. All other kinetic parameters (α, β, and $K_i$) were calculated from fitting data to the equations described in *Mogul et al*.[35] and in *Joshi et al*.[36] Each plot comprises data from 3-4 separate experiments and the reported error is the error calculated from non-linear regression. The wild-type 5-LOX from the ammonium sulfate preparation showed no inactivation for the 2 h duration of experiment and no 5(S)-HpETE inhibition was observed for the initial rates of AA catalysis. Finally, it should be noted that the ammonium sulfate preparation, without 5-LOX being present, did not include any fatty acid substrates or impurity proteins with LOX activity.

### 2.2.4 Measurement of the CMC with isothermal titration calorimetry

CMCs were measured as described by *McAuley et al*.[37] A MicroCal VP-ITC Calorimeter was used for data collection. A solution of highly concentrated AA, dissolved in Buffer A, was titrated into a sample cell containing Buffer A only. The final concentration of AA was determined by quantitating product concentration after

full turnover with soybean-1 lipoxygenase, and from this the molar amount of AA added per injection was extrapolated. Experiments were repeated 3 times and the reported error is the S.E.M. of each set of measurements.

### 2.2.5 HPLC determination of the 5(S)-HETE/5,12-DiHETE product ratio

5-LOX prepared by ammonium sulfate precipitation was incubated with 10 μM AA in Buffer A at room temperature (21 $^{o}$C). Enzymatic reactions were quenched with 1% glacial acetic acid (v/v) at varied levels of turnover between 5% and 60%, as determined by UV/vis spectrophotometry. Products were then extracted with dichloromethane, reduced with trimethylphosphite, and evaporated to dryness under nitrogen stream. The products were HPLC purified as described above for hydroperoxide products using a Phenomenex Luna (5 μm, 250 x 4.6 mm) C-18 column and an elution protocol consisting of 1 mL/min isocratic mobile phase of 55% solution A and 45% solution B. The molar amounts of 5(S)-HETE and 5,12-DiHETE were calculated by the corresponding peak areas determined by HPLC and normalized to their respective extinction coefficients, $\varepsilon_{234}$ = 27000 $M^{-1}$ $cm^{-1}$ and $\varepsilon_{280}$ = 50000 $M^{-1}$ $cm^{-1}$.[38,39] Reactions were repeated 12-26 times and the reported error is the S.E.M. of each set of measurements.

### 2.2.6 Structural determination of 5-LOX catalyzed products by LC-MS/MS

LC-MS/MS running solutions were made prior to experiment. Solution A was 99.9% $H_2O$ and 0.1% formic acid; solution B was 99.9% ACN and 0.1% formic acid. Ammonium sulfate precipitated 5-LOX was incubated with 10 μM AA substrate. A 2

mL sample of the reaction was monitored at 234 nm with a Perkin-Elmer Lambda 40 UV/vis spectrophotometer to determine when complete turnover had been reached. Reactions were quenched with 1% glacial acetic acid (v/v), extracted with dichloromethane, reduced with trimethylphosphite, evaporated to dryness, and reconstituted in MeOH. Products were injected onto a Phenomenex Synergi (4 μm, 150 mm x 4.6 mm) C-18 column attached to a Finnigan LTQ liquid chromatography - mass spectrometer (LC-MS/MS). The elution protocol consisted of 200 μL/min, with an isocratic mobile phase of 40% solution A and 60% solution B. The corresponding reduced product ion peak ratio was determined using negative ion MS/MS (collision energy of 35 eV) with the following masses: 5(S)-HETE, parent *m/z* = 319, fragments *m/z* = 115, 203, 129; 5,12-DiHETE, parent *m/z* = 335, fragments *m/z* = 317, 273, and 195.[40,41]

### 2.2.7 $^{18}$O-labeling of PUFA substrates

HPLC running solutions were made prior to experiment. Solution A was 99.9% MeOH and 0.1% acetic acid; solution B was 99.9% $H_2O$ and 0.1% acetic acid. Arachidonoyl chloride and eicosapentaenoyl chloride (>99%) were purchased from Nu-Chek Prep, Inc. $H_2{}^{18}O$ (97%) was purchased from Cambridge Isotope Laboratories. One molar equivalent of acyl chloride substrate was reacted with 15 molar equivalents of $H_2{}^{18}O$ in the presence of dried pyridine for 10 minutes in a nitrogen-sparged flask. Lipids were extracted twice with dichloromethane, evaporated to dryness, and reconstituted in MeOH for HPLC purification. Sample was injected onto a Higgins Haisil Semi-Preparative (5 μm, 250 × 10 mm) C-18 column and eluted

with an isocratic program of 75% solution A and 25% solution B. Substrate purity was calculated to be greater than 99% on an LC-MS/MS, although we measured a range of $^{18}O$ labeling efficiencies from 57% to 78% in different labeling experiments. Isotope ratios of labeled/unlabeled PUFA substrate were used to normalize data.

### 2.2.8 Competitive substrate capture investigations of PUFA and hydroperoxide catalysis

LC-MS/MS running solutions were made prior to experiment. Solution A was 99.9% $H_2O$ and 0.1% formic acid; solution B was 99.9% ACN and 0.1% formic acid. Competitive substrate capture method experiments were performed using a reaction mixture of labeled PUFA substrate and its respective hydroperoxide product ([$^{18}O$]AA/5(S)-HpETE) with a known molar ratio (1:1) and were initiated with ammonium sulfate precipitated 5-LOX in Buffer A in the presence or absence of 200 μM ATP. The ratio of the simultaneous product formation (5,12-[$^{18}O$]dihydroxides and 5,12-dihydroxides) by 5-LOX was determined at a total substrate concentration of 1 μM (substrate limiting conditions). A 2 mL sample of the reaction was monitored at 234 nm with a Perkin-Elmer Lambda 40 UV/vis spectrophotometer to determine time points to achieve ~5% total substrate consumption (~0.05 μM) [27,42]. Reactions were timed and quenched with 1% glacial acetic acid (v/v), extracted with dichloromethane, reduced with trimethylphosphite, evaporated to dryness, and reconstituted in MeOH. Products were injected onto a Phenomenex Synergi (4 μm, 150 mm x 4.6 mm) C-18 column attached to a Finnigan LTQ liquid chromatography - tandem mass spectrometer (LC-MS/MS). The elution protocol consisted of 200

μL/min, with an isocratic mobile phase of 40% solution A and 60% solution B. The corresponding reduced product ion peak ratio was determined using negative ion MS/MS (collision energy of 35 eV) with the following masses: 5,12-DiHETE, parent *m/z* = 335, fragments *m/z* = 317, 273, and 195; 5,12-[$^{18}$O]DiHETE, parent *m/z* = 337, fragments *m/z* = 319, 273, and 197.[40] The ratio of the peak areas for the labeled and unlabeled dihydroxides was then used to determine the $(V_{max}/K_m)^{AA}/(V_{max}/K_m)^{5(S)\text{-}HpETE}$ ratio, modeled after our previous report [42]. Reactions were repeated 14-21 times and the reported error is the S.E.M. of each set of measurements.

**2.2.9 Measurement of solvent isotope effects**

Steady-state kinetics were performed in $H_2O$ and $^2H_2O$ at room temperature (21 $^oC$) as previously described to reveal SIEs.[43,44] Reactions were performed in Buffer A ($H_2O$, pH 7.5) or in the same buffer made with $^2H_2O$ (pH meter reading was 7.1[45]), and all kinetic parameters were determined as described above. A Hewlett-Packard diode-array 8453 UV/vis spectrometer was used to simultaneously observe 5(S)-HpETE and $LTA_4$ formation and thus determine the SIE for either step of catalysis.

**2.2.10 Measurement of viscosity effects**

Steady-state kinetics were performed in the absence or presence of a viscogen (dextrose) at room temperature (21 $^oC$) to reveal any diffusion-linked effects on catalysis as previously described.[44,46] Maltose, sucrose, ethylene glycol, glycerol, and PEG-8000 were also tested as viscogens but all of these inhibited (>50%) enzymatic catalysis and thus were not further used. Reactions were carried out at different relative viscosities ($\eta_{rel} = \eta/\eta_0$, where $\eta_0$ is the viscosity of $H_2O$ at 20 °C) in 25 mM

Hepes, 0.05 mM EDTA, pH 7.5, normalized to 25 mM ionic strength with NaCl. All kinetic parameters were determined as described above in the absence ($\eta_{rel} = 1$) or presence of 1.873 M dextrose ($\eta_{rel} = 3$).

## 2.3 Results and Discussion

### 2.3.1 Steady-state kinetic dependence on ATP and $Ca^{2+}$

Steady-state kinetics of hydroperoxidation with AA demonstrated that the addition of saturating ATP (200 μM) produced a 4.9-fold increase in $V_{max}$ and a nearly 2-fold increase in $V_{max}/K_m$, due to the large increase in $V_{max}$, relative to the small increase in $K_m$ (Table 2.1). The kinetic results indicate that ATP increases the rate of product release more so than substrate capture. These observations are consistent with the ATP activation reported by *Ochi et al.* for 5-LOX purified from guinea pig neutrophils,[27] underscoring a similarity between human and guinea pig 5-LOX isozymes, with respect to ATP activation. It should be noted that *Aharony et al.* observed a decrease in $K_m$ upon addition of $Ca^{2+}$ and ATP, leading to a larger increase in $k_{cat}/K_m$ (25-fold) than we observed.[30] We occasionally saw a decrease in $K_m$ but it was only with a small percentage of our 5-LOX preparations and so we did not consider it relevant. Interestingly, these infrequent preparations of 5-LOX, which demonstrated a decrease in $K_m$, also exhibited substrate inhibition, and manefested artificially lower $K_m$ values. This substrate inhibition was not due to a change in the critical micelle concentration (CMC) for AA because substrate concentrations used were well below the CMC values (CMC = 43 ± 3 μM (no ATP) and 52 ± 1 μM (200 μM ATP)), as measured by isothermal titration calorimetry. In addition, we

| | AA Hydroperoxidation | | | 5(S)-HpETE Epoxidation | | |
|---|---|---|---|---|---|---|
| [ATP] (μM) | Relative $V_{max}$* | $K_m$ (μM) | Relative $V_{max}/K_m$ | Relative $V_{max}$ | $K_m$ (μM) | Relative $V_{max}/K_m$ |
| 0 | 1.0 ± 0.02 | 1.9 ± 0.2 | 0.53 ± 0.05 | 0.33 ± 0.01 | 14 ± 1 | 0.023 ± 0.002 |
| 200 | 4.9 ± 0.3 | 5.3 ± 0.8 | 0.90 ± 0.1 | 1.6 ± 0.09 | 19 ± 2 | 0.090 ± 0.01 |

**Table 2.1.** Steady-state parameters of ammonium sulfate precipitated 5-LOX with ATP. *The relative $V_{max}$ of 5-LOX (ammonium sulfate precipitated) and AA, with no cofactors added, is set to one. All other $V_{max}$ values are standardized to this value and are unitless. $V_{max}$ values with 5(S)-HpETE as a substrate were multiplied by 0.54 to account for the difference in exctinction coefficients between HETE (234 nm) and diHETE (280 nm) products. For comparison to other studies, the absolute kinetic activity of all of our wildtype 5-LOX preparations, without ATP added, were ≈ 60 μmol/min/mg.

confirmed with our 5-LOX preparation that calcium is not required for ATP activation (data not shown), as previously reported with recombinant human 5-LOX, obtained from insect cell expression.[31,47] However, we did notice that calcium slightly diminished the ATP activation (~10%), but the cause of this small reduction in activation is unclear. 1,2-Dimyristoyl-sn-glycero-3-phosphocholine (DMPC), with and without $Ca^{2+}/Mg^{2+}$, also showed no observable kinetic effect on ATP activation. Furthermore, DMPC hindered accurate absorption detection due to its high background absorption and thus it was not included in further experiments (data not shown).

Steady-state kinetics of epoxidation with 5(S)-HpETE demonstrated a 3-fold smaller $V_{max}$ and a 23-fold smaller $V_{max}/K_m$, compared to hydroperoxidation of AA (Table 2.1). This difference in rates was caused by a nearly 10-fold larger $K_m$ measured for 5(S)-HpETE. These results highlight a prominent difference between AA and 5(S)-HpETE in their rate of substrate capture and suggest that leukotriene formation could occur more readily from sequential steps of hydroperoxidation and then epoxidation with the same molecule of AA (*vide infra*) (Scheme 2.1). The addition of saturating ATP (200 μM) produced a 4.8-fold increase in $V_{max}$ with 5(S)-HpETE as substrate, which was identical to the magnitude of activation seen for AA hydroperoxidation (Table 2.1). In contrast, ATP induced a nearly 4-fold increase in $V_{max}/K_m$, which indicates a 2-fold greater ATP-induced activation of $V_{max}/K_m$ for 5(S)-HpETE epoxidation relative to AA hydroperoxidation, and demonstrates a distinction in the ATP activation mechanism for epoxidation and hydroperoxidation. Due to this

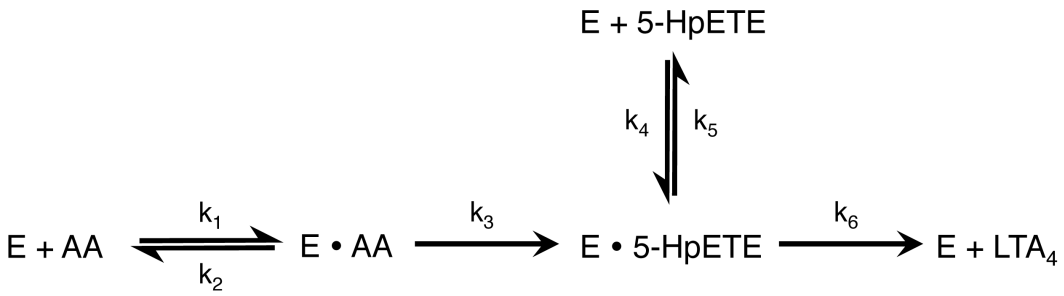


**Scheme 2.1.** 5-LOX catalysis proceeds with hydroperoxidation of AA to 5(S)-HpETE and either product release or subsequent epoxidation to $LTA_4$. Kinetic pathways involved in 5-LOX catalyzed formation of $LTA_4$ from AA, originally published by *Wiseman et al.*[38]

observed difference, more extensive investigations were realized in order to understand ATP activation in more detail (*vide infra*).

### 2.3.2 Effect of ATP-induced activation on hydroperoxide retention and epoxide formation

As described above, ATP activates both AA hydroperoxidation and 5(S)-HpETE epoxidation. However, it is unclear if the epoxidation reaction affects the rate of hydroperoxidation due to the consumption of the hydroperoxidation substrate, 5(S)-HpETE and/or production of the 5,6-epoxide. The kinetic data above would suggest that 5(S)-HpETE production does not affect the rate of AA hydroperoxidation due to its low rate. To confirm this conclusion, a diode-array UV/vis spectrophotometer was used to observe both 5(S)-HpETE (234 nm) and $LTA_4$ (280 nm) formation simultaneously from 0 to 20% product formation, to determine if slight changes in the 5(S)-HpETE concentration could affect the rate of either hydroperoxide or epoxide formation. The $LTA_4$/5(S)-HpETE ratio of products (the efficiency of epoxide formation) was calculated throughout the reaction and observed to remain constant up to 20% product formation ($LTA_4$/5(S)-HpETE ratio = 0.161 ± 0.004, Figure 2.2). This value increases to a constant value of 0.247 ± 0.005 up to 20% product formation, with the addition of 200 μM ATP (Figure 2.2) and matches the value determined for rat PMNL 5-LOX.[38] In addition, 5(S)-HETE and 5,12-DiHETE concentrations were quantified through HPLC and comparable product ratios were observed (0.19 ± 0.02 (no ATP) and 0.25 ± 0.02 (200 μM ATP)), confirming the accuracy of the dual wavelength assay (Figure 2.2). These data

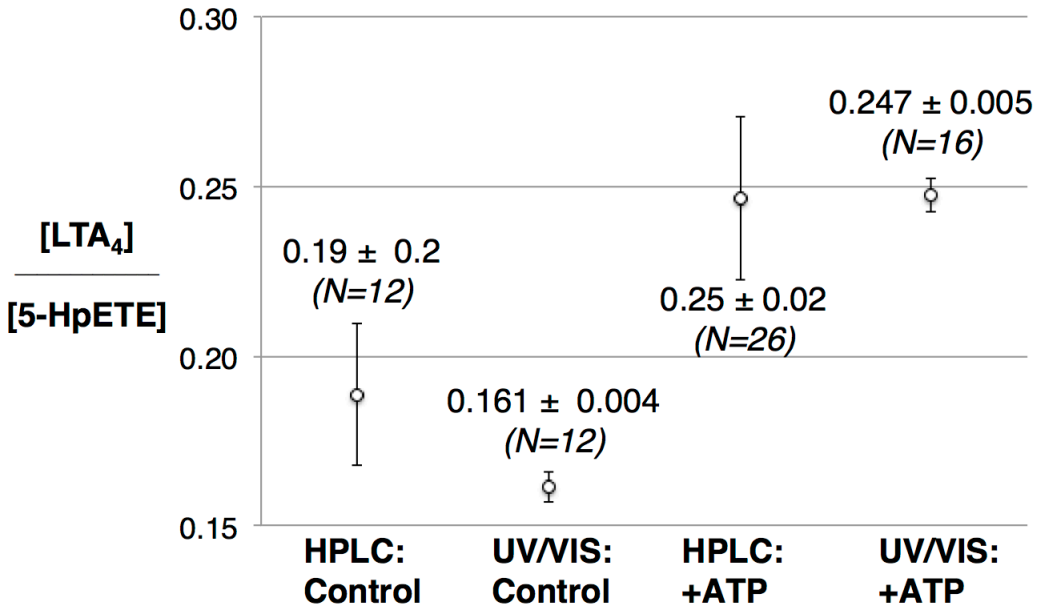


**Figure 2.2**. Effect of 200 μM ATP on the efficiency of epoxide formation. [$LTA_4$] / [5(S)-HpETE] turnover ratio from 10 μM AA substrate as measured by HPLC and UV/vis spectrophotometry. [$LTA_4$] was measured at 280 nm, [5(S)-HpETE] was measured at 234 nm, and both were normalized to their respective extinction coefficients. The absolute kinetic activity of wildtype 5-LOX ammonium sulfate preparations was ≈ 60 μmol/min/mg.

confirm the hypothesis that the consumption of 5(S)-HpETE, or the production of the 5,6-epoxide, does not affect the rates of either hydroperoxidation or epoxidation.

### 2.3.3 Hyperbolic activation of 5-LOX by ATP

In order to compare the allosteric effect of ATP activation for AA hydroperoxidation and 5(S)-HpETE epoxidation in more detail, extensive allosteric titrations were performed (Table 2.2). From the data, it was observed that 5-LOX and AA exhibited a hyperbolic response to increasing amounts of ATP with an increase in $K_m$ (app) from 1.9 ± 0.2 μM to 5.3 ± 0.8 μM and an increase in $V_{max}/K_m$ (app) from 0.53 ± 0.05 to 0.9 ± 0.1. The saturation behavior of $K_m$ (app) and $V_{max}/K_m$, with AA as the substrate, is indicative of hyperbolic activation (i.e. partial activation). Similar hyperbolic allostery has been observed for other LOX isozymes with different allosteric regulators, such as soybean 15-LOX-1 with oleyl sulfate[35] and human 15-LOX-2 with 13(S)-HODE.[36] These data indicate the presence of an allosteric binding site in 5-LOX that affects the catalysis by changing the microscopic rate constants of 5-LOX, as described in Scheme 2.2. From Scheme 2.2, equations 1-4 allow for the determination of $K_i$, the strength of binding, α, the change in $K_m$, β, the change in $V_{max}$ and β/α, the change in $V_{max}/K_m$.

$$1/v = (\alpha K_m/V_{max})*[([I] + K_i)/(\beta[I] + \alpha K_i)]*1/[S] + 1/V_{max}*[([I] + \alpha K_i)/(\beta[I] + \alpha K_i)] \quad (1)$$

$$K_m \text{ (app)} = (\alpha K_m)*[([I] + K_i)/([I] + \alpha K_i)] \quad (2)$$

$$V_{max}/K_m \text{ (app)} = (V_{max}/\alpha K_m)*[(\beta[I] + \alpha K_i)/([I] + K_i)] \quad (3)$$

$$V_{max} \text{ (app)} = V_{max}*[(\beta[I] + \alpha K_i)/([I] + \alpha K_i)] \quad (4)$$

| Substrate | α | β | β / α | $K_i$ (μM) |
|---|---|---|---|---|
| AA | 3.0 ± 0.4 | 5.4 ± 0.08 | 1.8 ± 0.2 | 8.0 ± 6 |
| 5(S)-HpETE | 1.6 ± 0.08 | 5.1 ± 0.1 | 3.3 ± 0.2 | 12 ± 5 |

**Table 2.2.** Kinetic parameters for ATP-induced activation of 5-LOX Hyperbolic fit parameters of 5-LOX with ATP and AA or 5(S)-HpETE as substrates

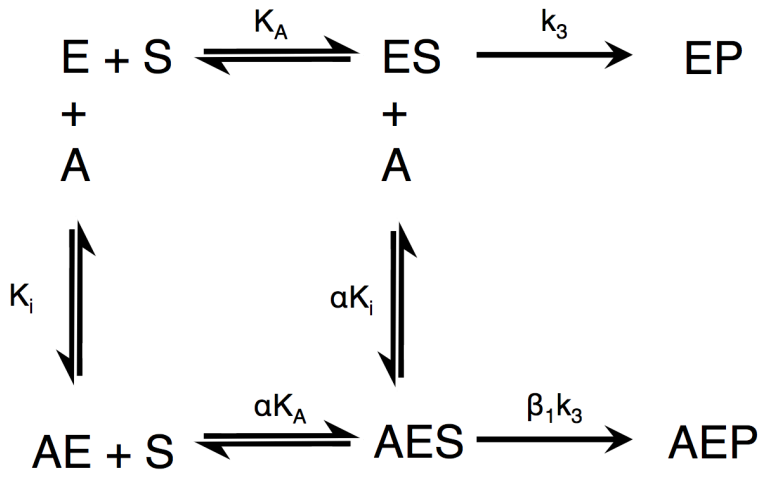


**Scheme 2.2.** 5-LOX catalysis including hyperbolic partial activation induced by ATP. Similar hyperbolic allostery has been observed for other LOX isozymes with different allosteric regulators, such as soybean 15-LOX-1 with oleyl sulfate[35] and human 15-LOX-2 with 13(S)-HODE.[36]

A plot of $K_m$ (app) versus ATP concentration, with AA as the substrate (Figure 2.3) yielded an α of 3.0 ± 0.4 and a $K_i$ of 8 ± 6 μM, when fitted with equation 2. The values of α and $K_i$ were then utilized in equation 3 and fit to the $V_{max}/K_m$ data, which yielded a β of 5.5 ± 0.5. The value of β was also determined from the $V_{max}$ data (fitted with equation 4 and the above values of α and $K_i$), which yielded a β of 5.4 ± 0.08 (Figure 2.4) and matched well with the β value from the $V_{max}/K_m$ plot. These values indicate mixed hyperbolic allostery, α > 1 (K-type inhibition) and β > 1 (V-type activation),[48] with the majority of kinetic change being seen in the value of $V_{max}$. This $V_{max}$ allosteric effect is best observed the $V_{max}/K_m$ value, which is greater than 1 (β/α = 1.8 ± 0.2) and indicates $V_{max}/K_m$ allosteric activation. These hyperbolic data suggest the formation of a catalytically active ternary complex (A□E□S) between 5-LOX and ATP and are consistent with previous finding of an allosteric site in 5-LOX.[31,49]

Similar ATP titration experiments were also performed with 5(S)-HpETE as substrate, which showed an α value of 1.56 ± 0.08 (K-type inhibition) and a $K_i$ value of 12 ± 5 μM from the $K_m$ (app) plot (Figure 2.5). The α value was half that of the α value for AA activation, indicative of a weaker ATP allosteric effect on $K_m$ with 5(S)-HpETE as the substrate. However, the $K_i$ value was comparable to that of AA activation, indicating similar ATP binding affinities and most likely the same binding site. The β value was determined to be 5.1 ± 0.1 (Figure 2.6), which is V-type activation, similar to that seen for AA. The β/α ratio is nearly 2-fold greater for 5(S)-HpETE (3.3 ± 0.2) than for AA (1.8 ± 0.2), indicating that ATP activates the rate of

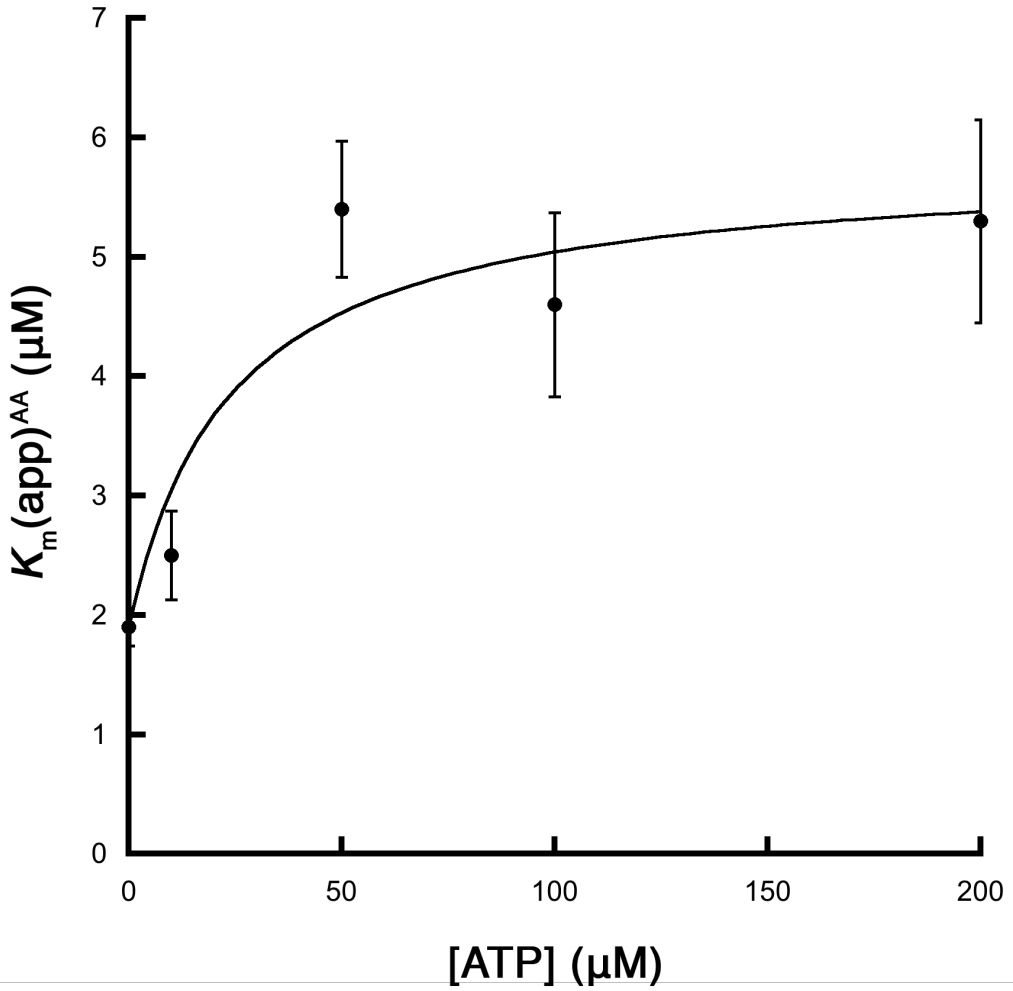


**Figure 2.3**. Effect of ATP on the $K_m$ (app) of 5-LOX with AA substrate. The data are fit to eq 2 (Scheme 2.2), where $K_m$ = 1.9 μM. α and $K_i$ were determined to be 3.0 ± 0.4 and 8 ± 6 μM, respectively.

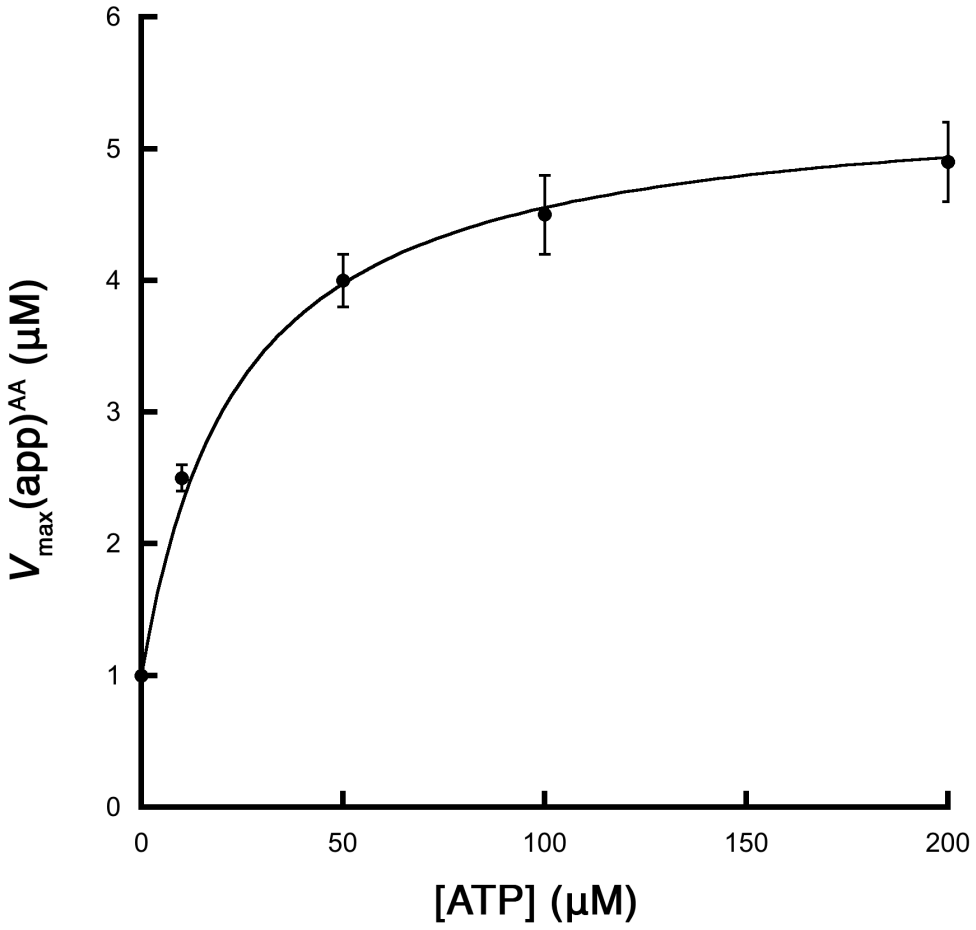


**Figure 2.4**. Effect of ATP on the $V_{max}$ (app) of 5-LOX with AA substrate. The data are fit to eq 4 (Scheme 2.2) with $K_m$ = 1.9 μM, α = 3.0, and $K_i$ = 8, where β was determined to be 5.41 ± 0.08.

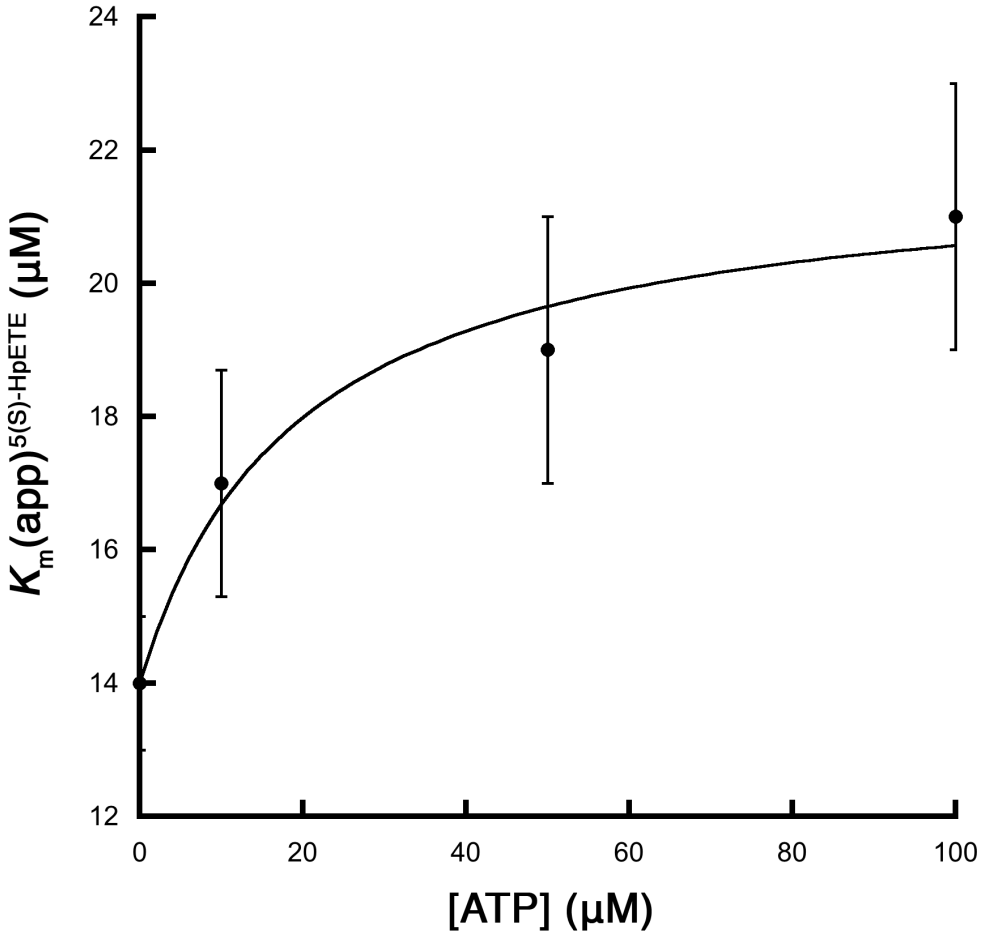


**Figure 2.5**. Effect of ATP on the $K_m$ (app) of 5-LOX with 5(S)-HpETE substrate. The data are fit to eq 2 (Scheme 2.2), where $K_m$ = 14 μM. α and $K_i$ were determined to be 1.56 ± 0.08 and 12 ± 5 μM, respectively.

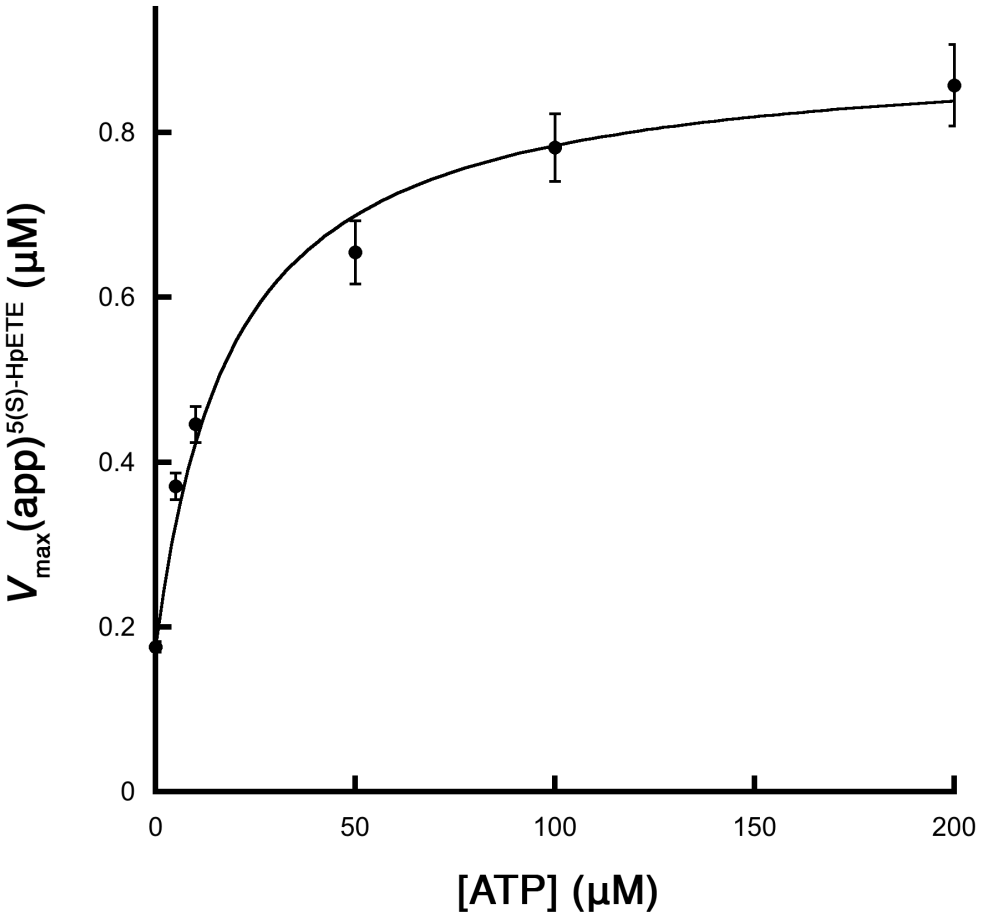


**Figure 2.6**. Effect of ATP on the $V_{max}$ (app) of 5-LOX with 5(S)-HpETE substrate. The data are fit to eq 4 (Scheme 2.2) with $K_m$ = 14 μM, α = 1.56, and $K_i$ = 12, where β was determined to be 5.1 ± 0.1.

substrate capture for 5(S)-HpETE more so than AA. These results agree with our kinetic results (Table 2.1), suggesting that the allosteric structural effect caused by ATP binding has related but altered consequences for the two substrates and thus for the two processes, hydroperoxidation and epoxidation.

### 2.3.4 Endogenous and exogenous rates of epoxide formation

As mentioned above, 5-LOX can produce $LTA_4$ from AA or from 5(S)-HpETE directly. To better understand the differences of endogenous 5(S)-HpETE (*in situ* generated) epoxidation versus exogenous 5(S)-HpETE epoxidation, steady-state experiments with AA and 5(S)-HpETE were performed by indirectly observing the formation of the epoxide by measuring its decomposition product (5,12-diHETE) at 280 nm (Table 2.3). The epoxidation $V_{max}$ for both substrates was the same, which is an expected result since 5-LOX abstracts the same hydrogen atom from C10 of 5(S)-HpETE, regardless if the 5(S)-HpETE is endogenous or exogenous. However, the epoxidation of endogenous 5(S)-HpETE was found to have a nearly 10-fold larger $V_{max}/K_m$ than the epoxidation of exogenous 5(S)-HpETE, due to a nearly 10-fold smaller $K_m$. These data indicate that the nature of the rate-limiting step for substrate capture changes depending on whether 5(S)-HpETE is made endogenously or exogenously. Two possible explanations for this data are either that diffusion is a rate-limiting step or that a slow rearrangement step is required for exogenous 5(S)-HpETE, both possible steps being avoided if endogenously produced 5(S)-HpETE is already positioned in the active site properly. Interestingly, saturating ATP (200 μM) activated the $V_{max}$ of epoxidation of endogenous 5(S)-HpETE more so than

| | AA Epoxidation | | | 5(S)-HpETE Epoxidation | | |
|---|---|---|---|---|---|---|
| [ATP] (μM) | Relative $V_{max}$* | $K_m$ (μM) | Relative $V_{max}/K_m$ | Relative $V_{max}$ | $K_m$ (μM) | Relative $V_{max}/K_m$ |
| 0 | 1.0 ± 0.05 | 1.6 ± 0.3 | 0.6 ± 0.1 | 1.1 ± 0.1 | 15 ± 4 | 0.07 ± 0.01 |
| 200 | 6.3 ± 0.3 | 4.5 ± 0.7 | 1.4 ± 0.2 | 4.6 ± 0.3 | 21 ± 3 | 0.22 ± 0.01 |

**Table 2.3.** Steady-state parameters of ammonium sulfate precipitated 5-LOX with ATP. *The relative $V_{max}$ of 5-LOX (ammonium sulfate precipitated) and AA, with no cofactors added, is set to one. All other $V_{max}$ values are standardized to this value and are unitless. For comparison to other studies, the absolute kinetic activity of all of our wildtype 5-LOX preparations, without ATP added, were ≈ 60 μmol/min/mg.

exogenous 5(S)-HpETE (6-fold versus 4-fold, respectively), but ATP activated the $V_{max}/K_m$ of epoxidation of exogenous 5(S)-HpETE more so than endogenous 5(S)-HpETE (3-fold versus 2-fold, respectively). Clearly, allosteric activation by ATP is distinct, depending on the source of 5(S)-HpETE. Enhanced activation of $V_{max}/K_m$ for epoxidation may arise from the fact that epoxidation requires an easier substrate rearrangement step due to a postulated suprafacial homolytic cleavage of the hydroperoxide relative to iron.[50] In contrast, hydroperoxidation requires larger rearrangement of the substrate after antarafacial di-oxygen attack so that the iron can transfer a hydrogen atom back to the oxygen radical (Scheme 2.3).

### 2.3.5 Competitive substrate capture investigations of AA/5(S)-HpETE catalysis

To further investigate the kinetics of AA and 5(S)-HpETE catalysis, a competitive substrate capture experiment was performed with a mixture of [$^{18}$O]AA (0.5 μM) and unlabeled 5(S)-HpETE (0.5 μM). The results without ATP demonstrated that the amount of 5,12-DiHETEs produced from [$^{18}$O]AA was larger than those produced from exogenous 5(S)-HpETE, with a measured $(V_{max}/K_m)^{AA}/(V_{max}/K_m)^{5(S)\text{-HpETE}}$ epoxide efficiency ratio of 1.8 ± 0.06. These results confirm the steady-state results (*vide supra*) that 5-LOX is more likely to retain the nascent 5(S)-HpETE in its active site than bind exogenous 5(S)-HpETE in order to generate the epoxide, however the magnitude is different. The steady-state results indicate a $(V_{max}/K_m)^{AA}/(V_{max}/K_m)^{5(S)\text{-HpETE}}$ ratio of 8.6. The competitive experiment was repeated with saturating ATP (200 μM) and the $(V_{max}/K_m)^{AA}/(V_{max}/K_m)^{5(S)\text{-HpETE}}$

ratio increased to 2.2 ± 0.06, indicating an increase in the epoxide efficiency of AA conversion, relative to 5(S)-HpETE conversion. This is in contrast to the steady-state $(V_{max}/K_m)^{AA}/(V_{max}/K_m)^{5(S)\text{-HpETE}}$ ratio, which decreases from 8.6 to 6.4 with the addition of ATP. These differences between the two methods could be due to the fact that the competitive measurements were performed with both substrates present, while the steady-state experiments only had one substrate at a time. As seen previously for 15-LOX-1 and 15-LOX-2, [35,36] differences between competitive and steady-state measurements can be indicative of allosteric effects by either the substrate or product. Therefore, while these data confirm that the majority of $LTA_4$ produced by 5-LOX is made from AA and not 5(S)-HpETE, additional experiments are required to investigate why the two methods do not correlate. It should be noted that *Puustinen et al.* observed a $(V_{max}/K_m)^{AA}/(V_{max}/K_m)^{5(S)\text{-HpETE}}$ epoxide efficiency ratio of approximately 3.2 for 5-LOX from human leukocyte homogenate, with ATP being present,[51] while *Wiseman et al.* measured a $(V_{max}/K_m)^{AA}/(V_{max}/K_m)^{5(S)\text{-HpETE}}$ ratio of 32 ± 1 for 5-LOX from rat PMNLs in the presence of ATP,[38], indicating a possible difference between species.

### 2.3.6 Solvent effects of the hydroperoxidation and epoxidation kinetics

The mechanism of hydroperoxidation for soybean 15-LOX,[45,52] human 12-LOX,[43,44] human 15-LOX-1[43,44] and human 15-LOX-2[46] has been shown previously to manifest multiple rate-limiting steps, defined by substrate diffusion, hydrogen bond rearrangement and hydrogen atom abstraction. However, the mechanisms employed by 5-LOX for hydroperoxidation and epoxidation are less well understood (Scheme

2.1).[30,38] The 5-LOX mechanism for hydroperoxidation has historically been assumed to be similar to that of other lipoxygenases,[53] but with little experimental evidence. The epoxidation reaction is also proposed to proceed through a hydrogen atom abstraction mechanism, similar to that of hydroperoxidation,[50] which is supported by a large primary kinetic isotope effect of >10,[6,54,55] and inhibition of $LTA_4$ formation by reductive inhibitors.[4] With respect to ATP activation, it is unclear if molecular steps in the reaction coordinate for either hydroperoxidation or epoxidation (Scheme 2.3) are accelerated, or if activation proceeds through an alternative process that does not affect the catalytic mechanism, such as protein stabilization.[31]

In this current work, hydroperoxidation kinetic studies of AA in the absence of ATP revealed a normal solvent isotope effect (SIE) for $V_{max}$ [AA] (1.8 ± 0.2) and an inverse SIE for $V_{max}/K_m$[AA] (0.66 ± 0.3) (Table 2.4). Under ATP activation (200 μM ATP), the normal SIE increased for $V_{max}$ [AA] to 3.1 ± 0.6, while the inverse SIE for $V_{max}/K_m$[AA] changed to a normal SIE of 1.8 ± 0.6, demonstrating that ATP affects the molecular mechanisms of both substrate capture and product release. In general, SIE values of 2 to 3 typically correspond to general acid/base catalysis, while solvation of catalytic bridges range from 1.5 to 4.[57,58] Previous studies of LOX isozymes[43-46,52] attribute their observed SIE results to a solvent-dependent hydrogen transfer from multiple hydrogen bond rearrangements, presumably due to an enzymatic conformational change upon substrate binding. Interestingly, although all four LOX isozymes manifested SIEs, their magnitude and temperature dependence varied, indicating subtle differences in their rate-limiting steps. For 5-LOX, the

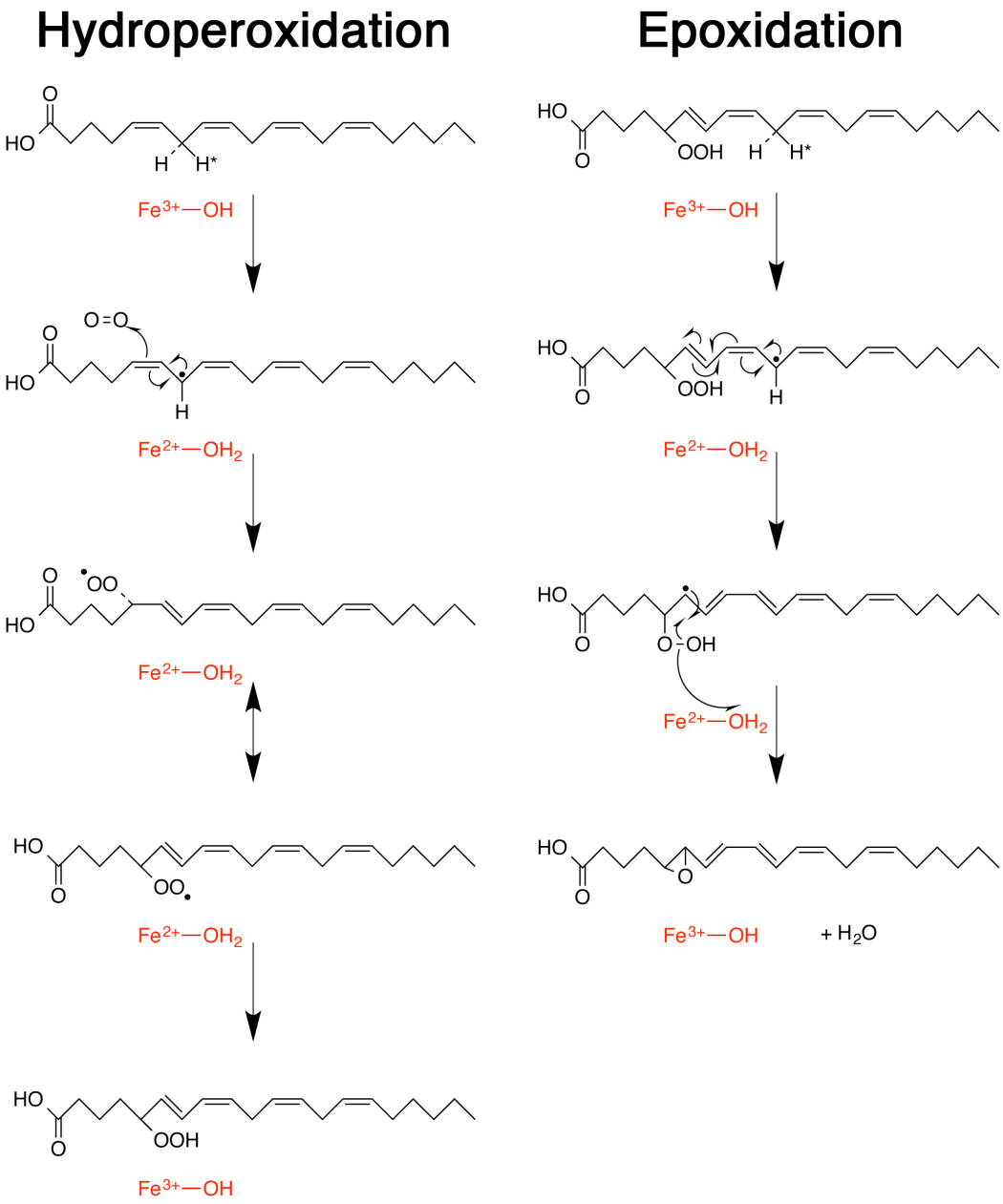


**Scheme 2.3.** Detailed scheme of hydroperoxidation and epoxidation. Hydroperoxidation proceeds after initial abstraction of pro-S hydrogen at C7, whereas epoxidation proceeds after abstraction of pro-R hydrogen at C10.[54] The antarafacial nature of hydroperoxidation is well known,[31,45,56] while a suprafacial arrangement for epoxidation is postulated by *Jin et al*.[50]

| | AA Hydroperoxidation (234 nm) | | 5(S)-HpETE Epoxidation (280 nm) | |
|---|---|---|---|---|
| [ATP] (μM) | $V_{max}$ SIE | $V_{max}/K_m$ SIE | $V_{max}$ SIE | $V_{max}/K_m$ SIE |
| 0 | 1.8 ± 0.2 | 0.66 ± 0.3 | 0.81 ± 0.1 | 0.49 ± 0.09 |
| 200 | 3.1 ± 0.6 | 1.8 ± 0.6 | 2.6 ± 0.3 | 1.2 ± 0.2 |

**Table 2.4.** SIEs for 5-LOX catalysis with AA or 5(S)-HpETE as a substrate. Solvent isotope effect values for hydroperoxidation of AA and epoxidiation of 5(S)-HpETE.

magnitude of the normal SIE for both $V_{max}$[AA] and $V_{max}/K_m$[AA], with ATP added, indicates a hydrogen bond rearrangement step (i.e. general conformational change), similar to that seen for other LOX isozymes. The increase in the normal $V_{max}$ SIE value, with addition of ATP, indicates that the solvent dependence of the rate-limiting step increases with added ATP and that the activation of 5-LOX by ATP is in part due to a change in its microscopic rate constants. It should be noted that lower values of SIE (below 1.5) are typically ascribed to proton transfer coupled to heavy atom motion in the transition state[59] or to increased viscosity of $D_2O$ relative to $H_2O$.[60] These are unlikely explanations for our data, given their larger SIE values.

In contrast to the $V_{max}$ SIE, the $V_{max}/K_m$ of AA manifests an inverse SIE without ATP (SIE = 0.66 ± 0.3), which becomes a normal SIE (SIE = 1.80 ± 0.61) upon ATP addition. Previously, our laboratory observed inverse SIE values for both $V_{max}$ and $V_{max}/K_m$ for a soybean 15-LOX mutant[61] and wild-type 15-LOX-2,[46] which was ascribed to the participation of a ferric-hydroxide in the abstraction of the hydrogen atom. It is possible that the observed inverse SIE for 5-LOX with AA is also due to the ferric-hydroxide moiety, however due to its large error, it is difficult to state this with certainty. Nonetheless, the change to a normal SIE upon ATP addition is significant and indicates a shift in the nature of the rate-determining step, possibly from a dependence on the ferric hydroxide to a dependence on hydrogen-bond rearrangement. It should be noted that $V_{max}/K_m$ includes the bimolecular encounter of substrate and enzyme, up to the first irreversible step (hydrogen atom abstraction), but $V_{max}$ includes steps after the enzyme substrate complex formation, and therefore the

SIE observed for $V_{max}$ and $V_{max}/K_m$ could be from the same step or from different steps.

Identical solvent dependence studies, with 5(S)-HpETE as a substrate, were also performed (Table 2.4). Interestingly, the $V_{max}$ SIE for 5(S)-HpETE epoxidation was markedly different than that for AA ($V_{max}$ SIE = 0.8 ± 0.1). This result clearly demonstrates an inverse SIE for 5(S)-HpETE epoxidation and indicates the participation of the ferric-hydroxide in the hydrogen abstraction mechanism as a contributor to the rate-limiting step (*vide infra*). Adding ATP, with 5(S)-HpETE as the substrate, increased the epoxidation SIE to 2.6 ± 0.3. This increase in SIE is nearly identical to that with AA as a substrate, showing that both processes, AA hydroperoxidation and 5(S)-HpETE epoxidation, display an ATP-induced increase in SIE, suggesting a shift in their rate-limiting step to being more dependent on hydrogen bond rearrangement and less on the hydrogen atom abstraction by the Fe(III)-OH moiety.

For the $V_{max}/K_m$ data, the 5(S)-HpETE epoxidation SIE is 0.49 ± 0.09. This value is similar to that seen previously for AA hydroperoxidation (SIE = 0.66 ± 0.3), and indicates that the rate-limiting step of $V_{max}/K_m$, for both AA hydroperoxidation and 5(S)-HpETE epoxidation, is dominated by the hydrogen-atom abstraction of the Fe(III)-OH moiety. Adding ATP, the 5(S)-HpETE epoxidation SIE increased to 1.2 ± 0.2, similar to the increase seen for the AA hydroperoxidation (SIE = 1.8 ± 0.6). However, given the small magnitude of the SIE, the resultant SIE could be due to either offsetting SIE effects (inverse SIE from the Fe(III)-OH and normal SIE from

hydrogen-bond rearrangement) or the complete loss of the rate-limiting step's dependency on solvent. More information is needed to distinguish between these two hypotheses, and is beyond the scope of the present work.

In summary, the above results indicate that the ATP-induced allosteric effect on hydroperoxidation and epoxidation changes the solvent dependency of the rate-limiting step, which cannot be explained by an ATP-induced stabilization of the 5-LOX protein structure.[31] We could not determine if ATP also affects the rate of hydrogen atom abstraction, since isotopically labeled AA was not available to us. However, the increase in the magnitude of the normal SIE for $V_{max}$, as well as the change to a normal $V_{max}/K_m$ SIE with the addition of ATP, is suggestive of a shift in the rate-limiting step towards hydrogen bond rearrangement relative to hydrogen atom abstraction for both hydroperoxidation and epoxidation.

### 2.3.7 Viscosity effects of the hydroperoxidation and epoxidation kinetics

To further probe the nature of the rate-limiting step, viscosity experiments ($\eta/\eta^\circ$ = 1 and 3) were performed in the absence and presence of 200 μM ATP (Table 2.5). The $(V_{max}/K_m^\circ)/(V_{max}/K_m)$ for AA substrate was calculated to be 1.5 ± 0.3 without ATP and 1.2 ± 0.2 with ATP, where $V_{max}/K_m^\circ$ has an $\eta/\eta^\circ$ of 1 and $V_{max}/K_m$ has an $\eta/\eta^\circ$ of 3. These data indicate that the rate of substrate capture is not diffusion controlled, with or without ATP. However, it is interesting to note that $V_{max}^\circ/V_{max}$ increased from 1.0 ± 0.1 to 1.6 ± 0.2 upon ATP activation. Since there is no viscosity effect seen for $V_{max}/K_m$, this data is best explained by decreased translational diffusion

| | AA Hydroperoxidation (234 nm) | | 5(S)-HpETE Epoxidation (280 nm) | |
|---|---|---|---|---|
| [ATP] (μM) | $V_{max}°/V_{max}$ | $(V_{max}/K_m°)$ / $(V_{max}/K_m)$ | $V_{max}°/V_{max}$ | $(V_{max}/K_m°)$ / $(V_{max}/K_m)$ |
| 0 | 1.0 ± 0.1 | 1.5 ± 0.3 | 1.0 ± 0.2 | 0.65 ± 0.1 |
| 200 | 1.6 ± 0.2 | 1.2 ± 0.2 | 1.3 ± 0.2 | 1.6 ± 0.4 |

**Table 2.5.** Viscosity effects for 5-LOX catalysis with AA or 5(S)-HpETE as a substrate

rates and/or conformational changes upon substrate binding,[62-64] the latter being consistent with the SIE results.

In contrast to the viscosity effect with AA as substrate, an inverse viscosity effect can be seen on $V_{max}/K_m$ with 5(S)-HpETE as the substrate ($(V_{max}/K_m°)/(V_{max}/K_m) = 0.65 \pm 0.1$). Considering there is no viscosity effect observed under the same conditions for the faster reaction of 5-LOX and AA, the inverse viscosity effect on $V_{max}/K_m$ with 5(S)-HpETE clearly arises through a different mechanism. A change in the dielectric environment[65] could result in an inverse effect, but the dielectric constant of water (~80) is reduced by only 10% with the addition of 30% by mass dextrose[66]. Moreover, the finding that this inverse viscosity effect is removed by the addition of ATP also suggests dielectric constants are not inducing the effect. Experiments with PEG-8000 were attempted to confirm that the viscosity effect is independent of a change in dielectric constants, but unfortunately PEG was observed to inactivate 5-LOX and thus no conclusion was possible (data not shown). The only other conclusion is that inverse viscosity effect on $(V_{max}/K_m°)/(V_{max}/K_m)$ is most likely due to a partially rate-determining conformational change during catalysis.[60] This is supported by the fact that the SIE results also indicate a conformational change. Upon addition of ATP, the $(V_{max}/K_m°)/(V_{max}/K_m)$ viscosity effect with 5(S)-HpETE as substrate becomes $1.6 \pm 0.4$. Given the slow rate of 5(S)-HpETE epoxidation relative to AA hydroperoxidation, and the fact that no viscosity effect was seen for AA hydroperoxidation, the normal viscosity effect on 5(S)-HpETE $V_{max}/K_m$ induced by

ATP is most likely not due to a diffusion-controlled mechanism. Therefore, the small $(V_{max}/K_m°)/(V_{max}/K_m)$ viscosity effect with ATP may possibly be due to a conformational change during catalysis. The $V_{max}°/V_{max}$ viscosity effect did not change upon ATP addition (1.0 ± 0.2 to 1.3 ± 0.2), indicating diffusion is not rate-limiting, with or without ATP. Future experiments are needed to further press into these kinetic possibilities.

**2.4 Conclusions**

It has been known in the literature for many years that 5-LOX has two catalytic functions, hydroperoxidation of AA and epoxidation of 5(S)-HpETE, but a detailed kinetic investigation comparing these two processes has never been undertaken. In the current work, we demonstrate that the $V_{max}$ of epoxidation is 3-fold slower than the $V_{max}$ of hydroperoxidation and that the $V_{max}/K_m$ is 23-fold slower, indicating that the rate of substrate capture is markedly less efficient for epoxidation relative to hydroperoxidation. However, if one measures the rate of epoxidation on the endogenous 5(S)-HpETE (i.e. 5(S)-HpETE generated *in situ* from AA), one observes that the rate of $V_{max}/K_m$ is nearly 10-fold larger compared to exogenous 5(S)-HpETE epoxidation (i.e. not generated from AA), while their $V_{max}$ values are the same. These results indicate that 5-LOX has overcome a significant catalytic barrier during the process of 5(S)-HpETE capture by retaining the 5(S)-HpETE in its active site for subsequent epoxidation, possibly by avoiding a costly structural rearrangement. In the recently solved crystal structure for human 5-LOX, a unique FY cork feature is observed that blocks the entrance to the active site.[32] We

hypothesize that this FY cork could be the source of this structural rearrangement, highlighting future research directions for studying the epoxidation mechanism.

Along this same line of investigation, we determined the allosteric ATP activation of hydroperoxide and epoxide (leukotriene) formation for 5-LOX and found that ATP activates the $V_{max}$ of AA 4.9-fold and the $V_{max}$ of 5(S)-HpETE by a similar degree (4.8-fold). However, ATP activates the $V_{max}/K_m$ to a lesser extent (1.7-fold for AA and 3.9-fold for 5(S)-HpETE), indicating ATP may enhance distinct rate-limiting steps for the two processes. Titration with ATP yielded hyperbolic kinetic parameters supporting the similarity between the activation of hydroperoxidation and epoxidation. Both processes displayed similar V-type activation, but the K-type inhibition was greater with AA as the substrate, resulting in a greater activation for $V_{max}/K_m$ for 5(S)-HpETE. Given that the $V_{max}/K_m$ for 5(S)-HpETE is over 20-fold smaller than that for AA, it is tempting to speculate that the larger ATP effect on $V_{max}/K_m$ may be a structural compensation for this difference. Comparing the hydroperoxidation and epoxidation mechanisms, one possible explanation for this differential activation is the rearrangement of the intermediate structure to allow for oxidation of the ferric iron. For hydroperoxidation, a more pronounced rearrangement step is required due to the nature of antarafacial insertion of molecular oxygen leading to the hydroperoxide positioned away from the catalytic iron. In contrast, epoxidation presumably only requires suprafacial homolytic cleavage of the hydroperoxide relative to the catalytic iron. Thus, an ATP-induced conformational

change may allow for better activation of a smaller rearrangement step needed during epoxidation.

The SIE experiments demonstrated inverse SIE $V_{max}/K_m$ values for both AA and 5(S)-HpETE. Inverse SIE values were previously observed for LOX isozymes and indicate the rate-limiting step for substrate capture is dominated by the hydrogen atom abstraction by the Fe(III)-OH moiety. Given that there is a 23-fold difference in their $V_{max}/K_m$ values, this data supports the hypothesis that the rate of hydrogen atom abstraction is slower for epoxidation than hydroperoxidation (*vide infra*). However, ATP shifts the inverse $V_{max}/K_m$ SIE for both AA and 5(S)-HpETE to normal SIE values, indicating an increased dependence of the rate-limiting step on solvent. Given the previous assignment of the SIE to hydrogen-bond rearrangement for other LOX isozymes,[43-46,52] it appears that addition of ATP increases the dependence of the rate-limiting step on hydrogen-bond rearrangement relative to hydrogen-atom abstraction. This conclusion is supported by the fact that no viscosity effect is observed, and thus the reactions are not diffusion-controlled.

In comparing the mechanisms of hydroperoxidation and epoxidation (Scheme 2.3), it is observed that there are three key differences: first, the hydrogen atom is abstracted from C7 for hydroperoxidation, but C10 for epoxidation; second, molecular oxygen does not attack the radical intermediate for epoxidation; and third, the Fe(II)-$OH_2$ moiety donates a hydrogen atom to the peroxyl radical intermediate on C5 for hydroperoxidation, but donates a hydrogen atom to the hydroxide radical, which is homolytically cleaved from the hydroperoxide during epoxidation.

Considering that neither mechanism is limited by substrate diffusion, but both substrate capture rates are limited by hydrogen atom abstraction (inverse SIE), it appears that the 23-fold faster rate for hydroperoxidation is due to an increased rate of hydrogen atom abstraction compared to epoxidation. This hypothesis is chemically reasonable because subtle changes in the positioning of the abstracted hydrogen relative to the Fe(III)-OH moiety have a dramatic effect on rate. [45,52] And considering the carbon from which the hydrogen atom is abstracted for the two mechanisms is distinct (C7 versus C10), and the overall structure of the substrates are also distinct (AA versus 5(S)-HpETE), it is reasonable to assume changes in substrate positioning. It should be noted that the positioning of the substrate relative to the active site iron has also large implications for the final step in both mechanisms. For hydroperoxidation, the Fe(III)-OH moiety abstracts a hydrogen atom from C7 on one face of the substrate, and then must donate the hydrogen atom back to the peroxyl radical intermediate 2 carbons away (C5) on the opposite face of the substrate, requiring repositioning of substrate in the active site. For epoxidation, this conformational change is less, since the hydrogen atom abstraction occurs on C10 and the hydrogen atom donation occurs at the epoxyl radical on the same side as the iron. Nevertheless, these rearrangements are not observed kinetically since neither the $V_{max}$ nor the $V_{max}/K_m$ manifest a structural rearrangement as a rate-limiting step for epoxidation with no ATP present (i.e. inverse SIE values for $V_{max}/K_m$). We are currently investigating this process further to gain insight into this amazing chemical process.

With respect to the larger implications of these ATP results, 5-LOX has a unique role in the inflammatory response by catalyzing the formation of potent pro- and anti-inflammatory molecules, and as such the cell has devised several strategies for regulating its control.[8,19,21,31,49,67] Along these lines, we note that ATP has a well-established role as an up-regulated mediator in inflammation[68-70] and that extracellular ATP is measured at elevated levels for patients suffering from inflammatory diseases, such as Chronic Obstructive Pulmonary Disease (COPD) and emphysema, which are known to involve leukotrienes as causal factors in their pathology.[71-76] *Lommatzsch et al.* recently established that ATP concentrations in bronchoalveolar lavage fluid increased from <10 μM in a control group of patients to upward of 300 μM in patients with increasing stages of COPD. They also presented *in vitro* results suggesting that increasing concentrations of extracellular ATP, from 1 to 100 μM, increased the chemotactic index of human neutrophils, an effect that saturated and resisted any further changes even when probed with 1000 μM extracellular ATP.[72] While a direct link to 5-LOX activity was not tested, we note that these results correlate with our measured $K_i$ of ATP-induced activation for 5-LOX (approximately 10 μM), suggesting a possible connection between increasing chemotactic index and ATP-induced activation of 5-LOX in disease. There is also evidence of intracellular compartmentalization of ATP itself up to low mM concentrations[77] and for high μM amounts of ATP being released extracellularly from HEK293 and ACN neuroblastoma cells through nonlytic ATP release,[78] further demonstrating that the concentration of ATP necessary for ATP-induced activation is

biologically relevant. We reason that these divergent lines of evidence could suggest that the ATP-induced allosteric effect of 5-LOX we have characterized herein may be another biologically relevant form of 5-LOX regulation through which inflammation control can be modulated. The distinction between extracellular and intracellular ATP is an important one, and while ATP is thought to be released from neutrophils[74], 5-LOX activation would still require an elevated intracellular ATP prior to release. The critical question is whether the ATP concentration in the 5-LOX localized cellular compartment is changing as the above experiments predict, suggesting future directions for *in vivo* research.

**2.5 Acknowledgments**

We would like to thank Qiangli Zhang for her assistance in operating the LC-MS/MS and Eric K. Hoobler for thoughtful discussions and advice.

## 2.6 References

(1) Jakschik, B. A., and Lee, L. H. (1980) Enzymatic assembly of slow reacting substance. *Nature 287*, 51–52.

(2) Rådmark, O. (2002) Arachidonate 5-lipoxygenase. *Prostaglandins Other Lipid Mediators 68-69*, 211–234.

(3) Samuelsson, B. (1983) Leukotrienes: mediators of immediate hypersensitivity reactions and inflammation. *Science 220*, 568–575.

(4) Shimizu, T., Radmark, O., and Samuelsson, B. (1984) Enzyme with dual lipoxygenase activities catalyzes leukotriene A4 synthesis from arachidonic acid. *Proc. Natl. Acad. Sci. U.S.A. 81*, 689–693.

(5) Borgeat, P., and Samuelsson, B. (1979) Metabolism of arachidonic acid in polymorphonuclear leukocytes. Structural analysis of novel hydroxylated compounds. *J. Biol. Chem. 254*, 7865–7869.

(6) Ueda, N., Yamamoto, S., Oates, J. A., and Brash, A. R. (1986) Stereoselective hydrogen abstraction in leukotriene A4 synthesis by purified 5-lipoxygenase of porcine leukocytes. *Prostaglandins 32*, 43–48.

(7) Fitzpatrick, F., Liggett, W., McGee, J., Bunting, S., Morton, D., and Samuelsson, B. (1984) Metabolism of leukotriene A4 by human erythrocytes. A novel cellular source of leukotriene B4. *J. Biol. Chem. 259*, 11403–11407.

(8) Sala, A., Folco, G., and Murphy, R. C. (2010) Transcellular biosynthesis of eicosanoids. *Pharmacol Rep 62*, 503–510.

(9) Serhan, C. N. (2002) Lipoxins and aspirin-triggered 15-epi-lipoxin biosynthesis: an update and role in anti-inflammation and pro-resolution. *Prostaglandins Other Lipid Mediators 68-69*, 433–455.

(10) Serhan, C. N., and Savill, J. (2005) Resolution of inflammation: the beginning programs the end. *Nat. Immunol. 6*, 1191–1197.

(11) Rouzer, C. A., and Samuelsson, B. (1987) Reversible, calcium-dependent membrane association of human leukocyte 5-lipoxygenase. *Proc. Natl. Acad. Sci. U.S.A. 84*, 7393–7397.

(12) Hammarberg, T., and Radmark, O. (1999) 5-lipoxygenase binds calcium. *Biochemistry 38*, 4441–4447.

(13) Allard, J. B., and Brock, T. G. (2005) Structural organization of the regulatory domain of human 5-lipoxygenase. *Curr. Protein Pept. Sci. 6*, 125–131.

(14) Reddy, K. V., Hammarberg, T., and Radmark, O. (2000) Mg2+ activates 5-lipoxygenase in vitro: dependency on concentrations of phosphatidylcholine and arachidonic acid. *Biochemistry 39*, 1840–1848.

(15) Noguchi, M., Miyano, M., Matsumoto, T., and Noma, M. (1994) Human 5-lipoxygenase associates with phosphatidylcholine liposomes and modulates LTA4 synthetase activity. *Biochim. Biophys. Acta 1215*, 300–306.

(16) Hill, E., Maclouf, J., Murphy, R. C., and Henson, P. M. (1992) Reversible membrane association of neutrophil 5-lipoxygenase is accompanied by retention of activity and a change in substrate specificity. *J. Biol. Chem. 267*, 22048–22053.

(17) Evans, J. F., Ferguson, A. D., Mosley, R. T., and Hutchinson, J. H. (2008) What's all the FLAP about?: 5-lipoxygenase-activating protein inhibitors for inflammatory diseases. *Trends Pharmacol. Sci. 29*, 72–78.

(18) Dixon, R. A., Diehl, R. E., Opas, E., Rands, E., Vickers, P. J., Evans, J. F., Gillard, J. W., and Miller, D. K. (1990) Requirement of a 5-lipoxygenase-activating protein for leukotriene synthesis. *Nature 343*, 282–284.

(19) Rakonjac, M., Fischer, L., Provost, P., Werz, O., Steinhilber, D., Samuelsson, B., and Rådmark, O. (2006) Coactosin-like protein supports 5-lipoxygenase enzyme activity and up-regulates leukotriene A4 production. *Proc. Natl. Acad. Sci. U.S.A. 103*, 13150–13155.

(20) Esser, J., Rakonjac, M., Hofmann, B., Fischer, L., Provost, P., Schneider, G., Steinhilber, D., Samuelsson, B., and Rådmark, O. (2009) Coactosin-like protein functions as a stabilizing chaperone for 5-lipoxygenase: role of tryptophan 102. *Biochem. J. 425*, 265–274.

(21) Newcomer, M. E., and Gilbert, N. C. (2010) Location, location, location: compartmentalization of early events in leukotriene biosynthesis. *J. Biol. Chem. 285*, 25109–25114.

(22) Peters-Golden, M., and Brock, T. G. (2001) Intracellular compartmentalization of leukotriene synthesis: unexpected nuclear secrets. *FEBS Lett. 487*, 323–326.

(23) Brock, T. G. (2005) Regulating leukotriene synthesis: The role of nuclear 5-lipoxygenase. *J. Cell. Biochem. 96*, 1203–1211.

(24) Luo, M., Flamand, N., and Brock, T. G. (2006) Metabolism of arachidonic acid

to eicosanoids within the nucleus. *Biochim. Biophys. Acta 1761*, 618–625.

(25) Lepley, R. A., Muskardin, D. T., and Fitzpatrick, F. A. (1996) Tyrosine kinase activity modulates catalysis and translocation of cellular 5-lipoxygenase. *J. Biol. Chem. 271*, 6179–6184.

(26) Häfner, A.-K., Cernescu, M., Hofmann, B., Ermisch, M., Hörnig, M., Metzner, J., Schneider, G., Brutschy, B., and Steinhilber, D. (2011) Dimerization of human 5-lipoxygenase. *Biol. Chem. 392*, 1097–1111.

(27) Ochi, K., Yoshimoto, T., Yamamoto, S., Taniguchi, K., and Miyamoto, T. (1983) Arachidonate 5-lipoxygenase of guinea pig peritoneal polymorphonuclear leukocytes. Activation by adenosine 5'-triphosphate. *J. Biol. Chem. 258*, 5754–5758.

(28) Rouzer, C. A., Thornberry, N. A., and Bull, H. G. (1988) Kinetic effects of ATP and two cellular stimulatory components on human leukocyte 5-lipoxygenase. *Ann. N.Y. Acad. Sci. 524*, 1–11.

(29) Noguchi, M., Miyano, M., and Matsumoto, T. (1996) Physiochemical characterization of ATP binding to human 5-lipoxygenase. *Lipids 31*, 367–371.

(30) Aharony, D., and Stein, R. L. (1986) Kinetic mechanism of guinea pig neutrophil 5-lipoxygenase. *J. Biol. Chem. 261*, 11512–11519.

(31) Rådmark, O., and Samuelsson, B. (2005) Regulation of 5-lipoxygenase enzyme activity. *Biochem. Biophys. Res. Commun. 338*, 102–110.

(32) Gilbert, N. C., Bartlett, S. G., Waight, M. T., Neau, D. B., Boeglin, W. E., Brash, A. R., and Newcomer, M. E. (2011) The structure of human 5-lipoxygenase. *Science 331*, 217–219.

(33) Robinson, S. J., Hoobler, E. K., Riener, M., Loveridge, S. T., Tenney, K., Valeriote, F. A., Holman, T. R., and Crews, P. (2009) Using enzyme assays to evaluate the structure and bioactivity of sponge-derived meroterpenes. *J. Nat. Prod. 72*, 1857–1863.

(34) Mogul, R., and Holman, T. R. (2001) Inhibition studies of soybean and human 15-lipoxygenases with long-chain alkenyl sulfate substrates. *Biochemistry 40*, 4391–4397.

(35) Mogul, R., Johansen, E., and Holman, T. R. (2000) Oleyl sulfate reveals allosteric inhibition of soybean lipoxygenase-1 and human 15-lipoxygenase. *Biochemistry 39*, 4801–4807.

(36) Joshi, N., Hoobler, E. K., Perry, S., Diaz, G., Fox, B. G., and Holman, T. R. (2013) Kinetic and structural investigations into the allosteric and pH effect on substrate specificity of human epithelial 15-lipoxygenase-2. *Biochemistry 52*, 8026–8035.

(37) McAuley, W. J., Jones, D. S., and Kett, V. L. (2009) Characterisation of the interaction of lactate dehydrogenase with Tween-20 using isothermal titration calorimetry, interfacial rheometry and surface tension measurements. *J. Pharm. Sci. 98*, 2659–2669.

(38) Wiseman, J. S., Skoog, M. T., Nichols, J. S., and Harrison, B. L. (1987) Kinetics of leukotriene A4 synthesis by 5-lipoxygenase from rat polymorphonuclear leukocytes. *Biochemistry 26*, 5684–5689.

(39) Petrich, K., Ludwig, P., Kuhn, H., and Schewe, T. (1996) The suppression of 5-lipoxygenation of arachidonic acid in human polymorphonuclear leucocytes by the 15-lipoxygenase product (15S)-hydroxy-(5Z, 8Z, 11Z, 13E)-eicosatetraenoic acid: structure-activity relationship and mechanism of action. *Biochem. J. 314*, 911–916.

(40) Deems, R., Buczynski, M. W., Bowers-Gentry, R., Harkewicz, R., and Dennis, E. A. (2007) Detection and quantitation of eicosanoids via high performance liquid chromatography-electrospray ionization-mass spectrometry. *Methods Enzymol. 432*, 59–82.

(41) Derogis, P. B. M. C., Freitas, F. P., Marques, A. S. F., Cunha, D., Appolinário, P. P., de Paula, F., Lourenço, T. C., Murgu, M., Di Mascio, P., Medeiros, M. H. G., and Miyamoto, S. (2013) The development of a specific and sensitive LC-MS-based method for the detection and quantification of hydroperoxy- and hydroxydocosahexaenoic acids as a tool for lipidomic analysis. *PLoS One 8*, e77561.

(42) Lewis, E. R., Johansen, E., and Holman, T. R. (1999) Large competitive kinetic isotope effects in human 15-lipoxygenase catalysis measured by a novel HPLC method. *J. Am. Chem. Soc. 121*, 1395–1396.

(43) Wecksler, A. T., Jacquot, C., van der Donk, W. A., and Holman, T. R. (2009) Mechanistic investigations of human reticulocyte 15- and platelet 12-lipoxygenases with arachidonic acid. *Biochemistry 48*, 6259–6267.

(44) Segraves, E. N., and Holman, T. R. (2003) Kinetic investigations of the rate-limiting step in human 12- and 15-lipoxygenase. *Biochemistry 42*, 5236–5243.

(45) Glickman, M. H., and Klinman, J. P. (1995) Nature of rate-limiting steps in the soybean lipoxygenase-1 reaction. *Biochemistry 34*, 14077–14092.

(46) Wecksler, A. T., Kenyon, V., Garcia, N. K., Deschamps, J. D., van der Donk, W. A., and Holman, T. R. (2009) Kinetic and structural investigations of the allosteric site in human epithelial 15-lipoxygenase-2. *Biochemistry 48*, 8721–8730.

(47) Skorey, K. I., and Gresser, M. J. (1998) Calcium is not required for 5-lipoxygenase activity at high phosphatidyl choline vesicle concentrations. *Biochemistry 37*, 8027–8034.

(48) Reinhart, G. D. (2004) Quantitative analysis and interpretation of allosteric behavior. *Methods Enzymol. 380*, 187–203.

(49) Rådmark, O., Werz, O., Steinhilber, D., and Samuelsson, B. (2007) 5-Lipoxygenase: regulation of expression and enzyme activity. *Trends Biochem. Sci. 32*, 332–341.

(50) Jin, J., Zheng, Y., Boeglin, W. E., and Brash, A. R. (2012) Biosynthesis, isolation, and NMR analysis of leukotriene A epoxides: substrate chirality as a determinant of the cis or trans epoxide configuration. *J. Lipid Res. 54*, 754–761.

(51) Puustinen, T., Scheffer, M. M., and Samuelsson, B. (1987) Endogenously generated 5-hydroperoxyeicosatetraenoic acid is the preferred substrate for human leukocyte leukotriene A4 synthase activity. *FEBS Lett. 217*, 265–268.

(52) Glickman, M. H., Wiseman, J. S., and Klinman, J. P. (1994) Extremely large isotope effects in the soybean lipoxygenase-linoleic acid reaction. *J. Am. Chem. Soc. 116*, 793–794.

(53) Borgeat, P., Hamberg, M., and Samuelsson, B. (1976) Transformation of arachidonic acid and homo-gamma-linolenic acid by rabbit polymorphonuclear leukocytes. Monohydroxy acids from novel lipoxygenases. *J. Biol. Chem. 251*, 7816–7820.

(54) Maas, R. L., Ingram, C. D., Taber, D. F., Oates, J. A., and Brash, A. R. (1982) Stereospecific removal of the DR hydrogen atom at the 10-carbon of arachidonic acid in the biosynthesis of leukotriene A4 by human leukocytes. *J. Biol. Chem. 257*, 13515–13519.

(55) Panossian, A., Hamberg, M., and Samuelsson, B. (1982) On the mechanism of biosynthesis of leukotrienes and related compounds. *FEBS Lett. 150*, 511–513.

(56) Hamberg, M., and Hamberg, G. (1980) On the mechanism of the oxygenation of arachidonic acid by human platelet lipoxygenase. *Biochem. Biophys. Res. Commun. 95*, 1090–1097.

(57) Schowen, K. B., and Schowen, R. L. (1982) Solvent isotope effects of enzyme systems. *Methods Enzymol. 87*, 551–606.

(58) Quinn, D. M., and Sutton, L. D. (1991) Theoretical basis and mechanistic utility of solvent isotope effects. *Enzyme mechanism from isotope effects* (Cook, P. F., Ed.) 73–126.

(59) Bott, R. R., Chan, G., Domingo, B., Ganshaw, G., Hsia, C. Y., Knapp, M., and Murray, C. J. (2003) Do enzymes change the nature of transition states? Mapping the transition state for general acid-base catalysis of a serine protease. *Biochemistry 42*, 10545–10553.

(60) Raber, M. L., Freeman, M. F., and Townsend, C. A. (2009) Dissection of the stepwise mechanism to beta-lactam formation and elucidation of a rate-determining conformational change in beta-lactam synthetase. *J. Biol. Chem. 284*, 207–217.

(61) Tomchick, D. R., Phan, P., Cymborowski, M., Minor, W., and Holman, T. R. (2001) Structural and functional characterization of second-coordination sphere mutants of soybean lipoxygenase-1. *Biochemistry 40*, 7509–7517.

(62) Pocker, Y., and Janjić, N. (1987) Enzyme kinetics in solvents of increased viscosity. Dynamic aspects of carbonic anhydrase catalysis. *Biochemistry 26*, 2597–2606.

(63) Pocker, Y., and Janjić, N. (1988) Origin of viscosity effects in carbonic anhydrase catalysis. Kinetic studies with bulky buffers at limiting concentrations. *Biochemistry 27*, 4114–4120.

(64) Kanosue, Y., Kojima, S., and Ohkata, K. (2004) Influence of solvent viscosity on the rate of hydrolysis of dipeptides by carboxypeptidase Y. *J. Phys. Org. Chem. 17*, 448–457.

(65) Almagor, A., Yedgar, S., and Gavish, B. (1992) Viscous cosolvent effect on the ultrasonic absorption of bovine serum albumin. *Biophys. J. 61*, 480–486.

(66) Malmberg, C. G., and Maryott, A. A. (1950) Dielectric constants of aqueous solutions of dextrose and sucrose. *J. Res. Nat. Bur. Stand. 45*, 299–303.

(67) Mandal, A. K., Jones, P. B., Bair, A. M., Christmas, P., Miller, D., Yamin, T.-T. D., Wisniewski, D., Menke, J., Evans, J. F., Hyman, B. T., Bacskai, B., Chen, M., Lee, D. M., Nikolic, B., and Soberman, R. J. (2008) The nuclear membrane organization of leukotriene synthesis. *Proc. Natl. Acad. Sci. U.S.A. 105*, 20434–20439.

(68) Bodin, P., and Burnstock, G. (1998) Increased release of ATP from endothelial cells during acute inflammation. *Inflamm. Res. 47*, 351–354.

(69) Burnstock, G., Brouns, I., Adriaensen, D., and Timmermans, J. P. (2012) Purinergic signaling in the airways. *Pharmacol. Rev. 64*, 834–868.

(70) Gourine, A. V., Dale, N., Llaudet, E., Poputnikov, D. M., Spyer, K. M., and Gourine, V. N. (2007) Release of ATP in the central nervous system during systemic inflammation: real-time measurement in the hypothalamus of conscious rabbits. *J. Physiol. 585*, 305–316.

(71) Esther, C. R., Alexis, N. E., and Picher, M. (2011) Regulation of airway nucleotides in chronic lung diseases. *Subcell. Biochem. 55*, 75–93.

(72) Lommatzsch, M., Cicko, S., Müller, T., Lucattelli, M., Bratke, K., Stoll, P., Grimm, M., Dürk, T., Zissel, G., Ferrari, D., Di Virgilio, F., Sorichter, S., Lungarella, G., Virchow, J. C., and Idzko, M. (2010) Extracellular adenosine triphosphate and chronic obstructive pulmonary disease. *Am. J. Respir. Crit. Care Med. 181*, 928–934.

(73) Mortaz, E., Folkerts, G., Nijkamp, F. P., and Henricks, P. A. J. (2010) ATP and the pathogenesis of COPD. *Eur. J. Pharmacol. 638*, 1–4.

(74) Mortaz, E., Braber, S., Nazary, M., Givi, M. E., Nijkamp, F. P., and Folkerts, G. (2009) ATP in the pathogenesis of lung emphysema. *Eur. J. Pharmacol. 619*, 92–96.

(75) Rorke, S. (2002) Role of cysteinyl leukotrienes in adenosine 5`-monophosphate induced bronchoconstriction in asthma. *Thorax 57*, 323–327.

(76) Idzko, M., Hammad, H., van Nimwegen, M., Kool, M., Willart, M. A. M., Muskens, F., Hoogsteden, H. C., Luttmann, W., Ferrari, D., Di Virgilio, F., Virchow, J. C., and Lambrecht, B. N. (2007) Extracellular ATP triggers and maintains asthmatic airway inflammation by activating dendritic cells. *Nat. Med. 13*, 913–919.

(77) Miller, D. S., and Horowitz, S. B. (1986) Intracellular compartmentalization of adenosine triphosphate. *J. Biol. Chem. 261*, 13911–13915.

(78) Pellegatti, P., Falzoni, S., Pinton, P., Rizzuto, R., and Di Virgilio, F. (2005) A novel recombinant plasma membrane-targeted luciferase reveals a new pathway for ATP secretion. *Mol. Biol. Cell 16*, 3659–3665.

# Chapter 3

# Investigating substrate preferences for hydroperoxidation and epoxidation in human lipoxygenase enzymes

## 3.1 Introduction

Lipoxins are downstream lipid mediators responsible for key anti-inflammatory processes during an inflammatory event.[1-3] Lipoxins are important for their vasoactive properties, stimulating either vasoconstriction or vasodilation in different contexts, however the biological mechanisms for these processes are not entirely clear.[4,5] In addition, lipoxins are immunoregulators and antagonize leukotriene-mediated pro-inflammatory processes.[6,7] Lipoxins also have their own dedicated cell surface receptors that may be important for inducing some of these anti-inflammatory effects.[8]

Originating from the poly-unsaturated fatty acid (PUFA) arachidonic acid (AA), the transcellular biosynthesis of lipoxins highlights a complex series of catalytic events whereby multiple lipoxygenases act in concert in different cellular milieus to generate its distinct trihydroxylated structure. Two biosynthetic routes have been proposed in the literature.[9,10] The first route involves the function of 15-LOX found in eosinophils, macrophages, and monocytes to convert AA into 15(S)-HpETE, whereupon this hydroperoxide product is transported into leukocytes and/or PMNLs to be directly converted into lipoxins by 5-LOX, through epoxidation.[1,11] In contrast, the second route highlights 5-LOX as the initial catalytic event to take AA and form leukotriene $A_4$ ($LTA_4$), which is then acted on by 12-LOX in platelet cells for the

final biosynthetic step.[12,13] Both of these routes involve the generation of epoxide-containing intermediates by 5-LOX, although the starting material for 5-LOX epoxidation is distinct, AA versus 15(S)-HpETE.

Despite the wealth of cellular and biological evidence of the functional importance of lipoxins in initiating clearance of exudate and cell debris, kinetic evidence of these two biosynthetic pathways and how they individually contribute to forming higher-order oxylipins, is lacking. Frequently, assays intended to observe lipoxin formation involved extended periods of cellular incubations and analysis of only a single time-point, obscuring important details of the initial stages of catalysis. Despite these long incubation times, small amounts of lipoxin are recorded, suggesting slow rates of formation. Despite the complexity of these assays, certain specific intermediates along the transcellular biosynthetic pathway have been found. For example, a recent publication by *Jin et al*.[14] confirmed the formation of a 14,15-epoxy intermediate (eoxin $A_4$), generated from 15-LOX-1 catalysis of 15(S)-HpETE, by a mechanism suggested by previous research.[15,16] However, kinetic data detailing the microscopic rate constants of this mechanism is lacking. Likewise, the epoxidation by 5-LOX of 5(S)-HpETE to form the 5,6-epoxide product ($LTA_4$) has not been investigated directly and thus there is little molecular understanding of how 5-LOX can contribute to lipoxin formation. Finally, 12-LOX is thought to hydroperoxidate other epoxide-containing substrates on the path toward lipoxin formation,[9,17,18] However, direct biochemical assays with recombinant protein showed that the $V_{max}/K_m$ of 12-LOX hydroperoxidation with AA is ~60-fold greater than the

$V_{max}/K_m$ of 12-LOX hydroperoxidation with $LTA_4$.[18] This suggests that more *in vitro* experiments with recombinant protein are needed to better determine the relative rates of these mechanisms and, by extension, their potential biological relevance for inflammation control and disorder.

In our first attempt to understand the generation of higher-order oxylipin formation, we examined both the hydroperoxidation and epoxidation by 5-LOX. The mechanisms utilized during these biosynthetic processes include hydroperoxidation, a mechanism shared by all major lipoxygenase isoforms to catalyze di-oxygen attack at *cis*,*cis*-1,4-pentadiene moieties of various PUFAs,[19,20] and epoxidation, a mechanism through which hydroperoxidated lipid substrates are converted into epoxide-containing products.[14,21] Our data demonstrated subtle differences in their kinetic parameters, as well as their ability to be activated by ATP. These differences were primarily due to differences in the substrates used (AA versus 5(S)-HpETE) and the specific catalytic steps of each mechanism (Scheme 3.1).

As outlined above, there are many examples of oxylipins in biology where multiple LOX isozymes are implicated in their biosynthesis, however there is confounding evidence with respect to the sequence and nature of the specific isozymes involved. In this paper, a variety of primary hydroperoxides (5(S)-HpETE, 12(S)-HpETE, and 15(S)-HpETE) were investigated as substrates against the three common LOX isoforms (5-LOX, 12-LOX, and 15-LOX) for catalysis via hydroperoxidation and epoxidation, which have been implicated in the generation of complex oxylipin biosynthesis. These data confirm that all three tested LOX isoforms

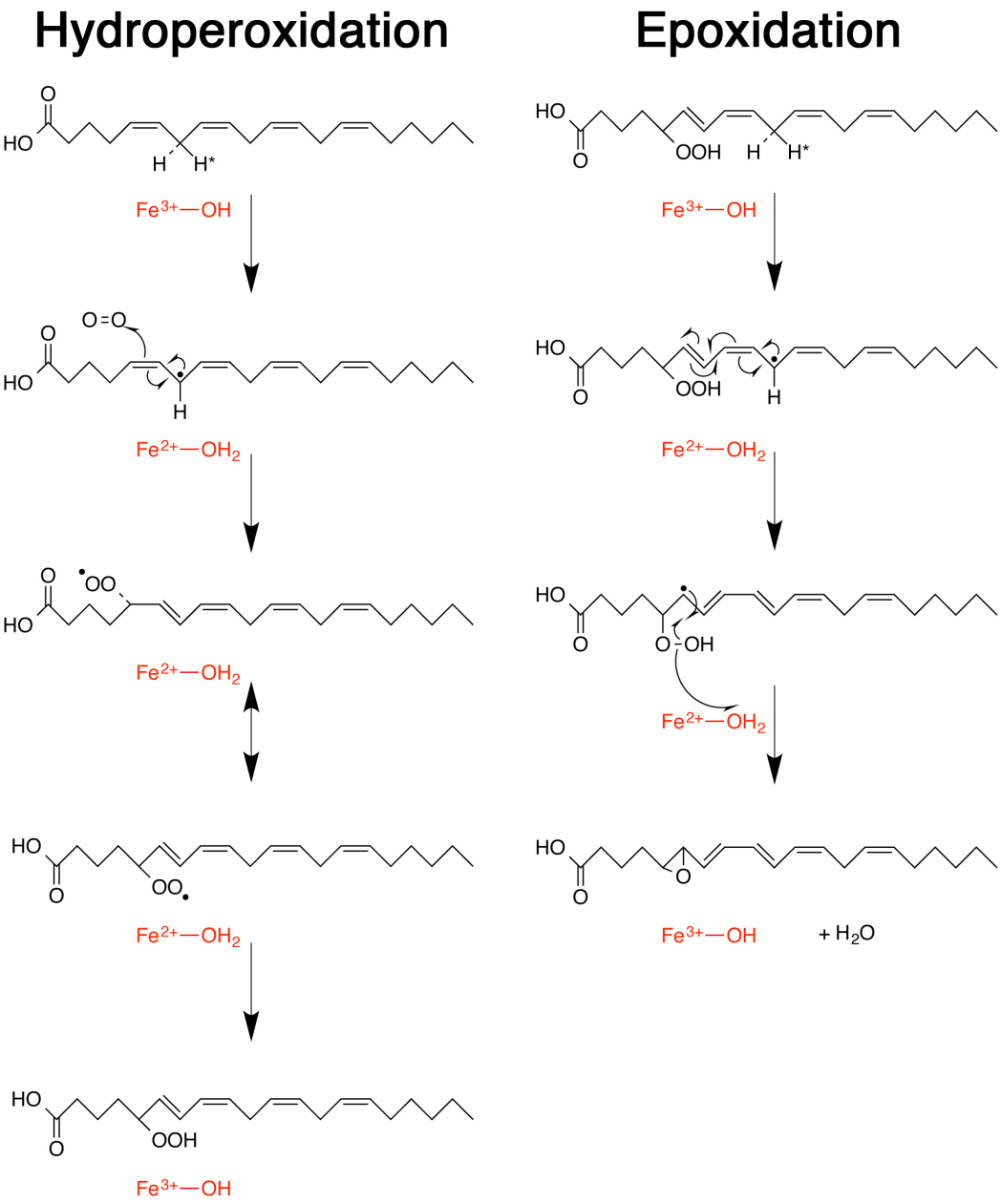


**Scheme 3.1.** Detailed scheme of hydroperoxidation and epoxidation. Hydroperoxidation proceeds after initial abstraction of pro-S hydrogen at C7, whereas epoxidation proceeds after abstraction of pro-R hydrogen at C10.[29] The antarafacial nature of hydroperoxidation is well known,[19,30,31] while a suprafacial arrangement for epoxidation is postulated by *Jin et al*.[14]

are capable of hydroperoxidation with a variety of hydroxide and hydroperoxide substrates, while the epoxidation mechanism is viable with certain hydroperoxide substrates, confirming preferences for stereo- and regioselectivity. We present relative kinetic parameters for these mechanisms in comparison to AA hydroperoxidation to determine which biosynthetic pathways are most biologically relevant. In addition, we present further evidence for substrate-specific changes induced by ATP on 5-LOX catalysis, extending results from a previous paper (submitted to *Biochemistry*). Finally, we note that lipoxin and other higher-order oxylipin formation is undetectable in nearly all of our assays, and we discuss what this may imply for anti-inflammatory processes in the cell.

## 3.2 Materials and Methods

### 3.2.1 Ammonium sulfate precipitation of 5-LOX

Recombinant human 5-LOX in a pET21 plasmid was expressed and precipitated with ammonium sulfate as published previously (submitted to *Biochemistry*). Frozen ammonium sulfate precipitated pellets were resuspended in a nitrogen-sparged, 4 $^{o}$C chilled buffer of 50 mM Hepes, 0.1 mM EDTA, pH 7.5, normalized to 50 mM ionic strength with NaCl (referred to as Buffer A in all subsequent methods) when needed for enzymatic assays. Enzyme activity was not normalized to iron content.

### 3.2.2 Overexpression and purification of 12-LOX and 15-1 LOX

Recombinant human 12-LOX and human reticulocyte 15-1 LOX were expressed and purified as published previously.[22] 12-LOX and 15-1 LOX were both

purified to >80% purity, as evaluated by SDS-PAGE analysis. Enzyme activity was not normalized to iron content.

### 3.2.3 Purification of LOX hydroperoxide and hydroxide enzymatic products

Hydroperoxide and hydroxide enzymatic products were made using AA as a substrate as published previously (submitted to *Biochemistry*). Briefly, 5-LOX was utilized to make 5(S)-HETE and 5(S)-HpETE in Buffer A, while 12-LOX and sLO-1 were utilized to make products oxygenated either at the 12 or the 15 position of AA, respectively, in a buffer of 50 mM Hepes, 0.1 mM EDTA, pH 8.0, normalized to 50 mM ionic strength with NaCl (referred to as Buffer B in all subsequent methods). All of these products were tested using both analytical HPLC and LC-MS/MS. 5(S)-HpETE was generated at greater than 90% purity, with the other <10% being hydrolysis products of the hydroperoxide (5-hydroxides and 5-ketones). All other generated products demonstrated greater than 99% purity.

### 3.2.4 One-point activity screens of 5-LOX, 12-LOX, and 15-LOX-1 against HETE and HpETE substrates

Enzyme was incubated with 10 μM PUFA substrate at room temperature (21 $^{o}$C) and initial rates of product turnover were compared in the presence and absence of ATP. Approximately 100-300 nM ammonium sulfate precipitated wildtype 5-LOX or IDA-$Ni^{2+}$ affinity purified 12-LOX or 15-LOX-1 was used. Catalytic activity relative to protein weight was measured to be ≈0.2 abs/sec/mg for 5-LOX, ≈0.3 abs/sec/mg for 12-LOX, and ≈0.5 abs/sec/mg for 15-LOX-1. Initial rates of catalysis

were determined by following the formation of the conjugated diene-containing hydroperoxides at 234 nm and the conjugated triene-containing diHETEs at 280 nm with a *Hewlett-Packard* diode-array 8453 UV/vis spectrophotometer. All reactions were 2 mL in volume and constantly stirred using a magnetic stir bar in Buffer A (for reactions with 5-LOX and 15-LOX-1) or Buffer B (for reactions with 12-LOX). All rates of diHETE formation for each enzyme were normalized to control rates of HETE formation from AA substrate using a normalization factor of 0.54 to account for the different extinction coefficients of HETEs and diHETEs. No photodegradation of the product was observed during the time of reaction. Enzymatically generated products were identified by LC-MS/MS as previously described (submitted to *Biochemistry*).[23,24] Reactions were repeated 3-6 times and the reported error is the S.E.M. of each set of measurements.

### 3.2.5 Determination of substrate specificity of 5-LOX by the competitive substrate capture method

Competitive substrate capture experiments were modeled after similar experiments in a previous publication (submitted to *Biochemistry*). Briefly, a reaction mixture of AA, 12(S)-HETE, and 15(S)-HETE with a known molar ratio was incubated with ammonium sulfate precipitated 5-LOX in Buffer A in the presence of 200 μM ATP. Reactions were performed in 3 mL cuvettes and quenched at low total substrate consumption (~5-10%). Samples were prepared and analyzed by LC-MS/MS. The corresponding reduced product ion peaks were first identified by their parent size (*m/z* = 319.5 for 5(S)-HETE and *m/z* = 335.5 for the DiHETEs) using

negative ion full MS mode (collision energy of 35 eV). Due to peak overlap between 5(S)-HETE and 12(S)-HETE, negative ion MS/MS data were collected and 5(S)-HETE was identified based on its unique ion fragment (*m/z* = 115). A sample of 5(S)-HETE was used to calculate the ratio of signal responses for this unique fragment and for the 5(S)-HETE parent ion, and this ratio was then used to determine the size of the parent ion signal peak of 5(S)-HETE from the measured amount of its unique fragment. A calibration curve determined that signal responses for 5(S)-HETE and the DiHETEs were the same, and so the size of each parent ion peak gave information on the quantity of each product made. After normalizing for initial molar ratios used, the ratio of products made (5(S)-HETE: 5,12-DiHETE: 5,15-DiHETE) was calculated. Reactions were repeated 22 times and the reported error is the S.E.M. of all measurements.

### 3.2.6 Determination of substrate specificity of 12-LOX by the competitive substrate capture method

Similar experiments as detailed above were also performed with 12-LOX and a reaction mixture with a known molar ratio of AA, 5(S)-HETE, and 15(S)-HETE. Due to peak overlap between 5,12-diHETE and 12,15-diHETE products, negative ion MS/MS data were collected and each diHETE was identified based on its unique ion fragment (*m/z* = 195 and *m/z* = 235, respectively). The ratio of signal responses for each unique fragment relative to its diHETE parent ion signal was determined from a set of control experiments using each individual HETE substrate, and these ratios were then used to determine the size of the parent ion signal peak of each diHETE

from the measured amount of its unique fragment. After normalizing for initial molar ratios used, the ratio of products made (12(S)-HETE: 5,12-DiHETE: 12,15-DiHETE) was calculated. Reactions were repeated 8 times and the reported error is the S.E.M. of all measurements.

### 3.2.7 Steady-state kinetic measurements

Steady-state kinetic rates were determined by following the formation of hydroperoxide products at 234 nm ($\varepsilon$ = 27000 $M^{-1}$ $cm^{-1}$) and triene-containing diHETE products at 280 nm ($\varepsilon$ = 50000 $M^{-1}$ $cm^{-1}$) with a *Hewlett-Packard* diode-array 8453 UV/vis spectrophotometer as detailed previously (submitted to *Biochemistry*). Initial rates (up to the first 20% of the reaction) for each substrate were fitted to the Michaelis-Menten equation using KaleidaGraph (Synergy) and $V_{max}$ and $K_m$ kinetic parameters determined by non-linear regression.

## 3.3 Results and Discussion

### 3.3.1 One-point activity and MS competitive substrate capture screens with 5-LOX, 12-LOX, and 15-LOX-1 against HETE substrates

It is well known in the literature that 5-LOX has two functions, hydroperoxidation and epoxidation. 5-LOX abstracts the pro-S hydrogen atom from C7 of AA to generate an S-hydroperoxide on C5, but abstracts the pro-R hydrogen atom from C10 of 5(S)-HpETE to convert the S-hydroperoxide to an S,R-epoxide (Scheme 3.1). Interestingly, even though 5-LOX is capable of abstracting the pro-R hydrogen atom from C10 from 5(S)-HpETE, it cannot abstract a hydrogen atom from C10 of AA to generate HpETE products, most likely due to substrate orientation. This

selectivity raised the question of LOX hydroperoxidation specificity in general and which specific LOX isozyme could hydroperoxidate which specific HETEs. With this in mind, we performed one-point activity screens with three LOX isozymes, 5-LOX, 12-LOX and 15-LOX-1, against 5(S)-HETE, 12(S)-HETE and 15(S)-HETE in an effort to determine relative catalysis of these products compared to AA.

For 5-LOX, no oxidation products, which absorb at 234 nm or 280 nm, were observed with 5(S)-HETE as substrate, indicating its specificity for hydroperoxidation at C5 and not the other *cis*,*cis*-1,4-pentadiene moieties of 5(S)-HETE. 5-LOX also did not produce 234 nm or 280 nm products with 12(S)-HETE or 15(S)-HETE either, despite C7 and C10 being available to hydrogen atom abstraction (i.e. a 1,4-diene moiety). Given that the one point assays described above only detect products that absorb at 234 and 280 nm, MS competitive kinetic experiments were performed to collect relative $k_{cat}/K_m$ parameters and account for products that do manifest an absorbance change at 234 nm or 280 nm. For the competitive substrate capture experiments, 5-LOX, AA, 12(S)-HETE, and 15(S)-HETE were mixed and the results demonstrated a 12(S)-HETE/AA consumption ratio of 0.0055 ± 0.0005, while the 15(S)-HETE/AA consumption ratio was measured to be 0.08 ± 0.006. These numbers show that 12(S)-HETE is hydroperoxidated only at a rate of 0.6% of the AA hydroperoxidation activity, agreeing with our one-point screen data (Table 3.1). However, 15(S)-HETE gave a rate of 8% of the AA hydroperoxidation activity, which could not be detected in our UV/vis one-point screens because the main product, 5,15-diHETE, does not absorb at 280 nm and the expected change in 234 nm

| Substrate | 5-LOX | 12-LOX | 15-LOX |
|---|---|---|---|
| **AA (234 nm)** | 100% | 100% | 100% |
| **AA (280 nm)** | 18 ± 1% | 5 ± 2% | 5 ± 1% |
| **5(S)-HETE** | < 1% | < 1% | 27 ± 3% |
| **12(S)-HETE** | < 1% | < 1% | < 1% |
| **15(S)-HETE** | 8%* | < 1% | < 1% |

**Table 3.1.** Rates of triene formation from HETE substrates relative to AA turnover. One-point activity screens comparing rates of diHETE formation (280nm) with HETE substrates relative to rates of HETE formation (234 nm) and diHETE formation (280 nm) with AA (10 μM substrate). Absorbance changes at 280 nm, to observe triene formation, were multiplied by a factor of 0.54 to account for the difference in 234 nm and 280 nm extinction coefficients, 27000 $M^{-1}$ $cm^{-1}$ and 50000 $M^{-1}$ $cm^{-1}$ respectively. Relative rates are calibrated to each enzyme's ability to hydroperoxidate AA, which was normalized to 100%. * Noted value is measured from a competitive capture experiment, due to the 5,15-diHETE product absorbing at the same wavelength as 5(S)-HETE substrate.

is not seen, possibly due to the large absorbance of the starting material. These results demonstrate that 5-LOX can only abstract a hydrogen atom from C7 of AA resulting in a hydroperoxide product, but 5-LOX can abstract a hydrogen atom from C13 of 15(S)-HETE at a reasonable rate, generating 5(S)-hydroxy,15(S)-hydroxy-ETE.

12-LOX was similar to 5-LOX in that none of the three HETEs tested produced hydroperoxidation products that absorbed at 234 nm or 280 nm. For the MS competitive substrate capture experiments, 12-LOX, AA, 5(S)-HETE, and 15(S)-HETE were mixed, and the 5(S)-HETE/AA consumption ratio was measured to be 0.0006 ± 0.00008 (<1% of AA hydroperoxidation activity), and the 15(S)-HETE/AA consumption ratio was measured to be 0.0066 ± 0.0007 (<1% of AA hydroperoxidation activity). These data are indicative that even though there were available 1,4-pentadiene moieties for hydrogen atom abstraction, little hydroperoxidation occurred, confirming the one-point screen results. It should be noted that with 12-LOX, both 12(S)-HETE and 5(S)-HETE can produce 5,12-diHETE (Table 2) and therefore, 12(S)-HETE was excluded from the experiment to make quantification of product formation more accurate. In summary, 5-LOX and 12-LOX hydroperoxidate AA most efficiently, with 5-LOX and 15(S)-HETE manifesting the only other appreciable rate, at over 10-fold less, suggesting either ineffective hydrogen atom abstraction or ineffective oxygen attack of the radical intermediate for these HETEs.

For 15-LOX-1, neither 12(S)-HETE nor 15(S)-HETE were substrates despite the presence of 1,4-pentadiene moieties. However, 5(S)-HETE was a relatively good

substrate for 15-LOX-1, producing 5,12-diHETE (75%) and 5,15-diHETE (25%). This result indicates that the presence of the alcohol moiety on C5 does not inhibit 5-LOX from abstracting a hydrogen atom, or from the attack of molecular oxygen on C12 or C15. Interestingly, the product specificity of 15-LOX-1 changes dramatically with 5(S)-HETE as the substrate, compared to AA. The hydroperoxidation of C12 is significantly greater than that of C15 with 5(S)-HETE, generating a majority of 5,12-diHETE. This is in contrast to the hydroperoxidation preference for C15 with AA as substrate, indicating an altered substrate positioning of 5(S)-HETE, possibly due to the hydroxyl group or trans double bond. This altered positioning of 5(S)-HETE allows for not only abstraction of the C10 hydrogen atom over C13, but also the attack of the substrate radical by molecular oxygen on C12. Given the fact that 5(S)-HETE is the only HETE substrate with reasonable rates compared to AA for these three LOX isozyme, we must conclude that this is an unusual activity for 15-LOX-1, which may have large implications for higher order oxylipin formation. For example, 5-LOX and 15-LOX-1 could potentially act in sequence whereby 5-LOX epoxidates at positions C5,C6 and then 15-LOX-1 hydroperoxidates at position C15, generating lipoxin $A_4$ ($LXA_4$). We are currently investigating whether 15-LOX-1 can hydroperoxidate 5,6-diHETE, the decomposition product of $LTA_4$. It should be noted that for 15-LOX-1, all substrates were found to produce products that absorb at 280 nm (Table 3.2), making them amenable to UV/vis detection. MS experiments with 15-LOX were performed to confirm this.

| Substrate | 5-LOX | 12-LOX | 15-LOX |
|---|---|---|---|
| **AA** | 5(S)-HETE (80%)<br>5,12-diHETE* (20%) | 12(S)-HETE | 15(S)-HETE (75%)<br>12(S)-HETE (10%)<br>8,15-diHETE* (10%)<br>12,15-diHETE (5%) |
| **5(S)-HETE** | None | 5,12-diHETE*† (75%)<br>5,15-diHETE† (25%) | 5,12-diHETE* (75%)<br>5,15-diHETE (25%) |
| **12(S)-HETE** | 5,12-diHETE*† | 5,12-diHETE*† | 5,12-diHETE*† |
| **15(S)-HETE** | 5,15-diHETE | 12,15-diHETE† | 12,15-diHETE† (65%)<br>8,15-diHETE*† (35%) |

**Table 3.2.** Products formed by full enzymatic turnover of HETE substrates. A list of relative amounts of LOX products observed by LC-MS/MS with various LOX/HETE combinations. Samples were reduced with trimethylphosphite for added stability in water, and thus all hydroperoxides are reduced to hydroxides. *Indicated products absorb at 280 nm. †Indicated products were found only in trace amounts, and correspond to low enzymatic rates, presented in Table 3.1.

### 3.3.2 One-point activity screens with 5-LOX, 12-LOX, and 15-LOX-1 against HpETE substrates

As discussed above, 5-LOX is known to hydroperoxidate AA and epoxidate 5(S)-HpETE. The epoxidation reaction has one less step, in that molecular oxygen does not react with the substrate radical. Therefore, the fact that the LOX isozymes do not react with many of the HETEs (*vide supra*), does not exclude the possibility of the LOX isozyme epoxidating a particular HpETE. This possibility lead us to perform one-point activity screens to test the three LOX isozymes, 5-LOX, 12-LOX and 15-LOX-1, against a variety of HpETE substrates and compare their relative rates of catalysis to AA.

For 5-LOX, 5(S)-HpETE was epoxidated with only 2% the rate of that for AA hydroperoxidation, which is dramatically less than the 18% rate of epoxidation for 5(S)-HpETE, generated *in situ* from AA. This data corroborates our previous work and indicates that the exogenous 5(S)-HpETE is a poorer substrate for epoxidation than the endogenous 5(S)-HpETE produced *in situ*, possibly due to a slower structural rearrangement (submitted to *Biochemistry*). In contrast, 12(S)-HpETE is an excellent exogenous substrate for 5-LOX, producing 5,12-diHETE at a rate of 17% that of AA hydroperoxidation (Table 3.3). This is a significant rate and indicates that 5-LOX can effectively abstract a hydrogen atom from C7, producing an 11,12-epoxy intermediate, which is then converted to 5,12-diHETE by water attack on C5. This position of hydrogen atom abstraction, C7, is the same carbon where 5-LOX abstracts a hydrogen atom from AA for hydroperoxidation, however in the case of 12(S)-

| Substrate | 5-LOX | 12-LOX | 15-LOX |
|---|---|---|---|
| **AA (234 nm)** | 100% | 100% | 100% |
| **AA (280 nm)** | 18 ± 1% | 5 ± 2% | 5 ± 1% |
| **5(S)-HpETE** | 2 ± 1% | 3 ± 1% | 34 ± 5% |
| **12(S)-HpETE** | 17 ± 3% | 3 ± 1% | 4 ± 2% |
| **15(S)-HpETE** | < 1% | 18 ± 1% | 14 ± 3% |

**Table 3.3.** Rates of triene formation from HpETE substrates relative to AA turnover. One-point activity screens comparing rates of diHETE formation (280nm) with HpETE substrates relative to rates of HETE formation (234 nm) and diHETE formation (280 nm) with AA (10 μM substrate). Absorbance changes at 280nm, to observe triene formation, were multiplied by a factor of 0.54 to account for the difference in 234nm and 280nm extinction coefficients, 27000 $M^{-1}$ $cm^{-1}$ and 50000 $M^{-1}$ $cm^{-1}$ respectively. Relative rates are calibrated to each enzyme's ability to hydroperoxidate AA, which was normalized to 100%.

HpETE, molecular oxygen does not attack C5, but rather the radical induces the epoxidation of the C12 hydroperoxide to form the C11,C12-epoxide. This result has implications for oxylipin production, with 12-LOX and 5-LOX potentially acting in sequence with AA to produce the 11,12-epoxy intermediate, that in theory could be further converted to hepoxilin $A_3$ with an appropriate hydroxylase.[25,26] As expected, 5-LOX abstracts a hydrogen atom from C7 and hydroperoxidates C5 of 15(S)-HpETE to produce 5,15-diHETE, like it does with 15(S)-HETE, but no other oxidation products were observed. These data indicate that epoxidation of 15(S)-HpETE does not occur, even though C10 is available for hydrogen atom abstraction to produce an epoxide. In summary, these data demonstrate that 5-LOX can rapidly abstract a hydrogen atom on C7 from exogenous 12(S)-HpETE to form the 11,12-epoxide, compared to C10 of exogenous 5(S)-HpETE, and C13 of exogenous 15(S)-HpETE. However, it should be noted that 5-LOX can rapidly abstract a hydrogen atom from C10 of 5(S)-HpETE to form the 5,6-epoxide, but only if the 5(S)-HpETE is made endogenously from AA. We previously suggested that this difference in catalytic rates between endogenous and exogenous 5(S)-HpETE could be due to a structural rearrangement step, which is 10-fold slower for exogenous 5(S)-HpETE (previous publication submitted to *Biochemistry*). Therefore, the above data could suggest that this slow step is not present in the epoxidation of 12(S)-HpETE, however further kinetic investigations are required (*vide infra*).

12-LOX did not react with either 5(S)-HpETE or 12(S)-HpETE, but it did react with 15(S)-HpETE, producing a rate of 18% that of AA hydroperoxidation.

Given the lack of reactivity between 12-LOX and 15(S)-HETE, the 15(S)-HpETE activity suggests the necessity of the hydroperoxide moiety for catalysis and thus implicates an epoxidation mechanism. The main product found by reacting 12-LOX with 15(S)-HpETE was 8,15-diHETE, which is indicative of abstraction of a hydrogen atom from C10, generating the 14,15-epoxy intermediate. The 14,15-epoxide is then opened with water attack on C8 (Table 3.4). The activated carbon, C10, is the same carbon that 12-LOX activates upon hydroperoxidation of AA, and suggests a similar binding mode for both AA and 15(S)-HpETE, with the exception that molecular oxygen does not attack the radical intermediate, but rather an epoxide is formed. This result is similar to that of 5-LOX in that only the primary activated carbon for hydroperoxidation (C7 for 5-LOX and C10 for 12-LOX) is also activated for epoxidation. However, unlike 5-LOX, 12-LOX does not react with the primary hydroperoxidation product, 12(S)-HpETE, even if it is generated *in situ*, implying a more restrictive substrate binding site for 12-LOX than 5-LOX, since only C10 can be activated by 12-LOX, while both C7 and C10 can be activated by 5-LOX. This confirms that the role of 12-LOX in generating higher-order oxylipins must be confined to hydroperoxidation of AA and epoxidation of 15(S)-HpETE, and not for the direct formation of epoxide-containing products from a single PUFA substrate.

In contrast to 5-LOX and 12-LOX, 15-LOX-1 reacted with two hydroperoxides, 12(S)-HpETE and 15(S)-HpETE, but did not catalyze their corresponding HETEs. The necessity of the hydroperoxide for catalysis demonstrates an epoxidation mechanism for both 12(S)-HpETE and 15(S)-HpETE. For 12(S)-

| Substrate | 5-LOX | 12-LOX | 15-LOX |
|---|---|---|---|
| **AA** | 5(S)-HETE (80%)<br>5,12-diHETE* (20%) | 12(S)-HETE | 15(S)-HETE (75%)<br>12(S)-HETE (10%)<br>8,15-diHETE* (10%)<br>12,15-diHETE (5%) |
| **5(S)-HpETE** | 5,12-diHETE* | 5,12-diHETE* (50%)<br>5,15-diHETE (50%) | 5,12-diHETE* (75%)<br>5,15-diHETE (25%) |
| **12(S)-HpETE** | 5,12-diHETE* | 5,12-diHETE* | 5,12-diHETE* |
| **15(S)-HpETE** | 5,15-diHETE† | 8,15-diHETE* (20%)<br>12,15-diHETE (10%)<br>14,15-diHETE* (70%) | 8,15-diHETE* (60%)<br>12,15-diHETE (20%)<br>14-15-diHETE* (20%) |

**Table 3.4.** Products formed by full enzymatic turnover of HpETE substrates. A list of relative amounts of LOX products observed by LC-MS/MS with various LOX/HpETE combinations. Products made only from HpETE substrates compared to the corresponding HETE substrates are indicative of an epoxidation mechanism rather than through double hydroperoxidation. *Indicated products absorb at 280 nm. †Indicated products were found only in trace amounts, and correspond to low enzymatic rates, presented in Table 3.3.

HpETE, the hydrogen atom is removed from C7, generating the 11,12-epoxy intermediate, which is subsequently attacked by water at C5 producing mainly 5,12-diHETE (Table 3.4). For 15(S)-HpETE, the hydrogen atom is removed from C10, generating the 14,15-epoxy intermediate, which is subsequently attacked by water at C8 producing mainly 8,15-diHETE (Table 3.4). Smaller percentages of both 12,15-diHETE and 14,15-diHETE are also produced from the 14,15-epoxy intermediate, indicating water attack at C12 and C14, respectively. Interestingly, this product distribution is different from that observed with 12-LOX and 15(S)-HpETE, despite a similar epoxidation mechanism producing a 14,15-epoxy intermediate. Using $LTA_4$ as an example, it is known that through nonenzymatic hydrolysis, water preferentially will attack at the C12 position or the C6 position to open the epoxide and form either 5,12-diHETE or 5,6-diHETE, respectively. *Borgeat et al.* determined, from alcohol-trapping experiments, that the C12 position was found to be the most susceptible to water attack, compared to C6, C8 or C10, indicating an inherent chemical susceptibility, independent of 5-LOX activity.[27] The fact that both 12-LOX and 15-LOX-1 appear to produce the same 14,15-epoxide intermediate, but generate distinct hydrolysis products, mainly 14,15-diHETE for 12-LOX but mainly 8,15-diHETE for 15-LOX-1, could suggest an enzymatic component to directing specific hydrolysis attacks before the epoxide leaves the active site. Since the epoxidation mechanism generates one catalytic equivalent of $H_2O$, a rational hypothesis can be made that either water attack may be directed by either 12-LOX or 15-LOX after epoxidation, which would explain the enzyme-dependent epoxide decomposition products above.

Finally, it is interesting to note that the rate 15-LOX-1 produces the 14,15-epoxide intermediate from *in situ* generated 15(S)-HpETE at only 5% the rate of AA hydroperoxidation, while direct epoxidation of 15(S)-HpETE was 14 ± 3% the rate of AA hydroperoxidation. This data indicates two important features about 15-LOX-1. First, 15-LOX-1 can epoxidate its own primary hydroperoxidation product, like 5-LOX, but the epoxidation rate of exogenous 15(S)-HpETE is faster than the endogenous epoxidation rate of *in situ* generated 15(S)-HpETE. This is opposite of the trend found for 5-LOX, where endogenous 5(S)-HpETE was the better substrate for epoxidation, compared to exogenously added 5(S)-HpETE. This opposing trend suggests interesting functional differences between 5-LOX and 15-LOX-1, which may have both structural and biological implications (*vide infra*).

In summary, 15(S)-HpETE was the only relatively good epoxidation substrate for both 12-LOX and 15-LOX-1. The products generated implicate the abstraction of a hydrogen atom from C10 to form the 14,15-epoxy intermediate (eoxin $A_4$), for both 12-LOX and 15-LOX-1. The activated carbon, C10, is the primary position for hydrogen atom abstraction from AA for 12-LOX, however in the case of 15-LOX-1, C10 is the minor site, relative to C12 for hydrogen atom abstraction from AA, implicating 15-LOX-1 broader substrate specificity as a key component for this activity. These results have implications on oxylipin production, with 15-LOX-1 and 12-LOX potentially acting in sequence, or 15-LOX-1 acting twice on AA, to produce the 14,15-epoxide (eoxin $A_4$), which is the precursor molecule for proinflammatory eoxins found in human eosinophils.[28]

### 3.3.3 Steady-state kinetics comparing hydroperoxidation and epoxidation mechanisms in LOX isoforms

The HpETE substrates that had significant enzymatic activity were further investigated to determine their steady-state kinetics, as compared to the kinetics of AA. Steady-state results for 5-LOX show that while 5(S)-HpETE gives a $V_{max}$ value that is 18% of the $V_{max}$ for AA hydroperoxidation, 12(S)-HpETE gives a $V_{max}$ of 51% (Table 3.5). With large $K_m$ values relative to AA, 5(S)-HpETE and 12(S)-HpETE give $V_{max}/K_m$ values of 3% and 7% of the $V_{max}/K_m$ for AA hydroperoxidation, respectively. These results confirm 12(S)-HpETE is the better substrate than 5(S)-HpETE, but large $K_m$ values for both hydroperoxides suggest that exogenous HpETEs are not as effective substrates for 5-LOX as AA. Interestingly, introduction of ATP did not increase the rate of 12(S)-HpETE catalysis compared to 5(S)-HpETE (submitted to *Biochemistry*) This is a revealing discovery as it indicates that ATP activation of 5-LOX is substrate-dependent, with distinct conformational changes in the active site that favor 5(S)-HpETE being used as a substrate and not 12(S)-HpETE. The key differences between the catalysis of these two HpETE substrates include the position of the abstracted hydrogen atom (C10 for 5(S)-HpETE and C7 for 12(S)-HpETE) and the position where the epoxide is formed (5,6-epoxide from 5(S)-HpETE versus 11,12-epoxide from 12(S)-HpETE). If hydrogen atom abstraction were the major rate-determining step or epoxidation, as proposed in our previous work with 5-LOX epoxidation (submitted to *Biochemistry*), the data would imply that ATP is failing to activate hydrogen atom abstraction from C7 for 12(S)-HpETE

| Substrate | Relative $V_{max}$* | $K_m$ (μM) | Relative $V_{max}/K_m$ |
|---|---|---|---|
| **AA (234 nm)** | 1.00 ± 0.04 | 2.8 ± 0.3 | 0.36 ± 0.03 |
| **AA (234 nm) +200 uM ATP** | 4.6 ± 0.3 | 8.5 ± 1 | 0.54 ± 0.04 |
| **AA (280 nm)** | 0.171 ± 0.008 | 1.64 ± 0.35 | 0.10 ± 0.02 |
| **AA (280 nm) +200 uM ATP** | 1.08 ± 0.06 | 4.5 ± 0.7 | 0.24 ± 0.03 |
| **5(S)-HpETE** | 0.18 ± 0.02 | 15 ± 4 | 0.012 ± 0.002 |
| **5(S)-HpETE +200 uM ATP** | 0.78 ± 0.05 | 21 ± 3 | 0.037 ± 0.002 |
| **12(S)-HpETE** | 0.51 ± 0.04 | 20 ± 3 | 0.026 ± 0.002 |
| **12(S)-HpETE +200 uM ATP** | 0.74 ± 0.06 | 24 ± 4 | 0.031 ± 0.002 |

**Table 3.5.** 5-LOX steady state parameters with and without 200 μM ATP. *All $V_{max}$ values are unitless and are relative to AA hydroperoxidation (234 nm), which is set to one. The $V_{max}$ values, with HpETEs as substrates, were multiplied by 0.54 to account for the difference in exctinction coefficients between HETE (234 nm) and diHETE (280 nm) products. For comparison to other studies, the absolute kinetic activity of 5-LOX was approximately 60 μmol/min/mg.

substrate. Since ATP activates the rate of hydrogen atom abstraction from C7 for 5-LOX and AA, the lack of activation of 12(S)-HpETE catalysis by ATP could potentially indicate that the structural change by ATP does not affect the microscopic rate constants of 12(S)-HpETE catalysis. More kinetic and structure/activity relationship studies are required to fully realize the implications of this data on the epoxidation mechanism.

For 12-LOX, 15(S)-HpETE was clearly the best substrate for epoxidation and thus was further analyzed through steady state kinetics. As shown in Table 3.6, 12-LOX manefests a 7% $V_{max}$ with 15(S)-HpETE as substrate compared to AA hydroperoxidation, but due to a smaller $K_m$, the $V_{max}/K_m$ value is 16% compared to AA hydroperoxidation. This relative efficiency in 15(S)-HpETE catalysis by 12-LOX is partially due to a smaller $K_m$ value for 15(S)-HpETE ($K_m$ = 1.0 ± 0.2) than that of AA ($K_m$ = 2.0 ± 0.3). Since the product is 14,15-diHETE, it indicates that 12-LOX abstracts a hydrogen atom at C10, allowing formation of the 14,15-epoxide (eoxin A-$_4$), which decomposes to the 14,15-diHETE product upon attack of water at C14. This is an expected result since 12-LOX only produces 12(S)-HpETE from AA, indicating it has a strong preference for hydrogen abstraction at C10.

Lastly, 15-LOX-1 was analyzed through steady state kinetics with 15(S)-HpETE as substrate (Table 3.7). For comparison, both hydroperoxidation rates (234 nm) and epoxidation rates (280 nm) rates were collected for AA, so as to obtain endogenous 15(S)-HpETE reaction rates. The steady-state kinetics of 15(S)-HpETE confirmed it to be a good substrate, with an 8% $V_{max}$ compared to AA

| Substrate | Relative $V_{max}$* | $K_m$ (μM) | Relative $V_{max}/K_m$ |
|---|---|---|---|
| **AA** | 1.00 ± 0.07 | 2.0 ± 0.3 | 0.49 ± 0.05 |
| **15(S)-HpETE** | 0.073 ± 0.004 | 1.0 ± 0.2 | 0.08 ± 0.01 |

**Table 3.6.** 12-LOX steady state parameters. *All $V_{max}$ values are unitless and are relative to AA hydroperoxidation (234 nm), which is set to one. The $V_{max}$ values, with HpETEs as substrates, were multiplied by 0.54 to account for the difference in exctinction coefficients between HETE (234 nm) and diHETE (280 nm) products. For comparison to other studies, the absolute kinetic activity of 12-LOX was approximately 80 μmol/min/mg.

| Substrate | Relative $V_{max}$* | $K_m$ (μM) | Relative $V_{max}/K_m$ |
|---|---|---|---|
| **AA (234 nm)** | 1.00 ± 0.05 | 8.7 ± 0.9 | 0.115 ± 0.006 |
| **AA (280 nm)** | 0.043 ± 0.002 | 1.2 ± 0.2 | 0.035 ± 0.005 |
| **15(S)-HpETE** | 0.081 ± 0.002 | 1.9 ± 0.2 | 0.043 ± 0.003 |

**Table 3.7.** 15-LOX steady state parameters. *All $V_{max}$ values are unitless and are relative to AA hydroperoxidation (234 nm), which is set to one. The $V_{max}$ values, with HpETEs as substrates, were multiplied by 0.54 to account for the difference in exctinction coefficients between HETE (234 nm) and diHETE (280 nm) products. For comparison to other studies, the absolute kinetic activity of 15-LOX was approximately 120 μmol/min/mg.

hydroperoxidation and a 37% $V_{max}/K_m$ compared to AA, due to a smaller $K_m$ value. If these relative rates of 15(S)-HpETE epoxidation are translated to absolute rates for $V_{max}/K_m$ for both 12-LOX and 15-LOX-1 (80 μmol/min/mg/1 μM*0.08 = 6.4 μmol/min/mg/μM and 120 μmol/min/mg/8.7 μM*0.43 = 5.9 μmol/min/mg/μM, respectively), it is apparent that 12-LOX and 15-LOX-1 have similar rates of epoxidation of 15(S)-HpETE. Therefore the both biosynthetic pathway in the cell are possible to make the 14,15-epoxy intermediate (eoxin $A_4$). As stated above, the product distribution of the epoxidation of 15(S)-HpETE by 15-LOX-1 indicates hydrogen atom abstraction from C10, the minor position of hydrogen atom abstraction on AA. Given only 10% of AA turnover by 15-LOX-1 is due to C10 abstraction, the $V_{max}/K_m$ of 15(S)-HpETE epoxidation by 15-LOX-1 is thus 3.7-fold greater than the $V_{max}/K_m$ of AA hydroperoxidation to form 12(S)-HpETE. However, the $V_{max}$ of 15(S)-HpETE epoxidation by 15-LOX-1 is comparable to that of AA hydroperoxidation at C12. These data indicate that 15(S)-HpETE has a faster rate of substrate capture than AA, for C10 abstraction, but a comparable rate of product release, indicating the difference is due to a change in the rate-limiting step before the first irreversible step, hydrogen atom abstraction.

Another difference in 15-LOX-1 kinetics is that the $V_{max}$ of exogenous 15(S)-HpETE was twice as large as the $V_{max}$ of endogenous 15(S)-HpETE. This is in contrast with 5-LOX, where epoxidation of exogenous 5(S)-HpETE is slower than endogenous 5(S)-HpETE to form the same product (5,6-epoxide). These data indicate a unique difference between how 5-LOX and 15-LOX-1 bind and process their

respective hydroperoxide products, such as structural differences which could these catalytic distinctions. For example, we have previously proposed that the FY cork found in the 5-LOX crystal structure is a unique structural determinant that may possibly hinder substrate access to the 5-LOX active site. This FY cork is not found in 15-LOX-1 and thus could explain their kinetic differences, although future experiments are needed to confirm this hypothesis.

### 3.4 Conclusions

In summary, this work offers *in vitro* kinetic investigations of the three main LOX isoforms and how they can contribute to higher-order oxylipin biosynthesis. The key questions answered are as follows. First, only 15-LOX-1 can effectively hydroperoxidate an oxylipin, 5(S)-HETE and 5(S)-HpETE. Second, the positional specificity of 15-LOX-1 hydroperoxidation is reversed for 5(S)-HETE and 5(S)-HpETE, relative to AA. For 5(S)-HETE and 5(S)-HpETE, the main hydroperoxidation product is on C12 (abstraction at C10), whereas the main hydroperoxidation product for AA is on C15 (abstraction at C13), indicating a significantly different substrate binding mode. Thus, a specific mode of binding for hydroxide/hydroperoxide lipids occurs within the 15-LOX-1 active site to allow for an additional hydroperoxidation event, a unique feature compared to the other LOX isozymes tested. Third, the ability of all three LOX isozymes to epoxidate hydroperoxides is dependent on their respective hydrogen atom abstraction specificity. For example, each LOX isozyme can only abstract hydrogen atoms from specific carbons, and therefore a particular LOX isozyme only epoxidates oxylipins

when those hydrogen atoms are available for that particular abstraction. This is highlighted by the fact that 5-LOX catalyzes the hydrogen atom abstraction at C7 for only AA and 12(S)-HpETE, but the rate for 12(S)-HpETE epoxidation is approximately half the rate of AA hydroperoxidation. Fourth, the degradation products of these epoxides vary with respect to LOX isozyme, and not with the epoxide intermediate, such as 15(S)-HpETE and 12-LOX/15-LOX-1. This suggests that water does not attack the epoxide based on chemical principles alone, but the water may be partially directed by the active site of the enzyme to attack a specific carbon. Fifth, the mechanism for ATP activation of 5-LOX is only valid for AA and 5(S)-HpETE and not for 12(S)-HpETE catalysis. This is unusual since the rate of 12(S)-HpETE epoxidation and the position of hydrogen atom abstraction (C7) are comparable to that of AA hydoperoxidation, suggesting the structural change upon ATP binding is highly substrate-selective. Sixth, the $V_{max}/K_m$ of 15(S)-HpETE epoxidation by 15-LOX-1 is 4-fold greater than the $V_{max}/K_m$ of AA hydroperoxidation to form 12(S)-HpETE. Considering that both mechanisms involve the abstraction of a hydrogen atom from C10, it appears that 15(S)-HpETE manifests a better position in the active site for catalysis than AA. Finally, the epoxidation rate of exogenous 15(S)-HpETE is faster than endogenous 15(S)-HpETE. This is the opposite trend seen for 5-LOX and 5(S)-HpETE and indicates the unique mechanism by which 5-LOX achieves epoxidation of endogenously produced 5(S)-HpETE.

In summary, each of the 3 LOX isoforms employs unique substrate preferences for hydroperoxidation and epoxidation, which may contribute to their

different biological functions. For example, 5-LOX and 15-LOX-1 are the the only isozymes able to effectively epoxidate their own hydroperoxide products, but 5-LOX preferentially retains its newly made 5(S)-HpETE, possibly as a mode of protection of 5(S)-HpETE from cellular attack. In addition, this paper offers the first demonstration of 5-LOX epoxidation capability with hydroperoxides made from 12-LOX, suggesting it may contribute to hepoxilin formation. 12-LOX has the most discerning active site allowing for only C10 hydrogen atom abstraction, suggesting it can either act as the first or second enzyme to form oxylipins with functional groups requiring C10 hydrogen atom abstraction, such as 12(S)-HpETE or 14,15-epoxide (eoxin $A_4$). 15-LOX-1 is the most promiscuous of the three isozymes, and can effectively catalyze secondary hydroperoxidation of 5-LOX hydroperoxides, in addition to carrying out epoxidation of its own released hydroperoxide product to form eoxin $A_4$. Finally, previous *in vivo* studies suggest biosynthetic pathways for lipoxin formation that implicate either a 5-LOX/12-LOX or 15-LOX/5-LOX order of enzymatic operations.[10] However, *in vitro* data presented here suggest either of these possibilities involve slow catalytic steps, with no observable rates of lipoxin formation detected. These results raise the question of whether the delayed formation of anti-inflammatory mediators in the cell is in part due to inefficient catalysis of pro-inflammatory mediators, or whether LOX isozymes are further regulated by an unknown factor in the cell to up-regulate higher-order oxylipin biosynthesis.

## 3.5 Acknowledgments

We would like to thank Qiangli Zhang for her assistance in operating the LC-MS/MS and Bill Fitch for thoughtful discussions and advice.

### 3.6 References

(1) Serhan, C. N., Hamberg, M., and Samuelsson, B. (1984) Trihydroxytetraenes: a novel series of compounds formed from arachidonic acid in human leukocytes. *Biochem. Biophys. Res. Commun. 118*, 943–949.

(2) Serhan, C. N., Hamberg, M., and Samuelsson, B. (1984) Lipoxins: novel series of biologically active compounds formed from arachidonic acid in human leukocytes. *Proc. Natl. Acad. Sci. U.S.A. 81*, 5335–5339.

(3) Serhan, C. N., and Savill, J. (2005) Resolution of inflammation: the beginning programs the end. *Nat. Immunol. 6*, 1191–1197.

(4) Dahlén, S. E., Raud, J., Serhan, C. N., Björk, J., and Samuelsson, B. (1987) Biological activities of lipoxin A include lung strip contraction and dilation of arterioles in vivo. *Acta Physiol. Scand. 130*, 643–647.

(5) Dahlén, S. E., Franzén, L., Raud, J., Serhan, C. N., Westlund, P., Wikström, E., Björck, T., Matsuda, H., Webber, S. E., and Veale, C. A. (1988) Actions of lipoxin A4 and related compounds in smooth muscle preparations and on the microcirculation in vivo. *Adv. Exp. Med. Biol. 229*, 107–130.

(6) Badr, K. F., DeBoer, D. K., Schwartzberg, M., and Serhan, C. N. (1989) Lipoxin A4 antagonizes cellular and in vivo actions of leukotriene D4 in rat glomerular mesangial cells: evidence for competition at a common receptor. *Proc. Natl. Acad. Sci. U.S.A. 86*, 3438–3442.

(7) Hedqvist, P., Raud, J., Palmertz, U., Haeggström, J., Nicolaou, K. C., and Dahlén, S. E. (1989) Lipoxin A4 inhibits leukotriene B4-induced inflammation in the hamster cheek pouch. *Acta Physiol. Scand. 137*, 571–572.

(8) Fiore, S., Ryeom, S. W., Weller, P. F., and Serhan, C. N. (1992) Lipoxin recognition sites. Specific binding of labeled lipoxin A4 with human neutrophils. *J. Biol. Chem. 267*, 16168–16176.

(9) Serhan, C. N. (1994) Lipoxin biosynthesis and its impact in inflammatory and vascular events. *Biochim. Biophys. Acta 1212*, 1–25.

(10) Serhan, C. N. (2005) Lipoxins and aspirin-triggered 15-epi-lipoxins are the first lipid mediators of endogenous anti-inflammation and resolution. *Prostaglandins Leukot. Essent. Fatty Acids 73*, 141–162.

(11) Samuelsson, B., Dahlén, S. E., Lindgren, J. A., Rouzer, C. A., and Serhan, C. N. (1987) Leukotrienes and lipoxins: structures, biosynthesis, and biological effects. *Science 237*, 1171–1176.

(12) Serhan, C. N., and Sheppard, K. A. (1990) Lipoxin formation during human neutrophil-platelet interactions. Evidence for the transformation of leukotriene A4 by platelet 12-lipoxygenase in vitro. *J. Clin. Invest. 85*, 772–780.

(13) Fiore, S., and Serhan, C. N. (1990) Formation of lipoxins and leukotrienes during receptor-mediated interactions of human platelets and recombinant human granulocyte/macrophage colony-stimulating factor-primed neutrophils. *J. Exp. Med. 172*, 1451–1457.

(14) Jin, J., Zheng, Y., Boeglin, W. E., and Brash, A. R. (2012) Biosynthesis, isolation, and NMR analysis of leukotriene A epoxides: substrate chirality as a determinant of the cis or trans epoxide configuration. *J. Lipid Res. 54*, 754–761.

(15) Bryant, R. W., Schewe, T., Rapoport, S. M., and Bailey, J. M. (1985) Leukotriene formation by a purified reticulocyte lipoxygenase enzyme. Conversion of arachidonic acid and 15-hydroperoxyeicosatetraenoic acid to 14, 15-leukotriene A4. *Journal of Biological ….*

(16) Maas, R. L., Brash, A. R., and Oates, J. A. (1981) A second pathway of leukotriene biosynthesis in porcine leukocytes. *Proc. Natl. Acad. Sci. U.S.A. 78*, 5523–5527.

(17) Romano, M., and Serhan, C. N. (1992) Lipoxin generation by permeabilized human platelets. *Biochemistry 31*, 8269–8277.

(18) Romano, M., Chen, X. S., Takahashi, Y., Yamamoto, S., Funk, C. D., and Serhan, C. N. (1993) Lipoxin synthase activity of human platelet 12-lipoxygenase. *Biochem. J. 296 ( Pt 1)*, 127–133.

(19) Hamberg, M., and Hamberg, G. (1980) On the mechanism of the oxygenation of arachidonic acid by human platelet lipoxygenase. *Biochem. Biophys. Res. Commun. 95*, 1090–1097.

(20) Yamamoto, S. (1992) Mammalian lipoxygenases: molecular structures and functions. *Biochim. Biophys. Acta 1128*, 117–131.

(21) Wiseman, J. S., Skoog, M. T., Nichols, J. S., and Harrison, B. L. (1987) Kinetics of leukotriene A4 synthesis by 5-lipoxygenase from rat polymorphonuclear leukocytes. *Biochemistry 26*, 5684–5689.

(22) Amagata, T., Whitman, S., Johnson, T. A., Stessman, C. C., Loo, C. P., Lobkovsky, E., Clardy, J., Crews, P., and Holman, T. R. (2003) Exploring sponge-derived terpenoids for their potency and selectivity against 12-human, 15-human, and 15-soybean lipoxygenases. *J. Nat. Prod. 66*, 230–235.

(23) Deems, R., Buczynski, M. W., Bowers-Gentry, R., Harkewicz, R., and Dennis, E. A. (2007) Detection and quantitation of eicosanoids via high performance liquid chromatography-electrospray ionization-mass spectrometry. *Methods Enzymol. 432*, 59–82.

(24) Derogis, P. B. M. C., Freitas, F. P., Marques, A. S. F., Cunha, D., Appolinário, P. P., de Paula, F., Lourenço, T. C., Murgu, M., Di Mascio, P., Medeiros, M. H. G., and Miyamoto, S. (2013) The development of a specific and sensitive LC-MS-based method for the detection and quantification of hydroperoxy- and hydroxydocosahexaenoic acids as a tool for lipidomic analysis. *PLoS One 8*, e77561.

(25) Pace-Asciak, C. R., and Martin, J. M. (1984) Hepoxilin, a new family of insulin secretagogues formed by intact rat pancreatic islets. *Prostaglandins*.

(26) Brash, A. R., Yu, Z., Boeglin, W. E., and Schneider, C. (2007) The hepoxilin connection in the epidermis. *FEBS Journal 274*, 3494–3502.

(27) Borgeat, P., and Samuelsson, B. (1979) Arachidonic acid metabolism in polymorphonuclear leukocytes: unstable intermediate in formation of dihydroxy acids. *Proc. Natl. Acad. Sci. U.S.A. 76*, 3213–3217.

(28) Feltenmark, S., Gautam, N., Brunnström, A., Griffiths, W., Backman, L.,

Edenius, C., Lindbom, L., Björkholm, M., and Claesson, H.-E. (2008) Eoxins are proinflammatory arachidonic acid metabolites produced via the 15-lipoxygenase-1 pathway in human eosinophils and mast cells. *Proceedings of the National Academy of Sciences 105*, 680–685.

(29) Maas, R. L., Ingram, C. D., Taber, D. F., Oates, J. A., and Brash, A. R. (1982) Stereospecific removal of the DR hydrogen atom at the 10-carbon of arachidonic acid in the biosynthesis of leukotriene A4 by human leukocytes. *J. Biol. Chem. 257*, 13515–13519.

(30) Rådmark, O., and Samuelsson, B. (2005) Regulation of 5-lipoxygenase enzyme activity. *Biochem. Biophys. Res. Commun. 338*, 102–110.

(31) Glickman, M. H., and Klinman, J. P. (1995) Nature of rate-limiting steps in the soybean lipoxygenase-1 reaction. *Biochemistry 34*, 14077–14092.

# Chapter 4

## Discovery of a novel dual fungal CYP51/human 5-lipoxygenase inhibitor: implications for anti-fungal therapy

### 4.1 Introduction

Human 5-lipoxygenase (5-LOX) has long been considered a possible therapeutic target for inflammatory diseases. Asthma is the principle disease target, however numerous other diseases have been postulated in the literature as possible targets for 5-LOX inhibition, such as allergic rhinitis, chronic obstructive pulmonary disease, idiopathic pulmonary fibrosis, atherosclerosis, ischemia-reperfusion injury, atopic dermatitis and acne vulgaris. [1-6] The role of 5-LOX in the latter disease, acne vulgaris, has been shown to be related to the production of sebum in the derma.[7] 5-LOX has also been implicated in another skin disease, seborrheic dermatitis (i.e. dandruff).[8] The involvement of 5-LOX in dandruff is because many systemic and superficial fungal infections are associated with inflammation. Ketoconazole is a widely used anti-fungal agent that is currently utilized as an active ingredient in anti-dandruff shampoo, [9,10] and previously for a wide range of fungal infections. Its mode of action is by inhibiting fungal sterol 14α-demethylase (Erg11 or CYP51) during ergosterol biosynthesis, thus retarding fungal growth.[11] However, it has been proposed that part of its effectiveness is due to its anti-inflammation activity, since it also weakly inhibits 5-LOX.[12] The anti-inflammatory activity of ketoconazole has also been seen for itraconazole, a similar anti-fungal therapeutic,[13] which suggests a common theme for effective dandruff agents, dual anti-fungal/anti-inflammatory

targeting. Nevertheless, the potency for ketoconazole and itraconazole against 5-LOX is poor, with $IC_{50}$ values greater than 50 μM for both molecules, which indicates a potential for improvement in their anti-inflammatory activity.[12,13]

Numerous inhibitors for 5-LOX have been reported,[14-17] which can be generally classified into three categories, reductive, iron ligands and competitive/mixed inhibitors[6,18,19] (Figure 4.1), however only one compound has been approved as a drug, zileuton.[20,21] Zileuton is a potent and selective 5-LOX inhibitor but its mode of action is unusual for a therapeutic.[19,22] It contains an *N*-hydroxyurea moiety, which is proposed to chelate to the active enzyme's ferric ion and reduce it to the inactive ferrous ion.[16,22,23] In general, chelation/reduction is not considered a viable mode of inhibition for a therapeutic since metal chelation tends toward promiscuous behavior with other metalloproteins and reductive inhibitors can be chemically inactivated in the cell.[16,18,19] Nevertheless, zileuton has been shown to not only be selective against 5-LOX but also efficacious in the cell,[20-22] which presents this class of inhibitors as a viable chemotype for 5-LOX inhibition. Other chelative inhibitors, such as nordihydroguaiaretic acid (NDGA)[24-26] are also reductive due to the facile nature of inner sphere electron reduction. NDGA contains a catechol moiety, which binds to the active site ferric ion, reducing it to the ferrous ion, with the concomitant oxidation of the catechol moiety to the semiquinone. This reactivity has previously been seen with the metalloenzyme, catechol dioxygenase, whose catechol substrate is activated to the semiquinone by the active site ferric ion for oxidation by molecular oxygen.[25,27,28] There is also a sub-classification of reductive

inhibitors that do not chelate the active site iron. The mechanism for these inhibitors is most likely long-range electron transfer, but no direct proof has been found for this mechanism. Recent efforts by the pharmaceutical industry have focused on non-reductive inhibitors of 5-LOX (see Figure 4.1; setileuton and PF-4191834), however, these appear to have been discontinued during Phase II clinical trials.[29,30] In the current publication, phenylenediamine derivatives are presented as highly selective, non-chelative, reductive inhibitors towards 5-LOX. For one derivative, the phenylenediamine core has been translated into the ketoconazole structure, generating a novel compound that demonstrates dual CYP51/5-LOX inhibitory properties. This new chemical entity, which combines anti-inflammatory and antifungal activities, is presented as a possible novel therapeutic against both the fungal and inflammatory causes of disease.

## 4.2 Materials and Methods

### 4.2.1 General methods for chemistry

All air or moisture sensitive reactions were performed under positive pressure of nitrogen with oven-dried glassware. Anhydrous solvents such as dichloromethane, *N,N*-dimethylformamide (DMF), acetonitrile, methanol and triethylamine were purchased from Sigma-Aldrich. Preparative purification was performed on a Waters semi-preparative HPLC system. The column used was a Phenomenex Luna C18 (5 micron, 30×75 mm) at a flow rate of 45 mL/min. The mobile phase consisted of acetonitrile and water (each containing 0.1% trifluoroacetic acid). A gradient of 10% to 50% acetonitrile over 8 minutes was used during the purification. Fraction

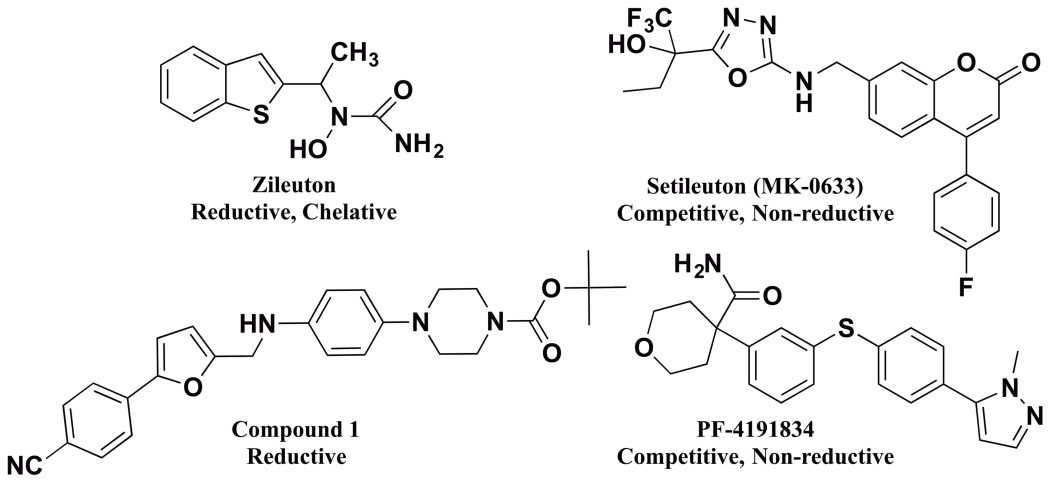


**Figure 4.1.** Structures of LOX inhibitors. This figure was made by coauthor Eric K. Hoobler.[62]

collection was triggered by UV detection (220 nm). Analytical analysis was performed on an Agilent LC/MS (Agilent Technologies, Santa Clara, CA). Method 1: A 7 minute gradient of 4% to 100% Acetonitrile (containing 0.025% trifluoroacetic acid) in water (containing 0.05% trifluoroacetic acid) was used with an 8 minute run time at a flow rate of 1 mL/min. A Phenomenex Luna C18 column (3 micron, 3×75 mm) was used at a temperature of 50°C. Method 2: A 3 minute gradient of 4% to 100% Acetonitrile (containing 0.025% trifluoroacetic acid) in water (containing 0.05% trifluoroacetic acid) was used with a 4.5 minute run time at a flow rate of 1 mL/min. A Phenomenex Gemini Phenyl column (3 micron, 3×100 mm) was used at a temperature of 50°C. Purity determination was performed using an Agilent Diode Array Detector for both Method 1 and Method 2. Mass determination was performed using an Agilent 6130 mass spectrometer with electrospray ionization in the positive mode. $^{1}$H NMR spectra were recorded on Varian 400 MHz spectrometers. Chemical shifts are reported in ppm with undeuterated solvent (DMSO-$d_6$ at 2.49 ppm) as internal standard for DMSO-$d_6$ solutions. All of the analogues tested in the biological assays have purity greater than 95%, based on both analytical methods. High resolution mass spectrometry was recorded on Agilent 6210 Time-of-Flight LC/MS system. Confirmation of molecular formula was accomplished using electrospray ionization in the positive mode with the Agilent Masshunter software (version B.02).

#### 4.2.2 Overexpression and purification of 5-human lipoxygenase, 12-human lipoxygenase, and the 15-human lipoxygenases

Human reticulocyte 15-lipoxygenase-1 (15-LOX-1)[31] and human platelet 12-

lipoxygenase (12-LOX)[31] and human prostate epithelial 15-lipoxygenase-2 (15-LOX-2)[32] were expressed as *N*-terminally, $His_6$-tagged proteins and purified to greater than 90% purity.[33] Human leukocyte 5-lipoxygenase was expressed as a non-tagged protein and used as a crude ammonium sulfate protein fraction, as published previously.[17]

### 4.2.3 Lipoxygenase UV-based inhibitor assay

Inhibitor potencies were evaluated through use of the standard UV-based inhibitor assay. The initial rates were determined by following the formation of the conjugated diene product at 234 nm ($\varepsilon = 25{,}000\ M^{-1}\ cm^{-1}$) with a Perkin-Elmer Lambda 40 UV/Vis spectrophotometer at one substrate concentration and varying inhibitor concentrations. All reactions were 2 mL in volume and constantly stirred using a magnetic stir bar at room temperature (23°C), with the enzyme specific buffer conditions outlined in Table 4.1. The substrate used for the various isozymes was arachidonic acid (AA) for 5-LOX, 12-LOX, and 15-LOX-2 and linoleic acid (LA) for 15-LOX-1, where concentrations were quantitatively determined by allowing the enzymatic reaction to go to completion. $IC_{50}$ values were obtained by determining the initial rate at various inhibitor concentrations and plotting them against inhibitor concentration, followed by a hyperbolic saturation curve fit. The data used for the saturation curves were performed in duplicate or triplicate, depending on the quality of the data. It should be noted that all of the potent inhibitors displayed greater than 80% maximal inhibition, unless otherwise stated in the tables. Inhibitors were stored at −20°C in DMSO. As a result of screening with a semi-purified protein there was

concern whether the 5-LOX concentration was approaching the inhibitor concentration for our most potent inhibitors, which would affect the Henri-Michaelis-Menten approximation. In order to investigate whether the enzyme concentration was approaching the $IC_{50}$ value, we compared our $IC_{50}$ values of two high potency 5-LOX inhibitors to that in the literature. Setileuton displayed an $IC_{50}$ value of 60±6 nM, in good agreement with the literature value of 45±10 nM, and zileuton displayed an $IC_{50}$ value of 560±80 nM, in good agreement with the literature value of 500±100 nM. [2,13] The solvent isotope effect of the inhibitor $IC_{50}$ was investigated utilizing the same conditions and methods as stated above. The pH of the buffered $D_2O$ was determined as reported previously.[34]

#### 4.2.4 Cyclooxygenase assay

Ovine COX-1 (Cat. No. 60100) and human COX-2 (Cat. No. 60122) were purchased from Cayman chemical. Approximately 2 μg of either COX-1 or COX-2 were added to buffer containing 100 μM AA, 0.1 M Tris-HCl buffer (pH 8.0), 5 mM EDTA, 2 mM phenol and 1 μM hematin at 37°C. Data was collected using a Hansatech DW1 oxygen electrode chamber, as described before.[35] Inhibitor or vehicle were mixed with the respective COX in buffer within the electrode cell, the reaction was initiated by the addition of AA, followed by monitoring of rate of oxygen consumption. Ibuprofen, aspirin and indomethacin, and the carrier solvent, DMSO, were used as positive and negative controls, respectively.

#### 4.2.5 Human blood LTB4 inhibition assay

Whole human blood was obtained from healthy volunteers from within the

| Enzyme | [Enyzme] | Substrate (μM) | pH | Buffer |
|---|---|---|---|---|
| 5-LOX | crude | 10 (μM) AA | 7.3 | 25 mM HEPES, 0.3 mM $CaCl_2$, 0.1 mM EDTA, 0.2 mM ATP, 0.01% Triton X-100 |
| 12-LOX | ~40 nM | 10 (μM) AA | 8.0 | 25 mM HEPES, 0.01% Triton X-100 |
| 15-LOX-1 | ~20 nM | 10 (μM) LA | 7.5 | 25 mM HEPES, 0.01% Triton X-100 |
| 15-LOX-2 | ~100 nM | 30 (μM) AA | 7.5 | 25 mM HEPES, 0.01% Triton X-100 |

[a]The UV-based manual inhibition data (3 replicates) were fit as described in the Materials and Methods section.
doi:10.1371/journal.pone.0065928.t001

**Table 4.1.** Buffer conditions for $IC_{50}$ assays, with constant substrate concentration and varying inhibitor concentration. This table and the data it contains was generated by coauthor Eric K. Hoobler.[62]

Student Health Center. These studies were approved by the UCSC Institutional Review Board (IRB) and informed consent was obtained from all donors before blood draw. The whole blood was dispensed in 150 μL samples followed by addition of inhibitor or control (vehicle, DMSO), and incubated for 15 min at 37°C. The mixture was then stimulated by introduction of the calcium ionophore, A23817, (freshly diluted from a 50 mM DMSO stock to 1.5 mM in Hanks balanced salt solution), and incubated for 30 min at 37°C. Samples were then centrifuged at 1,500 rpm (300 g) for 10 min at 4°C and the supernatant diluted between 20 and 50-fold (batch dependent) for LTB4 detection, using an ELISA detection kit (Cayman Chemicals Inc.). Inhibitors were added at 10 μM concentrations[36-38] and the $IC_{50}$ values were generated using a one point $IC_{50}$ estimation equation.

#### 4.2.6 Pseudoperoxidase activity assay

The reductive properties of the inhibitors were determined by monitoring the pseudoperoxidase activity of lipoxygenase in the presence of the inhibitor and 13-(S)-hydroperoxyoctadecadienoic acid (13-HPODE). Activity is monitored by direct measurement of the product degradation following the decrease of absorbance at 234 nm using a Perkin-Elmer Lambda 40 UV/Vis spectrometer (50 mM Sodium Phosphate (pH 7.4), 0.3 mM $CaCl_2$, 0.1 mM EDTA, 0.01% Triton X100, 10 μM 13-HPODE). All reactions were performed in 2 mL of buffer and constantly stirred with a rotating stir bar (23°C). Reaction was initiated by addition of 10 μM inhibitor (a 1 to 1 ratio to 13-HPODE), and a positive result for activity reflected a loss of greater

than 40% of product absorption at 234 nm. The control inhibitors for this assay were zileuton, a known reductive inhibitor,[18] and setileuton, a competitive inhibitor.[29]

### 4.2.7 Inhibitor modeling

Grid generation and flexible ligand docking were performed using Glide, while energy minimization and ligand preparation of inhibitors was done with LigPrep. LigPrep and Glide are both products of Schrodinger, Inc., and utilize energy functions to generate and rank models of ligand 3D structures and ligand-protein interactions, respectively. The crystal structure of Stable Human 5-Lipoxygenase (PDB ID: 3O8Y) was used to generate a Glide grid in which to carry out docking algorithms with our inhibitors. This structure contains several point mutations that remove destabilizing sequences, but since none of these are located at the active site of the enzyme, it is reasonable to assume the mutant structure is an accurate model of the wild-type active site. Positional constraints at the catalytic iron and at hydrophobic pockets within the active site were prepared and utilized intermittently during different docking calculations. Poses generated from ligand docking were ranked according to their GlideScores.

### 4.2.8 CYP51 protein studies

*C. albicans* CYP51 (CaCYP51) and *Homo sapiens* CYP51 (HsCYP51) proteins were expressed in *E. coli* using the pCWori$^{+}$ vector, isolated and purified as previously described to over 90% purity.[39,40] Native cytochrome P450 concentrations were determined by reduced carbon monoxide difference spectra,[41] based on an extinction coefficient of 91 $mM^{-1}$ $cm^{-1}$.[42,43] Binding of azole antifungal agents to 5

μM CaCYP51 and 5 μM HsCYP51 were performed as previously described using 0.25 and 0.5 mg $mL^{-1}$ stock solutions of ketoconazole and ketaminazole in DMSO.[39,44] Azole antifungal agents were progressively titrated against the CYP51 protein in 0.1 M Tris-HCl (pH 8.1) and 25% (wt/vol) glycerol, with the spectral difference determined after each incremental addition of azole. The dissociation constant ($K_d$) of the enzyme-azole complex was determined by nonlinear regression (Levenberg-Marquardt algorithm) of $\Delta A_{\text{peak-trough}}$ against azole concentration using a rearrangement of the Morrison equation[45] and fitted by the computer program ProFit 6.1.12 (QuantumSoft, Zurich, Switzerland).

$IC_{50}$ determinations were performed using the CYP51 reconstitution assay system previously described,[46,47] containing 1 μM CaCYP51 or 0.3 μM HsCYP51, 2 μM human cytochrome P450 reductase, 50 μM lanosterol, 50 μM dilaurylphosphatidylcholine, 4.5% (wt/vol) 2-hydroxypropyl-β-cyclodextrin, 0.4 mg $mL^{-1}$ isocitrate dehydrogenase, 25 mM trisodium isocitrate, 50 mM NaCl, 5 mM $MgCl_2$ and 40 mM MOPS (pH~7.2). Azole antifungal agents were added in 5 μL DMSO followed by incubation for 5 minutes at 37°C prior to assay initiation with 4 mM β-$NADPHNa_4$, with shaking for a further 10 minutes at 37°C. Sterol metabolites were recovered by extraction with ethyl acetate followed by derivatization with *N*,*O*-bis(trimethylsilyl)trifluoroacetamide and tetramethylsilane prior to analysis by gas chromatography mass spectrometry.[48] The term $IC_{50}$ is defined as the inhibitor concentration required for a 50% inhibition of the CYP51 reaction under the stated assay conditions.

## 4.3 Results and Discussion

Our laboratories have previously utilized a high-throughput screen to discover inhibitors against 12-LOX and 15-LOX-1.[35] In the process of screening the 15-LOX-1 "hits", we serendipitously discovered a novel 5-LOX inhibitor with a phenylenediamine core moiety, compound **1**. Due to its chemical nature, the mode of inhibition was postulated to be due to reduction of the active site ferric atom. As mentioned in the introduction, reductive inhibition of lipoxygenase is a very effective mode of action, with many reductive inhibitors having sub-micromolar $IC_{50}$ values.[5,6,16,19] This fact is indicative of both the ease with which the active site ferric can be reduced and the importance of the oxidation state of the iron. With this in mind, the phenylenediamine parent compound (**1**) was modified to change its reduction potential (Figure 4.2).[49] Modifications of the phenylenediamine core, such as atom substitutions of the nitrogens with carbon or oxygen (**2** and **3**, respectively), or the insertion of two additional nitrogen atoms into the core phenyl group (**4**, **5**), resulted in complete loss of inhibition. Interestingly, substitution of only one nitrogen into the core phenyl ring (**6**) did not lower potency dramatically, nor did methylation of the nitrogen (**7**).

The pseudoperoxidase assay was subsequently conducted with these inhibitors to establish their reductive activity against 5-LOX (Figure 4.2). From these data, it was demonstrated that the pseudoperoxidase activity paralleled their inhibitor potency, consistent with changes in the reductive potential of the inhibitors. Similar alterations of the core phenylenediamine structure were previously used in a similar

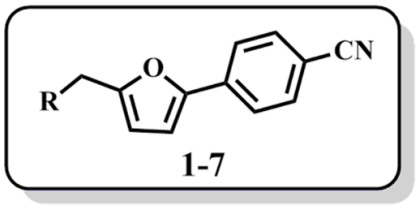


1-7

| Compound | R | Reductive Activity | $IC_{50}$ (μM) [± SD (μM)] |
|---|---|---|---|
| Zilueton | NA | Yes | 0.56 [0.08] |
| Setileuton | NA | No | 0.06 [0.007] |
| 1 | 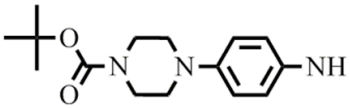 | Yes | 0.17 [0.05] |
| 2 | 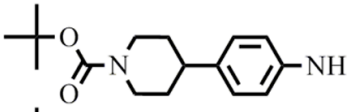 | No | >150 |
| 3 | 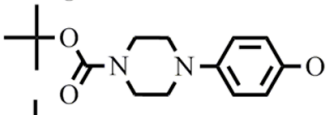 | No | >150 |
| 4 | 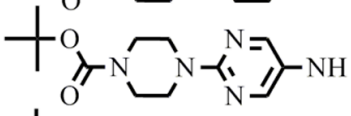 | No | >150 |
| 5 | 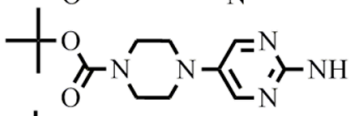 | No | >150 |
| 6 | 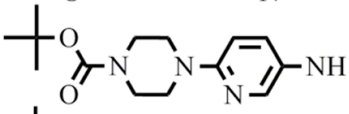 | Yes | 1.1 [0.2] |
| 7 | 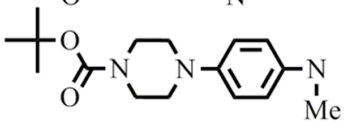 | Yes | 2.7 [0.4] |

**Figure 4.2.** Representative analogues evaluated for pseudoperoxidase activity and $IC_{50}$ potency (μM), with errors in brackets. The UV-based manual inhibition data (3 replicates) were fit as described in the materials and methods section. This figure and the data it contains was generated by coauthor Eric K. Hoobler.[62]

manner to determine the relationship between potency and reductive properties.[50-53] For comparison, zileuton and setileuton were screened as positive controls, with zileuton being reductive and setileuton being non-reductive in their mechanism of inhibition.

Interpreting $IC_{50}$ values for reductive inhibitors is challenging because their relative potency is dependent on a combination of both their reactivity with the active site iron and their binding affinity. The binding affinity was therefore investigated by changing the substituents on either side of the phenylenediamine core. As seen in Figure 4.3, the chemotype core tolerated a large range of modifications, such as changing the steric bulk on either side of the phenylenediamine core. Only one modification in this small set of compounds showed a greater than 10-fold decrease in potency, **10**, which was surprising given the activity of related oxazoles **8** and **9**. The lack of dependence between inhibitor potency and inhibitor structure suggests that the active site can accommodate a variety of inhibitor shapes and sizes. These findings are consistent with the large size of the 5-LOX active site[54] and the re-occurrence of large 5-LOX inhibitors discovered.[6,16,19]

Selectivity of the inhibitor chemotype was evaluated by screening a variety of LOX isozymes with a small subset of compounds (Table 4.2). Strong selectivity was displayed against 5-LOX relative to the other isozymes, with selectivity ratios ranging from 80-fold for 12-LOX, 75-fold for 15-LOX-1, and 30-fold for 15-LOX-2, for the least selective analogues (Table 4.2). The chemotype also displayed strong selectivity

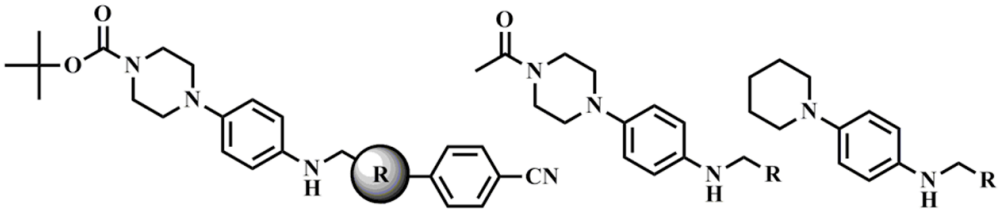

1, 8-10 11-13 14-15

| Compound | R | 5-LOX $IC_{50}$ (μM) [± SD (μM)] |
|---|---|---|
| 1 | 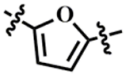 | 0.17 [0.05] |
| 8 | 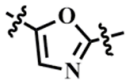 | 0.10 [0.06] |
| 9 | 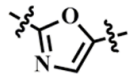 | 1.5 [0.2] |
| 10 | 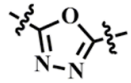 | >150 |
| 11 | 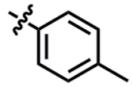 | 1.1 [0.10] |
| 12 | 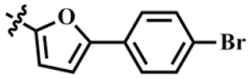 | 2.6 [0.3] |
| 13 | 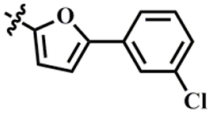 | 0.52 [0.07] |
| 14 | 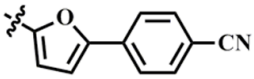 | 0.33 [0.07] |
| 15 | 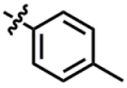 | 0.6 [0.1] |

**Figure 4.3.** 5-LOX $IC_{50}$ values of representative analogues (μM), with errors in brackets. The UV-based manual inhibition data (3 replicates) were fit as described in the materials and methods section. This figure and the data it contains was generated by coauthor Eric K. Hoobler.[62]

| Compound | 5-LOX | 12-LOX | 15-LOX-1 | 15-LOX-2 | COX-1 | COX-2 |
|---|---|---|---|---|---|---|
| **1** | 0.17 (0.05) | >150 | >150 | >150 | >50 | >150 |
| **13** | 0.52 (0.07) | >50 | >50 | >50 | >150 | >150 |
| **14** | 0.33 (0.07) | >150 | >25 | 10 | >150 | N/D[b] |
| **15** | 0.60 (0.1) | >50 | >150 | >50 | N/D | N/D |
| Setileuton | 0.060 (0.007) | >150 | >150 | >150 | >150 | >50 |
| Zileuton | 0.56 (0.08) | >150 | >50 | >150 | >150 | N/D |

[a]The UV-based manual inhibition data (3 replicates) were fit as described in the Materials and Methods section.
[b]N/D = Not determined.
doi:10.1371/journal.pone.0065928.t002

**Table 4.2.** Selectivity profile of representative analogues (μM), with errors in parentheses. This table and the data it contains was generated by coauthor Eric K. Hoobler.[62]

when assayed against cyclooxygenase (COX), with a 140-fold selectivity versus COX-1, and a 240-fold selectivity versus COX-2. These combined results indicate this chemotype has a strong preference/selectivity against 5-LOX versus other AA processing enzymes. As controls, setileuton and zileuton were utilized as selective inhibitors of 5-LOX.[20,21,29]

A few inhibitors were then tested for efficacy in whole human blood, which is known to express 5-LOX upon activation by an ionophore. **1** and **13** displayed roughly 50% inhibition at 10 μM drug dosing in the whole blood, while the positive control, setileuton, was found to inhibit 100% at 10 μM (Table 4.3). Compound **15** was also tested, but the potency was shown to be weak, with less than 10% inhibition at 10 μM (Table 4.3). The cellular enzyme inhibition for **1**, **13** and setileuton are diminished relative to the isolated-enzyme inhibitor values (Figure 4.2). This result, along with other analogues failing to display high potency, could indicate poor permeability, plasma protein binding, non-specific interactions or metabolism of the inhibitors by the cell.

The determination that the reductive phenylenediamine core was the key potency component and that the addition of large functionalities to either side of the phenylenediamine core was well tolerated led us to consider the similarity between the phenylenediamine chemotype and ketoconazole (Figure 4.4). Ketoconazole is a CYP51 inhibitor with an azole moiety that targets the active site heme and is a potent antifungal medication.[8,9] In addition, ketoconazole was previously determined to inhibit 5-LOX and have anti-inflammatory properties, although weakly.[12]

| Compound | Inhibition (%) |
|---|---|
| Setileuton | 100 (11) |
| Ciclopoxin | 34 (2) |
| Ketaminazole (**16**) | 45 (10) |
| Ketoconazole | 25 (3) |
| **1** | 65 (14) |
| **13** | 54 (11) |
| **15** | 8 (1) |

[a]The ELISA absorption-based inhibition data (3 replicates) were fit as described in the Materials and Methods section. Compounds were assayed at 10 μM.
doi:10.1371/journal.pone.0065928.t003

**Table 4.3.** Whole human blood activity profile of representative analogues. This table and the data it contains was generated by coauthor Eric K. Hoobler.[62]

| Compound | Structure | Reductive activity | 5-LOX | 12-LOX | 15-LOX-1 | 15-LOX-2 | COX-1 | COX-2 |
|---|---|---|---|---|---|---|---|---|
| ketoconazole | 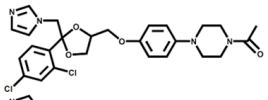 | No | >50 | >150 | >50 | >150 | >50 | >150 |
| ketaminazole (**16**) | 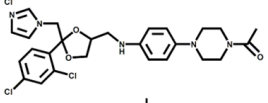 | Yes | 0.7 (0.01) | >150 | >150 | >150 | >150 | >150 |
| ciclopirox | 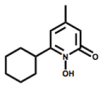 | N/D[b] | 11 (1) | >100 | >100 | N/D | >50 | >150 |

**Figure 4.4.** $IC_{50}$ values of dual anti-fungal, anti-inflammatory inhibitors (μM), with error in parentheses. The UV-based manual inhibition data (3 replicates) were fit as described in the materials and methods section. N/D = Not determined. This figure and the data it contains was generated by coauthor Eric K. Hoobler.[62]

Considering the similarity of ketoconazole to our chemotype, we hypothesized that by adding the phenylenediamine core to ketoconazole, we could improve its 5-LOX potency by making it a reductive inhibitor and thus increasing its anti-inflammatory properties. We subsequently modified the structure of ketoconazole to include a phenylenediamine core to generate a novel compound, ketaminazole (**16**) and found that its potency against 5-LOX increased over 70-fold compared to ketoconazole (Figure 4.4) and that it was a reductive inhibitor, as seen by its activity in the pseudoperoxidase assay (Figure 4.4). The selectivity of the ketaminazole (**16**) was also investigated and found to preferentially inhibit 5-LOX over 100 times better than that of 12-LOX, 15-LOX-1, 15-LOX-2, COX-1 and COX-2 (Figure 4.4). This is most likely due to the large active site of 5-LOX compared to the other human LOX isozymes. Ketaminazole (**16**) was also tested in whole human blood and shown to display cellular activity. Like the smaller phenylenediamine inhibitors (**1**, **13** and **15**), ketaminazole's cellular potency is lower relative to its *in vitro* potency, displaying an approximately 20-fold reduction (Table 4.3). The magnitude of the potency in whole blood is not consistent between all the phenylenediamine inhibitors tested. This indicates that the structural differences between the phenylenediamine inhibitors have an effect on their cellular potency, supporting the hypothesis that cellular factors, other than the phenylenediamine core, are important. Gratifyingly, ketaminazole (**16**) displayed a better potency against 5-LOX in whole blood relative to ketoconazole, however, the magnitude of this difference was not as great as their *in vitro* difference. This is surprising since their only structural difference is the substitution of an amine

for the ether linkage. It could be that the polarity change of the inhibitors changes their cellular uptake or that the reductive state of the ketaminazole is being compromised in the cell. Further cellular studies are required to probe these hypotheses further.

In addition to kinetic data, the importance of the phenylenediamine core for reductive inhibition was further supported using computational methods. Molecular modeling of possible inhibitor binding modes within the active site was initiated by deprotonation of the amine groups at the phenylenediamine core and energy minimization of the compounds with LigPrep.[55,56] The inhibitors listed in of the Figures/Tables above were then docked against the crystal structure of modified protein, Stable-5-LOX (3O8Y), using Glide's "XP" (extra-precision) mode.[55,56] Different trials, with varying Van der Waals scaling factors and alternating positional or hydrophobic constraints linking the inhibitor to the active site, resulted in the occurrence of high-ranking binding poses depicting the deprotonated amine nitrogen within 10 angstroms of the catalytic iron for several inhibitors. The docking results of these inhibitors support the hypothesis that the reduction of the ferric iron could be caused by the phenylenediamine core, either through an inner sphere (direct coordination to the iron) or outer sphere (through space) mechanism.[57] Docking of the larger inhibitors, ketoconazole (Figure 4.5A) and ketaminazole (**16**) (Figure 4.5B), generated poses with similar Glide docking scores to the other inhibitors studied, suggesting a comparable binding mode despite the differences in $IC_{50}$ values. In several high-ranking binding poses, the amine/ester core of ketaminazole (**16**) was

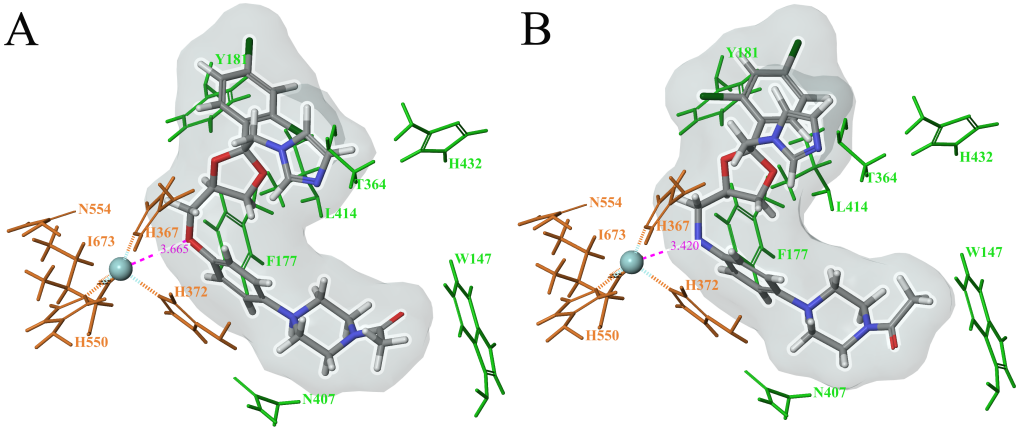


**Figure 4.5.** Docking ketoconazole (A) and ketaminazole (B) to the crystal structure of Stable-5-LOX (PDB ID: 3O8Y). Glide docking scores and poses were similar to other high-ranking docked inhibitors.

observed to be within 5 angstroms of the catalytic iron (Figure 4.5B), supportive of the hypothesis that the phenylenediamine core reduces the active site iron.

The docking poses of the phenylenediamine inhibitors suggest that their amine moieties could be possible conduits of iron reduction, through space via an outer sphere mechanism.[57] However, the docking poses also suggest the active site iron-hydroxide moiety could possibly abstract a hydrogen atom from the amine by an inner sphere mechanism, as is seen in the natural mechanism of LOX with its fatty acid substrate.[58] To test this hypothesis, **13** was incubated in $D_2O$ buffer, to deuterate the phenylenediamine core amine, and its $IC_{50}$ value compared to the protonated amine in $H_2O$. A 2.4-fold increase in the $IC_{50}$ for **13** was observed in $D_2O$, which is well below the kinetic isotope effect expected for hydrogen atom abstraction,[57] suggestive of a proton independent outer sphere reductive mechanism. To further verify this proton-independent reductive mechanism, **1** and **7** (containing the protonated and methylated amine, respectively) were also investigated and both were shown to have similar increases in $IC_{50}$ values in $D_2O$ relative to $H_2O$, suggesting the effect does not involve the amine proton.

In order to evaluate the concept of an improved anti-inflammatory effect combined with antifungal potency, we examined the selectivity of ketoconazole and ketaminazole (**16**) against the human and *C. albicans* CYP51 proteins, HsCYP51 and CaCYP51 respectively. Binding ketoconazole and ketaminazole (**16**) with both CaCYP51 and HsCYP51 produced strong type II difference spectra (Figure 4.6) signifying direct coordination as the sixth ligand of the heme prosthetic group of

CYP51. [58,59] Ketoconazole and ketaminazole (**16**) both bound tightly to CaCYP51 with $K_d$ values of 27±5 and 43±5 nM, respectively. Tight binding is observed when the $K_d$ for the ligand is similar to or less than the concentration of CYP51 present.[60] The similar $K_d$ values obtained for ketoconazole and ketaminazole (**16**) suggest both azoles would be equally effective as antifungal agents against wild-type CaCYP51. This is understandable since the CYP51 potency of this class of molecules is predominantly due to their azole moiety, which is quite distant from the phenylenediamine core of ketaminazole (**16**). This data also compares with $K_d$ values of 10 to 50 nM previously obtained for clotrimazole, econazole, fluconazole, itraconazole, ketoconazole, miconazole and voriconazole with CaCYP51.[39] Ketoconazole bound 17-fold more tightly to HsCYP51 ($K_d$ = 42±16 nM) compared to ketaminazole (**16**) ($K_d$ = 731±69 nM), in contrast to the 1.6-fold difference observed with CaCYP51, suggesting that ketaminazole would interfere less with the host HsCYP51 and possibly other human CYPs than ketoconazole, conferring a therapeutic advantage. These results compare well with the previously reported $K_d$ values of <100 nM for clotrimazole, econazole and miconazole, ~180 nM for ketoconazole and ~70 μM for fluconazole with HsCYP51.[40]

The $IC_{50}$ CYP51 reconstitution assay results (Figure 4.7) mirrored those of the azole binding results. CaCYP51 was strongly inhibited by both ketoconazole and ketaminazole (**16**) with $IC_{50}$ values of ~0.5 and ~0.9 μM, respectively, confirming that both azoles bound tightly to CaCYP51. Interestingly, at 4 μM ketaminazole (**16**), CaCYP51 retained ~15% CYP51 activity suggesting that lanosterol can displace

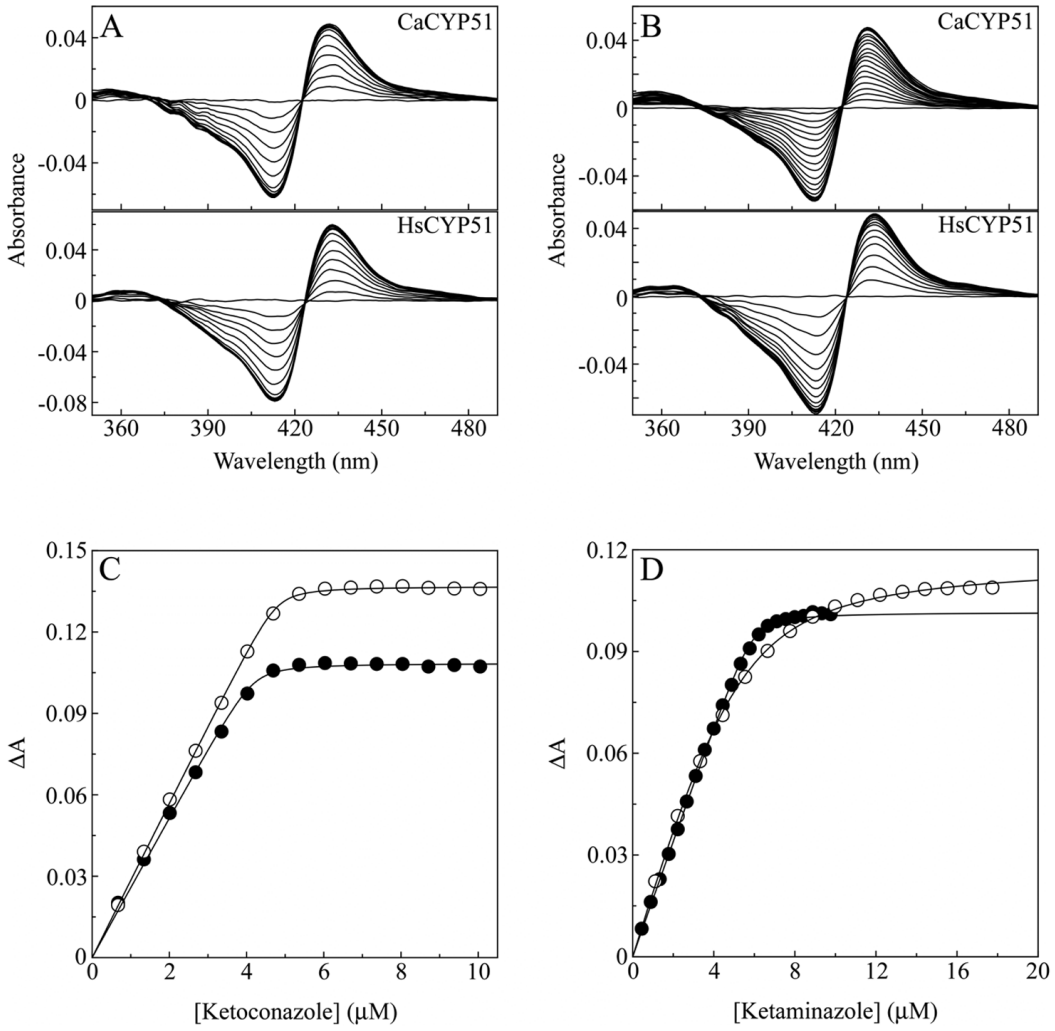


**Figure 4.6.** Binding properties of ketoconazole and ketaminazole with CaCYP51 and HsCYP51. Azole antifungals were progressively titrated against 5 μM CaCYP51 (filled circles) and 5 μM HsCYP51 (hollow circles). The resultant type II difference spectra are shown for ketoconazole (A) and ketaminazole (B). Saturation curves for ketoconazole (C) and ketaminazole (D) were constructed and a rearrangement of the Morrison equation was used to fit the data.[45] The data shown represent one replicate of the three performed. This figure and the data it contains was generated by coauthor Eric K. Hoobler.[62]

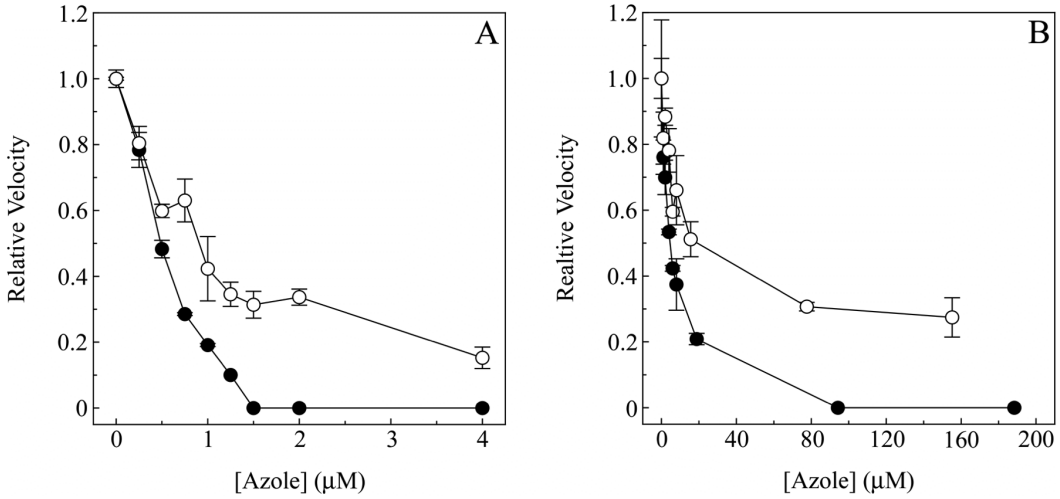


**Figure 4.7.** Determination of $IC_{50}$ values for ketoconazole and ketaminazole with CaCYP51 and HsCYP51. CYP51 reconstitution assays (0.5-ml total volume) containing 1 μM CaCYP51 (A) or 0.3 μM HsCYP51 (B) were performed as detailed in materials and methods. Ketoconazole (solid circles) and ketaminazole (hollow circles) concentrations were varied from 0 to 4 μM for CaCYP51 and up to 190 μM for HsCYP51 with the DMSO concentration kept constant at 1% (vol/vol). Mean values from two replicates are shown along with associated standard deviation bars. Relative velocities of 1.0 were equivalent to 1.04 and 2.69 nmoles 14α-demetylated lanosterol produced per minute per nmole CYP51 ($min^{-1}$) for CaCYP51 and HsCYP51, respectively. This figure and the data it contains was generated by coauthor Eric K. Hoobler.[62]

ketaminazole (**16**) from CaCYP51 leading to ketaminazole (**16**) being a less effective inhibitor of fungal CYP51 enzymes *in vitro* than ketoconazole. HsCYP51 was less severely inhibited by both ketoconazole and ketaminazole (**16**) with $IC_{50}$ values of ~5 and ~16 μM, respectively. This indicates that azole binding was less tight and suggested lanosterol can displace ketoconazole and especially ketaminazole (**16**) from HsCYP51. At 95 μM ketoconazole HsCYP51 was inactivated in contrast to the ~30% CYP51 activity remaining in the presence of 155 μM ketaminazole (**16**). The 3-fold higher $IC_{50}$ value of ketaminazole (**16**) over ketoconazole with HsCYP51 confirmed that ketaminazole (**16**) would be less disruptive to the CYP51 function of the host homolog than ketoconazole, conferring a therapeutic advantage for use as an antifungal agent. It should be noted that both itraconazole and posaconazole, both effective anti-fungal agents, could also have a phenylenediamine incorporated into their structures, thus conferring dual anti-fungal/anti-inflammatory properties on these therapeutics as well. We are currently investigating the properties of these modified anti-fungal agents further, with the hope of utilizing the phenylenediamine moiety as a simple modification for adding 5-LOX inhibitory potency to known therapeutics.

The fact that ketoconazole is both an anti-fungal and anti-inflammatory molecule is not a new phenomenon in the field of anti-fungal therapeutics. Previously, we determined that the common anti-fungal agent, chloroxine, was also a non-specific LOX inhibitor.[61] This fact suggested that the inherent selection process for the search for anti-seborrheic dermatitis agents could be responsible for the dual

nature of the anti-fungal/anti-inflammatory therapeutics, such as chloroxine and ketoconazole. With this hypothesis in mind, the anti-fungal agent, ciclopirox (trade name Loprox), presented a structure that could be interpreted as a LOX inhibitor, with the *N*-hydroxyamide being a possible chelator. This was confirmed and ciclopirox was found to be both a potent inhibitor of 5-LOX ($IC_{50}$ = 11±1 μM) and selective versus other AA processing enzymes (Figure 4.4). This dual nature of many anti-seborrheic dermatitis agents suggests that improving the 5-LOX potency of these therapeutics may be beneficial in their clinical efficacy.

**4.4 Conclusions**

The current data indicate that the phenylenediamine chemotype reported herein is a potent inhibitor against 5-LOX, demonstrating enzyme selectivity and cellular activity. The mechanism of action is consistent with reduction of the active site ferric ion, similar to that seen for zileuton, the only FDA approved LOX inhibitor. It is interesting to note that unlike zileuton, which chelates the iron through the *N*-hydroxyurea, the phenylenediamine chemotype lacks an obvious chelating moiety, thus differentiating it from zileuton. Structural modification around the phenylenediamine core was well tolerated, however, even relatively minor changes to the phenylenediamine moiety resulted in a loss of activity, presumably due to changes in its reduction potential. This attribute was utilized to modify the structure of ketoconazole to include the phenylenediamine moiety and produce a novel inhibitor, ketaminazole (**16**). This novel compound demonstrated an *in vitro* 40-fold increase in potency against 5-LOX relative to ketoconazole. However, in whole blood

ketaminazole demonstrated only a 2-fold greater potency than ketoconazole. In addition, the overall potency of ketaminazole was reduced by approximately 10-fold relative to its *in vitro* potency. It is currently unclear how the cellular environment is lowering the potency of ketaminazole, but pharmacokinetic investigations are currently underway to probe this further. Ketaminazole (**16**) had comparable potency against fungal CYP51 and improved selectivity against the human CYP51, relative to ketoconazole, which suggests a possible therapeutic advantage. This novel dual nature of ketaminazole (**16**), possessing both anti-fungal and anti-inflammatory activity, could potentially have therapeutic uses against fungal infections that have an anti-inflammatory component.

## 4.5 Supporting information

### 4.5.1 Representative procedures and characterization of phenylenediamine inhibitors

A mixture of tert-butyl 4-(4-aminophenyl)piperazine-1-carboxylate (1.94 g, 6.99 mmol, 1 eq) and 5-bromofuran-2-carbaldehyde (1.26 g, 7.34 mmol, 1.05 eq) in MeOH (35 mL) and $CH_2Cl_2$ (35 mL) was added sodium triacetoxyborohydride (4.45 g, 20.98 mmol, 3 eq). The reaction mixture was stirred at room temperature for 5 h. The product was extracted with ethyl acetate and the organic layer was subsequently washed with water, bicarbonate and brine. The crude product obtained after evaporation of the solvent was purified on a biotage flash system® eluting with 40% ethyl acetate in hexanes (Yield 1.94 g, 62 %)

***t*-Butyl-4-(4-(((5-(4-isocyanophenyl)furan-2-yl)methyl)amino)phenyl)piperazine-1-carboxylate (1)**: To a mixture of t-butyl 4-(4-(((5-bromofuran-2-yl)methyl)amino)phenyl)piperazine-1-carboxylate (0.172 mmol, 0.075 g, 1 eq) and (4-cyanophenyl)boronic acid (0.206 mmol, 30 mg, 1.2 eq) in 1 mL DME was added $Pd(PPh_3)_4$ (5 mol %, 0.09 mmol, 10 mg) and a 2.0 M aqueous solution of $Na_2CO_3$ (0.52 mmol). The mixture was irradiated in a microwave reactor for 30 minutes at 150 $^oC$. The solvent was removed by blowing air and the crude product was dissolved in DMF, passed through a palladium scavenger cartridge and finally purified in preparative HPLC. LC-MS: rt (min) = 5.10 (8.0 min run); $^1H$ NMR (400 MHz, DMSO-$d_6$) δ 7.86 – 7.74 (m, 3H), 7.10 (d, $J$ = 3.4 Hz, 1H), 6.78 – 6.69 (m, 2H), 6.62 – 6.53 (m, 2H), 6.44 – 6.38 (m, 1H), 5.72 (t, $J$ = 6.2 Hz, 1H), 4.24 (d, $J$ = 6.1 Hz, 2H), 3.47 – 3.34 (m, 4H), 2.81 (dd, $J$ = 6.1, 4.1 Hz, 4H), 1.38 (d, $J$ = 7.9 Hz, 9H); HRMS (ESI) $m/z$ (M+H)+ calcd. for $C_{27}H_{31}N_4O_3$, 459.2391; found 459.2374.

***t*-Butyl-4-(4-(((5-(4-isocyanophenyl)furan-2-yl)methyl)amino)phenyl)piperidine-1-carboxylate (2) :** LC-MS: rt (min) = 6.54 (8.0 min run); $^1H$ NMR (400 MHz, DMSO-$d_6$) δ 7.80 (m, 2H), 7.10 (d, $J$ = 3.3 Hz, 1H), 6.91 (d, $J$ = 8.2 Hz, 2H), 6.57 (d, $J$ = 8.2 Hz, 2H), 6.42 (d, $J$ = 3.3 Hz, 2H), 5.97 (t, $J$ = 6.2 Hz, 1H), 4.26 (d, $J$ = 6.0 Hz, 2H), 3.28 (m, 1H), 2.46 (m, 4H), 1.67 – 1.58 (m, 4H), 1.36 (s, 9H); HRMS (ESI) $m/z$ (M+H)+ calcd. for $C_{28}H_{32}N_3O_3$, 458.2438; found 458.2416.

***t*-Butyl-4-(6-(((5-(4-isocyanophenyl)furan-2-yl)methyl)amino)pyridin-3-yl)piperazine-1-carboxylate (6):** LC-MS: rt (min) = 4.886 (8.0 min run); $^1H$ NMR (400 MHz, DMSO-$d_6$) δ 7.81 (q, $J$ = 8.4 Hz, 4H), 7.69 (d, $J$ = 2.8 Hz, 1H), 7.22 (dd, $J$ = 8.9, 2.9 Hz, 1H), 7.11 (d, $J$ = 3.4 Hz, 1H), 6.62 (t, $J$ = 6.0 Hz, 1H), 6.52 (d, $J$ = 9.0

Hz, 1H), 6.37 (d, *J* = 3.4 Hz, 1H), 4.46 (d, *J* = 5.9 Hz, 2H), 3.41 (t, *J* = 5.2 Hz, 4H), 3.01 (s, 6H), 2.85 (t, *J* = 5.1 Hz, 4H), 1.47 (s, 1H), 1.39 (s, 9H), 1.22 (d, *J* = 5.7 Hz, 1H); ); HRMS (ESI) *m*/*z* (M+H)+ calcd. for $C_{26}H_{30}N_5O_3$, 460.2343; found 460.2343.

***t*-Butyl-4-(4-(((2-(4-cyanophenyl)oxazol-5-yl)methyl)amino)phenyl)piperazine-1-carboxylate (8) :** LC-MS: rt (min) = 4.645 (8.0 min run);$^1$H NMR (400 MHz, DMSO-$d_6$) δ 8.09 – 8.01 (m, 2H), 8.00 – 7.92 (m, 2H), 7.22 (s, 1H), 6.79 – 6.70 (m, 2H), 6.64 – 6.56 (m, 2H), 5.77 (t, *J* = 6.2 Hz, 1H), 4.33 (d, *J* = 6.2 Hz, 2H), 3.38 (t, *J* = 5.0 Hz, 4H), 2.82 (t, *J* = 5.1 Hz, 4H), 1.37 (s, 9H); HRMS (ESI) *m*/*z* (M+H)+ calcd. for $C_{26}H_{30}N_5O_3$, 460.2343; found 460.2323.

**1-(4-(4-(((5-(4-bromophenyl)furan-2-yl)methyl)amino)phenyl)piperazin-1-yl)ethanone (12) :** LC-MS: rt (min) = 4.645 (8.0 min run);$^1$H NMR (400 MHz, DMSO-$d_6$) δ 8.09 – 8.01 (m, 2H), 8.00 – 7.92 (m, 2H), 7.22 (s, 1H), 6.79 – 6.70 (m, 2H), 6.64 – 6.56 (m, 2H), 5.77 (t, *J* = 6.2 Hz, 1H), 4.33 (d, *J* = 6.2 Hz, 2H), 3.38 (t, *J* = 5.0 Hz, 4H), 2.82 (t, *J* = 5.1 Hz, 4H), 1.37 (s, 9H); HRMS (ESI) *m*/*z* (M+H)+ calcd. for $C_{25}H_{29}N_6O_3$, 461.2296; found 461.2288.

### 4.5.2 Synthesis of ketaminazole

A mixture of 2-((1H-imidazol-1-yl)methyl)-2-(2,4-dichlorophenyl)-1,3-dioxolan-4-yl)methyl methanesulfonate (0.9 g, 2.21 mmol, 1eq) [purchased from Toronto Research Chemicals] and 1-(4-(4-aminophenyl)piperazin-1-yl)ethanone (0.581 g, 2.65 mmol, 1.2 eq) in a microwave vial was stirred neat at 130 $^o$C for 1 h. The crude product was dissolved in DMSO and purified ISCO® reverse phase flash system using a water and acetonitrile solvent system. The product fractions were

pooled and lyophilized to get a brown solid. LC-MS: rt (min) = 3.64 (8.0 min run); $^{1}$H NMR (400 MHz, DMSO-$d_6$) δ 9.10 (t, $J$ = 1.4 Hz, 1H), 7.72 (d, $J$ = 2.1 Hz, 1H), 7.67 – 7.63 (m, 2H), 7.62 (s, 1H), 7.51 (dd, $J$ = 8.5, 2.1 Hz, 1H), 7.11 – 6.94 (m, 2H), 6.67 – 6.49 (m, 2H), 4.89 – 4.72 (m, 2H), 4.23 – 4.07 (m, 1H), 3.91 – 3.41 (m, 6H), 3.27 – 2.79 (m, 6H) and 2.05 (s, 3H)$^{\cdot}$; HRMS (ESI) $m/z$ (M+H)+ calcd. for $C_{26}H_{30}Cl_2N_5O_3$, 530.1720; found 530.1698.

## 4.6 References

(1) Rubin, P., and Mollison, K. W. (2007) Pharmacotherapy of diseases mediated by 5-lipoxygenase pathway eicosanoids. *Prostaglandins & Other Lipid Mediators 83*, 188–197.

(2) O'Byrne, P. M., Israel, E., and Drazen, J. M. (1997) Antileukotrienes in the treatment of asthma. *Ann. Intern. Med. 127*, 472–480.

(3) Rådmark, O. P. (2000) The Molecular Biology and Regulation of 5-Lipoxygenase.

(4) Ford-Hutchinson, A. W., Gresser, M., and Young, R. N. (1994) 5-Lipoxygenase. *Annu. Rev. Biochem. 63*, 383–417.

(5) Werz, O., and Steinhilber, D. (2006) Therapeutic options for 5-lipoxygenase inhibitors. *Pharmacol. Ther. 112*, 701–718.

(6) Pergola, C., and Werz, O. (2010) 5-Lipoxygenase inhibitors: a review of recent developments and patents. *Expert Opin Ther Pat 20*, 355–375.

(7) Zouboulis, C. C., Saborowski, A., and Boschnakow, A. (2005) Zileuton, an oral 5-lipoxygenase inhibitor, directly reduces sebum production. *Dermatology (Basel) 210*, 36–38.

(8) Faergemann, J. (2000) Management of seborrheic dermatitis and pityriasis versicolor. *Am J Clin Dermatol 1*, 75–80.

(9) Faergemann, J., Borgers, M., and Degreef, H. (2007) A new ketoconazole topical gel formulation in seborrhoeic dermatitis: an updated review of the mechanism. *Expert Opin Pharmacother 8*, 1365–1371.

(10) Borgers, M., and Degreef, H. (2007) The role of ketoconazole in seborrheic dermatitis. *Cutis 80*, 359–363.

(11) Scheinfeld, N. (2008) Ketoconazole: a review of a workhorse antifungal molecule with a focus on new foam and gel formulations. *Drugs Today 44*, 369–380.

(12) Beetens, J. R., Loots, W., Somers, Y., Coene, M. C., and De Clerck, F. (1986) Ketoconazole inhibits the biosynthesis of leukotrienes in vitro and in vivo. *Biochemical Pharmacology 35*, 883–891.

(13) Steel, H. C., Tintinger, G. R., Theron, A. J., and Anderson, R. (2007) Itraconazole-mediated inhibition of calcium entry into platelet-activating factor-

stimulated human neutrophils is due to interference with production of leukotriene B4. *Clin. Exp. Immunol. 150*, 144–150.

(14) Koeberle, A., Zettl, H., Greiner, C., Wurglics, M., Schubert-Zsilavecz, M., and Werz, O. (2008) Pirinixic acid derivatives as novel dual inhibitors of microsomal prostaglandin E2 synthase-1 and 5-lipoxygenase. *J. Med. Chem. 51*, 8068–8076.

(15) McMillan, R. M., and Walker, E. R. (1992) Designing therapeutically effective 5-lipoxygenase inhibitors. *Trends in Pharmacological Sciences 13*, 323–330.

(16) Musser, J. H., and Kreft, A. F. (1992) 5-lipoxygenase: properties, pharmacology, and the quinolinyl(bridged)aryl class of inhibitors. *J. Med. Chem. 35*, 2501–2524.

(17) Robinson, S. J., Hoobler, E. K., Riener, M., Loveridge, S. T., Tenney, K., Valeriote, F. A., Holman, T. R., and Crews, P. (2009) Using enzyme assays to evaluate the structure and bioactivity of sponge-derived meroterpenes. *J. Nat. Prod. 72*, 1857–1863.

(18) Falgueyret, J. P., Hutchinson, J. H., and RIENDEAU, D. (1993) Criteria for the identification of non-redox inhibitors of 5-lipoxygenase. *Biochemical Pharmacology 45*, 978–981.

(19) Young, R. (1999) Inhibitors of 5-lipoxygenase: a therapeutic potential yet to be fully realized? *European Journal of Medicinal Chemistry 34*, 671–685.

(20) Carter, G. W., Young, P. R., Albert, D. H., Bouska, J., Dyer, R., Bell, R. L., Summers, J. B., and Brooks, D. W. (1991) 5-lipoxygenase inhibitory activity of zileuton.

(21) McGill, K. A., and Busse, W. W. (1996) Zileuton. *Lancet 348*, 519–524.

(22) Bell, R. L., Young, P. R., Albert, D., Lanni, C., Summers, J. B., Brooks, D. W., Rubin, P., and Carter, G. W. (1992) The discovery and development of zileuton: an orally active 5-lipoxygenase inhibitor. *Int. J. Immunopharmacol. 14*, 505–510.

(23) Stewart, A. O., Bhatia, P. A., Martin, J. G., Summers, J. B., Rodriques, K. E., Martin, M. B., Holms, J. H., Moore, J. L., Craig, R. A., Kolasa, T., Ratajczyk, J. D., Mazdiyasni, H., Kerdesky, F. A., DeNinno, S. L., Maki, R. G., Bouska, J. B., Young, P. R., Lanni, C., Bell, R. L., Carter, G. W., and Brooks, C. D. (1997) Structure-activity relationships of N-hydroxyurea 5-lipoxygenase inhibitors. *J. Med. Chem. 40*, 1955–1968.

(24) Walenga, R. W., Showell, H. J., Feinstein, M. B., and Becker, E. L. (1980) Parallel inhibition of neutrophil arachidonic acid metabolism and lysosomal enzyme

secretion by nordihydroguaiaretic acid. *Life Sci. 27*, 1047–1053.

(25) Kemal, C., Louis-Flamberg, P., Krupinski-Olsen, R., and Shorter, A. L. (1987) Reductive inactivation of soybean lipoxygenase 1 by catechols: a possible mechanism for regulation of lipoxygenase activity. *Biochemistry 26*, 7064–7072.

(26) Whitman, S., Gezginci, M., Timmermann, B. N., and Holman, T. R. (2002) Structure-activity relationship studies of nordihydroguaiaretic acid inhibitors toward soybean, 12-human, and 15-human lipoxygenase. *J. Med. Chem. 45*, 2659–2661.

(27) Pham, C., Jankun, J., Skrzypczak-Jankun, E., Flowers, R. A., and Funk, M. O. (1998) Structural and thermochemical characterization of lipoxygenase-catechol complexes. *Biochemistry 37*, 17952–17957.

(28) Nelson, M. J., Cowling, R. A., and Seitz, S. P. (1994) Structural characterization of alkyl and peroxyl radicals in solutions of purple lipoxygenase. *Biochemistry 33*, 4966–4973.

(29) Ducharme, Y., Blouin, M., and Brideau, C. (2010) The Discovery of Setileuton, a Potent and Selective 5-Lipoxygenase Inhibitor *1*, 170–174.

(30) Masferrer, J. L., Zweifel, B. S., Hardy, M., Anderson, G. D., Dufield, D., Cortes-Burgos, L., Pufahl, R. A., and Graneto, M. (2010) Pharmacology of PF-4191834, a Novel, Selective Non-Redox 5-Lipoxygenase Inhibitor Effective in Inflammation and Pain. *Journal of Pharmacology and Experimental Therapeutics 334*, 294–301.

(31) Amagata, T., Whitman, S., Johnson, T. A., Stessman, C. C., Loo, C. P., Lobkovsky, E., Clardy, J., Crews, P., and Holman, T. R. (2003) Exploring sponge-derived terpenoids for their potency and selectivity against 12-human, 15-human, and 15-soybean lipoxygenases. *J. Nat. Prod. 66*, 230–235.

(32) Deschamps, J. D., Gautschi, J. T., Whitman, S., Johnson, T. A., Gassner, N. C., Crews, P., and Holman, T. R. (2007) Discovery of platelet-type 12-human lipoxygenase selective inhibitors by high-throughput screening of structurally diverse libraries. *Bioorg. Med. Chem. 15*, 6900–6908.

(33) Vasquez-Martinez, Y., Ohri, R. V., Kenyon, V., Holman, T. R., and Sepúlveda-Boza, S. (2007) Structure–activity relationship studies of flavonoids as potent inhibitors of human platelet 12-hLO, reticulocyte 15-hLO-1, and prostate epithelial 15-hLO-2. *Bioorg. Med. Chem. 15*, 7408–7425.

(34) Segraves, E. N., and Holman, T. R. (2003) Kinetic investigations of the rate-limiting step in human 12- and 15-lipoxygenase. *Biochemistry 42*, 5236–5243.

(35) Rai, G., Kenyon, V., Jadhav, A., Schultz, L., Armstrong, M., Jameson, J. B., Hoobler, E., Leister, W., Simeonov, A., Holman, T. R., and Maloney, D. J. (2010) Discovery of potent and selective inhibitors of human reticulocyte 15-lipoxygenase-1. *J. Med. Chem. 53*, 7392–7404.

(36) Hutchinson, J. H., Li, Y., Arruda, J. M., Baccei, C., Bain, G., Chapman, C., Correa, L., Darlington, J., King, C. D., Lee, C., Lorrain, D., Prodanovich, P., Rong, H., Santini, A., Stock, N., Prasit, P., and Evans, J. F. (2009) 5-lipoxygenase-activating protein inhibitors: development of 3-[3-tert-butylsulfanyl-1-[4-(6-methoxy-pyridin-3-yl)-benzyl]-5-(pyridin-2-ylmethoxy)-1H-indol-2-yl]-2,2-dimethyl-propionic acid (AM103). *J. Med. Chem. 52*, 5803–5815.

(37) Fogh, J., Poulsen, L. K., and Bisgaard, H. (1992) A specific assay for leukotriene B4 in human whole blood. *J Pharmacol Toxicol Methods 28*, 185–190.

(38) Spaethe, S. M., Snyder, D. W., Pechous, P. A., Clarke, T., and VanAlstyne, E. L. (1992) Guinea pig whole blood 5-lipoxygenase assay: utility in the assessment of potential 5-lipoxygenase inhibitors. *Biochemical Pharmacology 43*, 377–382.

(39) Warrilow, A. G. S., Martel, C. M., Parker, J. E., Melo, N., Lamb, D. C., Nes, W. D., Kelly, D. E., and Kelly, S. L. (2010) Azole binding properties of Candida albicans sterol 14-alpha demethylase (CaCYP51). *Antimicrob. Agents Chemother. 54*, 4235–4245.

(40) Strushkevich, N., Usanov, S. A., and Park, H.-W. (2010) Structural basis of human CYP51 inhibition by antifungal azoles. *J. Mol. Biol. 397*, 1067–1078.

(41) Estabrook, R. W., Peterson, J., Baron, J., and Hildebrandt, A. (1972) The spectrophotometric measurement of turbid suspensisons of cytochromes associated with drug metabolism. *Methods Pharmacol 2*, 303–350.

(42) Omura, T., and Sato, R. (1964) The carbon monoxide-binding pigment of liver microsomes. I. Evidence for its hemoprotein nature. *J. Biol. Chem. 239*, 2370–2378.

(43) Omura, T., and Sato, R. (1964) The carbon monoxide-binding pigment of liver microsomes. II. Solubilization, purification, and properties. *J. Biol. Chem. 239*, 2379–2385.

(44) Lamb, D. C., Kelly, D. E., Waterman, M. R., Stromstedt, M., Rozman, D., and Kelly, S. L. (1999) Characteristics of the heterologously expressed human lanosterol 14alpha-demethylase (other names: P45014DM, CYP51, P45051) and inhibition of the purified human and Candida albicans CYP51 with azole antifungal agents. *Yeast 15*, 755–763.

(45) Lutz, J. D., Dixit, V., Yeung, C. K., Dickmann, L. J., Zelter, A., Thatcher, J. E., Nelson, W. L., and Isoherranen, N. (2009) Expression and functional characterization of cytochrome P450 26A1, a retinoic acid hydroxylase. *Biochemical Pharmacology 77*, 258–268.

(46) Lepesheva, G. I., Ott, R. D., Hargrove, T. Y., Kleshchenko, Y. Y., Schuster, I., Nes, W. D., Hill, G. C., Villalta, F., and Waterman, M. R. (2007) Sterol 14alpha-demethylase as a potential target for antitrypanosomal therapy: enzyme inhibition and parasite cell growth. *Chem. Biol. 14*, 1283–1293.

(47) Lepesheva, G. I., Zaitseva, N. G., Nes, W. D., Zhou, W., Arase, M., Liu, J., Hill, G. C., and Waterman, M. R. (2006) CYP51 from Trypanosoma cruzi: a phyla-specific residue in the B' helix defines substrate preferences of sterol 14alpha-demethylase. *J. Biol. Chem. 281*, 3577–3585.

(48) Venkateswarlu, K., Denning, D. W., Manning, N. J., and Kelly, S. L. (1995) Resistance to fluconazole in Candida albicans from AIDS patients correlated with reduced intracellular accumulation of drug. *FEMS Microbiol. Lett. 131*, 337–341.

(49) Lo, H. Y., Man, C. C., Fleck, R. W., Farrow, N. A., Ingraham, R. H., Kukulka, A., Proudfoot, J. R., Betageri, R., Kirrane, T., Patel, U., Sharma, R., Hoermann, M. A., Kabcenell, A., and Lombaert, S. D. (2010) Substituted pyrazoles as novel sEH antagonist: investigation of key binding interactions within the catalytic domain. *Bioorg. Med. Chem. Lett. 20*, 6379–6383.

(50) Itoh, T., Nagata, K., Miyazaki, M., Ishikawa, H., Kurihara, A., and Ohsawa, A. (2004) A selective reductive amination of aldehydes by the use of Hantzsch dihydropyridines as reductant. *Tetrahedron 60*, 6649–6655.

(51) Ito, S., Kubo, T., Morita, N., Ikoma, T., Tero-Kubota, S., Kawakami, J., and Tajiri, A. (2005) Azulene-Substituted Aromatic Amines. Synthesis and Amphoteric Redox Behavior of N, N-Di(6-azulenyl)- p-toluidine and N, N, N‘, N‘-Tetra(6-azulenyl)- p-phenylenediamine and Their Derivatives. *J. Org. Chem. 70*, 2285–2293.

(52) Vouros, P., and Biemann, K. (1969) The structural significance of doubly charged ion spectra. Phenylenediamine derivatives. *Org. Mass Spectrom. 2*, 375–386.

(53) Sakurai, H., Ritonga, M. T. S., Shibatani, H., and Hirao, T. (2005) Synthesis and characterization of p-phenylenediamine derivatives bearing an electron-acceptor unit. *J. Org. Chem. 70*, 2754–2762.

(54) Gilbert, N. C., Bartlett, S. G., Waight, M. T., Neau, D. B., Boeglin, W. E., Brash, A. R., and Newcomer, M. E. (2011) The structure of human 5-lipoxygenase. *Science 331*, 217–219.

(55) Friesner, R. A., Banks, J. L., Murphy, R. B., Halgren, T. A., Klicic, J. J., Mainz, D. T., Repasky, M. P., Knoll, E. H., Shelley, M., Perry, J. K., Shaw, D. E., Francis, P., and Shenkin, P. S. (2004) Glide: a new approach for rapid, accurate docking and scoring. 1. Method and assessment of docking accuracy. *J. Med. Chem. 47*, 1739–1749.

(56) Halgren, T. A., Murphy, R. B., Friesner, R. A., Beard, H. S., Frye, L. L., Pollard, W. T., and Banks, J. L. (2004) Glide: a new approach for rapid, accurate docking and scoring. 2. Enrichment factors in database screening. *J. Med. Chem. 47*, 1750–1759.

(57) Lewis, E. R., Johansen, E., and Holman, T. R. (1999) Large competitive kinetic isotope effects in human 15-lipoxygenase catalysis measured by a novel HPLC method. *J. Am. Chem. Soc. 121*, 1395–1396.

(58) Jefcoate, C. R. (1978) Measurement of substrate and inhibitor binding to microsomal cytochrome P-450 by optical-difference spectroscopy. *Meth. Enzymol. 52*, 258–279.

(59) Jefcoate, C. R., Gaylor, J. L., and Calabrese, R. L. (1969) Ligand interactions with cytochrome P-450. I. Binding of primary amines. *Biochemistry 8*, 3455–3463.

(60) Copeland, R. A. (2005) Evaluation of enzyme inhibitors in drug discovery. A guide for medicinal chemists and pharmacologists. *Methods Biochem Anal 46*, 1–265.

(61) Kenyon, V., Rai, G., Jadhav, A., Schultz, L., Armstrong, M., Jameson, J. B., Perry, S., Joshi, N., Bougie, J. M., Leister, W., Taylor-Fishwick, D. A., Nadler, J. L., Holinstat, M., Simeonov, A., Maloney, D. J., and Holman, T. R. (2011) Discovery of potent and selective inhibitors of human platelet-type 12- lipoxygenase. *J. Med. Chem. 54*, 5485–5497.

(62) Hoobler, E. K. (2013) Structural and therapeutic investigations of human lipoxygenase. PhD dissertation, University of California, Santa Cruz. ProQuest/UMI. (ISBN: 9781303021152)

## 4.7 Credit to Coauthors

As noted in the figure captions above, the following experiments were performed by or under the supervision of the following people and not by Christopher J. Smyrniotis:

1) Cyclooxygenase assay
2) Human blood LTB4 inhibition assay
3) Pseudoperoxidase activity assay
4) CYP51 protein studies

**Eric K. Hoobler**
Department of Chemistry and Biochemistry, University of California, Santa Cruz, CA 95064